PROUROGUANYLIN'S ROLE IN THE HOMEOSTATIC RESPONSE TO DIETARY SODIUM: HORMONE PRECURSOR OR ACTIVE SIGNALING AGENT?

ROBERT C. FELLNER

A dissertation submitted to the faculty of the University of North Carolina at Chapel Hill in partial fulfillment of the requirements for the degree of Doctor of Philosophy in the Department of Cell and Molecular Physiology – School of Medicine

Chapel Hill

2010

Committee Members;

Michael F. Goy, PhD

William J. Arendshorst, PhD

Kathleen M. Caron, PhD

James E. Faber, PhD

Nobuyo N. Maeda, PhD

ABSTRACT

Robert C. Fellner

Prouroguanylin's Role in the Homeostatic Response to Dietary Sodium: Hormone Precursor or Active Signaling Agent? (Under the direction of Dr. Michael F. Goy)

High blood pressure affects more than 70 million Americans, putting them at a much greater risk for heart disease or a stroke. Sodium (Na^+) is a major determinant of blood osmolarity and volume, and therefore plays a critical role in blood pressure regulation. Prouroguanylin (proUgn) has been implicated as a signal being sent from the small intestine to the kidney, in response to oral Na^+ intake, that intestinal Na^+ adsorption is eminent and renal Na^+ excretion is necessary to maintain homeostasis. This concept, known as post-prandial natriuresis, is based on past observations of a faster natriuretic response from an oral salt load than from an equimolar intravenous infusion of NaCl. This role for proUgn is contentious however, as it has not been clearly shown if the role played by proUgn is that of a primary messenger from the intestine to the kidney in response to salt, if it is a intrarenal paracrine mechanism secondary to some other extrarenal signal in response to oral Na^+ or even if it is proUgn itself or one of its' metabolites that are acting in the kidney. My studies address identification and quantification of proUgn and Ugn in relevant tissue compartments and additionally, I look at the effects of dietary Na^+ on changes in the expression of proUgn and Ugn in these tissues. A novel adaptation of a binding

assay technique allowed for urinary Ugn measurements that were found to directly correlate with dietary Na^+ intake on a time scale that the prior techniques were insufficiently sensitive to achieve. Enteric and plasma proUgn do not change in response to dietary Na^+, however renal proUgn expression and Ugn in the urine do. Changes in plasma proUgn elicit a greater natriuretic response with a lower urinary Ugn concentration than urinary Ugn concentrations from infusions of Ugn into the blood. My conclusion is that proUgn is a secondary agent involved in volume and Na^+ homeostasis, acting though some as yet unidentified renal metabolite/receptor mechanism. Further studies should focus on if there is another active cleavage product of proUgn and what receptor it (proUgn or Ugn) acts through.

DEDICATION

This dissertation is dedicated to all my family and friends who have believed in me and inspired me throughout the process and especially in memory of my friend Andrew Rachlin.

ACKNOWLEDGEMENTS

I would like to thank first and foremost my dissertation advisor Dr. Michael Goy for all his support, patience and friendship throughout the process. He was there for me 100% from the very start in any way I could imagine both personally and professionally. Additionally, I owe a huge thanks to Dr. Nicholas Moss who has been a great guide, teacher and colleague, an excellent co-mentor for me throughout the process. I can be headstrong and determined to do things my way and both have shown great skill at steering me as much as possible to the right path and then patience in helping me recover from my mistakes and finding the best way to accomplish my goals. You both have helped greatly not only with professional but also personal growth.

I also owe a huge debt to all my committee members for not only their guidance in my dissertation quest but for overall assistance with my career; Dr. James Faber immediately took me under his wing both as an advisor and a friend, escorting me to both conferences and on climbing trips to learn about the world of academic science as well as my new home state of North Carolina. Dr. William Arendshorst showed me the world of renal microvasculature and introduced me to the important people in the field, opening the door for the next step in my academic career. Dr. Nobuyo Maeda had faith enough in me to grant me a fellowship in the IVB training program and to mentor me through such even before coming onto my

committee. Dr. Kathleen Caron was instrumental in helping me recognize how to set and accomplish realistic goals in my graduate career.

I have mentored a series of undergraduates in the lab and they have proved valuable both in helping achieve goals in my research and in teaching me to be a better teacher. Thanks Amanda Fitzgerald, Ariana Horvat-Fisher, Mark AbuMoussa, Sam AbuMoussa and Sharon Yu.

The bedrock of my graduate career comes from my friends, especially Julie Rasmussen, Dr. Dan Chalothorn, Ari Bowers, Dr. Nicole Ramocki, Mike Kerber and Dr. Kate Hamilton. Without these friendships this process might have broken my sanity. Many other great friends have assisted and accompanied me along the way; Alexis Mastromichalis, Dr. Aparna Bohil, Cathleen O'connell, Dr. Cauveh Erami, Caroline and Dr. Alex Couture, Dr. Damon Jacobs, Dana Williams, Erica Hauck, Jason Sayers, Jeremy Sadler, Dr. Marc Spingola, Dr. Matt Medlin, Dr. Melanie Schikore, Dr. Melinda Devito, Dr. Nikki Worthington, Rachel Liesman, Dr. Rebecca Sayers, Dr. Rob Tarran, Dr. Rob Onyenwoke, Dr. Suman Sen, and Dr. Vicki Newton have all been very close and their support is greatly appreciated.

Finally and especially I would like to thank my family for all the years of support and inspiration that I could and should try to achieve up to my greatest potential. Thanks to my brother Bill and wife Lora for allowing me to sleep in their basement. I thank my parents, Cindy and William Coty, and Thomas and Lanelle Fellner for all the efforts to make my continued education possible and the encouragement that the chosen path was the best thing for me. It would never have happened without all your support and inspiration… THANKS!!

TABLE OF CONTENTS

LIST OF TABLES

LIST OF FIGURES

FIGURE

ABBREVIATIONS

AALAC	Association for Assessment and Accreditation of Laboratory Animal Care
A/D	analog to digital
ADH	anti-diuretic hormone, also referred to as Vasopressin
ANOVA	analysis of variance
ANP	atrial natriuretic peptide
BDT	below detection threshold
BNP	brain or B-type natriuretic peptide
CΔ	recombinant rat proUgn missing the C-terminal 15 amino acids
cDNA	complementary deoxyribonucleic acid
CFTR	cystic fibrosis transmembrane conductance regulator
cGMP	cyclic guanosine monophosphate
CHF	congestive heart failure
CNP	C-type natriuretic peptide
C_t	cycle times to threshold detection for rt-PCR amplification
CTEP	carboxy-terminal extension peptide
Δ-C_t	differences in C_t between gene of interest (proUgn) to housekeeping gene (ß-Actin) in q-rt-PCR results
Δ-Δ-C_t	computational method for mRNA quantification analysis
DLAM	Division of Laboratory Animal Medicine
EC	enterochromaffin cell
ECF	extracellular fluid

GC-A	receptor guanylyl cyclase type A
GC-B	receptor guanylyl cyclase type B
GC-C	receptor guanylyl cyclase type C
GFR	glomerular filtration rate
Gn	guanylin
H_2O	water
HPLC	high-pressure liquid chromatography
hUgn-A, hUgn-B	human uroguanylin topoisomers A, and B
HS	diet study phase when rats are fed 3.1% Na^+ chow ad libitum
K^+	potassium
K_D	disassociation constant
K_I	binding inhibition constant (indicative of disassociation constant)
Lgn	lymphoguanylin
LI-COR	imaging system for western blot quantitation
LS	diet study phase when rats are fed 0.02% Na^+ chow ad libitum
MAP	mean arterial pressure
Meq	milliequivalents of an ion
mRNA	messenger ribonucleic acid
N	native proUgn molecule
Na^+	sodium
NHE3	Na^+/H^+ exchanger
NS	diet study phase when rats are fed 0.26% Na^+ chow ad libitum
OK-GC	receptor guanylyl cyclase type opossum kidney

Rgn	renoguanylin
rGC	receptor guanylyl cyclases
PKG II	cGMP-dependent protein kinase
PPN	post prandial natriuresis
proUgn	prouroguanylin
qRT-PCR	quantitative real time polymerase chain reaction
R	recombinant rat proUgn standard
RAAS	renin-angiotensin-aldosterone system
RP-HPLC	reverse phase high-pressure liquid chromatography
RIA	radioimmunoassay
SEM	standard error of the mean
SNS	sympathetic nervous system
STa	*E. coli*. Heat-stable bacterial toxin
UK^+v	urinary potassium excretion in milliequivalents per time
UNa^+v	urinary sodium excretion in milliequivalents per time
rtPCR	real time polymerase chain reaction
Ugn	uroguanylin
Ugn+/+	wild-type 129/SvJ mouse
Ugn-/-	129/SvJ mouse that has uroguanylin gene expression disabled
Y-Ugn	synthetic uroguanylin with a non-native tyrosine residue added to the amino terminus

CHAPTER I

BACKGROUND AND SIGNIFICANCE

A. The Discovery of Uroguanylin (Ugn) and Prouroguanylin (proUgn), and Their Hypothesized Participation in Sodium Homeostasis

Guanylin, Uroguanylin and their Enteric Receptor, Guanylyl Cyclase-C.

Guanylin (Gn) and uroguanylin (Ugn) are structurally related peptides that are produced in the gastrointestinal tract (40, 82, 113, 179). The discovery of these intestinal peptides was preceded by the cloning of their putative receptor, receptor guanylyl cyclase type C (GC-C), from an intestinal cDNA library (92). Ligand activation of GC-C leads to the synthesis of the second messenger cGMP, which affects transport of water and electrolytes across epithelial monolayers (61). GC-C was originally described as an orphan receptor, identified by cloning on the basis of its sequence homology with other members of the family of receptor guanylyl cyclases, including GC-A, the receptor for atrial natriuretic peptide (ANP), and GC-B, the receptor for C-type natriuretic peptide (CNP) (60, 104, 166). The initial cloning study showed that GC-C is highly expressed in the intestine (166) and that it serves as the receptor for a bacterial toxin (STa) that causes diarrheal disease (54, 188, 166). Although at the time there was no known endogenous ligand for GC-C, it was presumed that there would be one; otherwise, evolutionary pressure would have eliminated the receptor along with the lethal mechanism that it initiates.

Based on this presumption, intestinal extracts were screened for agents that induce cGMP production by GC-C (99). Active molecules were identified on the basis of their ability to elevate cyclic GMP levels in T-84 cells, a human colon carcinoma-derived cell line that expresses very high levels of GC-C (182). Using this assay, guanylin (Gn) was purified from extracts of the jejunum of rats, and identified

as a ligand for GC-C (40, 61). Subsequently, Ugn was found in the urine of possums (*Didelphis virginiana*)(83), rats (84), rabbits (55) and humans (99) using the same T-84 cell assay screening technique, and was subsequently shown to be produced in the intestine (82, 113, 116). Though 15 amino acid Ugn was the first form of the protein identified in the urine of opossum, the form shown to be produced and stored in the intestine is predominantly an 86 amino acid propeptide, prouroguanylin (proUgn)(82, 113).

The Concept of an Entero-Renal Endocrine Link

An entero-renal endocrine link was proposed by Robert Carey in the 70's based on experiments showing faster urinary excretion of sodium (Na^+) in response to an oral versus an intravenous salt load (19). In humans, dogs and rabbits, he subsequently showed that an oral NaCl load induced greater Na^+ excretion at comparable time points than did an equimolar salt load injected into the blood (19, 21, 111, 112).

The implication of these experiments is that the GI tract sends a signal to the kidney to indicate that intestinal Na^+ absorption is imminent and renal Na^+ excretion is necessary to maintain homeostasis (see figure 1.1). The slower time course of Na+ excretion in response to intravenous NaCl implies that there is a luminal sensing mechanism in the gut. This signal could be conveyed by either a humoral factor or by a neural signal. The component of Na^+ excretion that is dependent on oral intake is sometimes referred to as post-prandial natriuresis (64, 185). proUgn is a plausible candidate for mediating the post-prandial response, because it is

produced in an organ where such a signal could originate (the small intestine), has the ability to regulate epithelial electrolyte transport, and is present in the urine (indicating that it has access to the lumen of the nephron, a relevant target tissue for homeostatic regulation of Na^+ excretion).

B. Sodium and Volume Homeostasis

Volume and Sodium Homeostasis is a Crucial Biological Function with a Complex Regulatory System.

Sodium is a major determinant of extracellular fluid (ECF) osmolality and volume. Therefore, controlling Na^+ balance is essential for maintaining ECF volume homeostasis (70). ECF volume in the vascular system is a determinant of pressure in both the arterial and venous circulations (12, 175). Fluid and Na^+ levels in mammals must be tightly regulated to ensure proper biological functions as diverse as neural signaling and membrane transport (12). Dysregulation of water and Na^+ can result in pathologies such as hypertension, cardiac arrhythmia, and stroke (12, 124). Alternatively, underlying pathological conditions like heart and kidney failure can be the cause of such dysregulation (4, 115). Understanding the complex interrelationship between volume-regulatory mechanisms and disease is critical for improving clinical care for many pathological states.

Control mechanisms for fluid and Na^+ homeostasis typically detect fluctuations in plasma osmolality, blood pressure and atrial stretch, which serve as feedback signals for systems that adjust renal Na^+ excretion to match dietary Na^+ intake (121, 147). Some of the better-described mechanisms include anti-diuretic hormone (ADH), atrial natriuretic peptides (ANP and BNP), the sympathetic nervous

system (SNS), and the renin-angiotensin-aldosterone system (RAAS)(6, 10, 11, 12, 15, 37, 79, 98, 133, 158). Additionally, an autoregulatory system controls renal blood flow, and this has critically important effects on Na^+ retention and ECF volume (121, 175).

The Natriuretic Peptides

The natriuretic peptides ANP and BNP signal through guanylyl cyclases to affect Na^+ excretion by the kidney (15, 28, 122, 123). ANP is a 28-amino acid peptide produced and secreted by atrial myocytes in response to atrial distension (15). BNP, named because it was first discovered in the brain, is a 32-amino acid peptide also synthesized and secreted from the heart in response to stretch, mainly from the ventricles (12). Along with ANP, BNP is thought to induce natriuresis through Guanylyl Cyclase type-A (GC-A) in the kidney (28, 47).

Urodilatin is an alternate cleavage product of proANP produced selectively by the kidney (72, 183). Urodilatin was once thought to be involved in post-prandial natriuresis but is now generally believed to play a role as a feedback mediator that responds to expanded blood volume (90).

The Renin Angiotensin Aldosterone System (RAAS)

The RAAS provides critical control over Na^+ and fluid retention (37, 80, 88, 90). This hormone cascade is initiated by the release of renin into the blood stream from the cells of the juxtaglomerular apparatus of the kidney (11, 88, 90). This can be in response to baroreceptor stretch, SNS nerve activity or NaCl concentration

within the lumen of the nephron (88, 133). This initiates a sequence of catalytic events culminating in increased plasma angiotensin II (Ang II) and aldosterone (26, 31). Ang II is a potent regulator of general vascular tone, renal blood flow, glomerular filtration rate (GFR) and Na^+ reabsorption in the tubules (133, 158).

Aldosterone is mineralocorticoid that is produced in the adrenal gland (12). Production and release of aldosterone is stimulated by increases in plasma Ang II or plasma potassium (K^+) (6). Aldosterone acts in the distal tubule and collecting ducts to up-regulate and activate ion channels and pumps that promote Na^+ retention and K^+ excretion.

Other Sodium Homeostatic Feedback Mechanisms

The Sympathetic nervous system (SNS) modulates renal Na+ handling in multiple ways. Neurons terminate at various sites within the nephron to regulate renal blood flow, tubular Na^+ reabsorption and renin secretion (11). Under conditions of low SNS activation, Na^+ reabsorption increases and, as a result, the blood volume expands (6). At more intense activation of the SNS, through the effects of the SNS on Ang II and norepinephrine, there is a further modulation of vasoconstriction and renal blood flow (6, 98).

Anti-diuretic hormone (ADH, also referred to as Vasopressin) is a 9 amino acid peptide that is synthesized in the hypothalamus and stored and released from the pituitary gland in response to decreases in plasma osmolality (10). ADH acts in the distal tubule and collecting ducts to increase membrane permeability to H_2O via aquaporin-2 and thus promote renal retention of fluid and electrolytes (184).

Nitric oxide, prostaglandins, reactive oxygen species and other paracrine agents work in the kidney to alter GFR, ion transport, and water transport (70, 175). These agents act in various parts of the nephron to adjust renal Na^+ handling through mechanisms that affect renal vascular tone, ion transporters and channels, and renin secretion (175).

In general, these systems require a change of some physiological parameter that is affected by Na^+ in order to trigger a feedback loop. Such feedback systems can take many hours or days to accurately match Na^+ intake with excretion (80, 175). For this reason, the concept that the kidney (the body's salt excreting organ) and the intestine (the body's salt absorbing organ) could be linked by a rapid endocrine axis that helps to balance uptake and excretion over short time frames is attractive. The guanylin family of peptides, acting through a member of the receptor-guanylate cyclase family that mediates responses to other natriuretic peptides, are thought to play key roles in rapid fluid and Na^+ homeostasis, but their mechanisms are not clearly defined (60, 62, 73, 103).

C. The Guanylin family of Peptides, Regulators of Volume Homeostasis?

A Conserved Structure Among Family Members Based on Disulfide Bonds

Three mammalian peptides share the ability to stimulate GC-C-mediated catalysis of cGMP: Guanylin, Uroguanylin and Lymphoguanylin (Lgn)(64, 103, 113). In most mammals all three peptides have a high level of sequence homology with Ugn, being 55% homologous with Gn, and 80% homologous with Lgn. However, Lgn is only found in opossums (62, 64, 99). Additionally, GC-C can be stimulated by a

similar peptide, renoguanylin (Rgn), found in teleosts (190) and also the family of heat-stable bacterial toxin (STa) peptides (3, 35). All of these peptides share a common feature: they are cysteine rich and contain specific disulfide bonds (Figure 1.2). Gn, Ugn and Rgn contain 4 cysteines that form two specific disulfide bonds (1-3 and 2-4) but Lgn only has 3 cysteines and one disulfide bond (60, 64). The STa family has two additional cysteines forming a third disulfide bond, which stabilizes the molecule, but the cysteines homologous to those in Ugn and Gn still adopt the same 1-3 2-4 configuration (73). These specific disulfide configurations (1-3, 2-4) are required for potent activation of GC-C leading to the synthesis of the second messenger cGMP.

Lgn is unique not only for containing only 3 cysteines but also in that it has only ever been found as a transcript. No one to date reports finding this as an endogenous peptide, and the transcript has only been found in opossum, with no identified mammalian ortholog (64, 113). It is named for the fact that the expression has been noted most highly in opossum lymphoid tissue, with lesser amounts in testis, spleen and heart (64). Synthetic Lgn is able to fully activate GC-C; however, its potency is much lower than that of Ugn or Gn at any pH (64).

STa Activation of GC-C Induces Diarrhea

As described above, the first identified ligand for GC-C was the heat stable peptide produced by entero-toxigenic *E. coli*. This peptide can have 18 or more amino acids, depending on the strain but the 5 most common strains (2 human, 2 porcine and 1 bovine) all have 18 residues (3, 36, 46). The toxins have high

structural homology between strains, especially 6 key cysteine residues that are perfectly conserved between strains, including the 3 specific disulfide bonds they form (36). Two of these disulfide bonds (1-4 and 3-5) are required for GC-C activation (figure 1.2) (3). This enterotoxin is the secretagogue that is responsible for traveler's diarrhea, a condition that is still a prominent cause of mortality in underdeveloped countries, particularly in children under the age of 5 (3). It is through GC-C activation that STa induces the bulk movement electrolytes and water into the lumen of the colon to cause the rapid expulsion of enteric contents and allow the bacteria to colonize a new host. High mortality in children would constitute a special evolutionary burden. Thus, the high conservation of sequence in GC-C and the guanylin family of peptides, and the preservation of the genes that encode these polypeptides across a large number of mammalian species, implies an important function.

Guanylin

Guanylin is synthesized and stored as a 115 amino acid propeptide (proGn), predominantly in the intestine (33, 40, 41, 51, 82). It is expressed in a rostral to caudal gradient, with peptide and mRNA levels being lowest (barely detectable) in the duodenum and highest in the colon (33, 51). ProGn is produced by goblet cells, which are also responsible for the production of mucin. It is therefore hypothesized that Gn plays a role in hydrating the mucosal layer (required for conversion of mucin to mucus) and additionally in maintaining fluidity of the luminal contents of the colon (3, 113, 150).

A major structural difference between Gn and Ugn is that Gn has an internal aromatic residue (phenylalanine or tyrosine, depending on the species) instead of the asparagine that is characteristic of Ugn. This aromatic residue affects the potency of Gn and makes it more susceptible to proteolytic cleavage (82, 101). Proteolytic susceptibility is probably the reason why Gn is not found in the urine, even though proGn is present in plasma and kidney extracts (33, 51, 82, 101). The aromatic residue generates a consensus cleavage site for a chymotrypsin-like endopeptidase located on the brush border of proximal tubules in the kidney. This leads to degradation of any filtered peptide, prevents it from accumulating in the urine, and reduces the chance of it having any renal effects (12, 82).

The binding of Gn to GC-C is pH dependent. The peptide has less ability to stimulate cGMP production at lower pHs (73, 159). At a pH of 8.0, Gn, and Ugn have almost the same ability to stimulate cGMP synthesis, but Gn is 100-fold less potent than Ugn at a pH of 5.0 (73). This lends additional credence to the theory that Gn plays a physiological role in the colon but not the kidney, as the pH in the lumen of the colon is basic while the pH in the lumen of the nephron is acidic (156, 190).

Renoguanylin and Uroguanylin Play a Role in Adaptation to Water Salinity in Teleost Fish

Rgn is a Ugn-like peptide discovered in the kidney of teleosts (35, 120, 190). Euryhaline teleost fish migrate between marine and freshwater environments, making them an interesting model for adaptation to oral Na^+ handling (180). These fish also express homologues of Gn and Ugn, with sequence similarity to the rat and human forms at the critical cysteine residues and the aromatic position in Gn, which

determines proteolytic susceptibility (190). A third peptide (Rgn) has 55% sequence similarity to Ugn and, notably, contains the same four cysteines, disulfide bridges and the internal asparagine residue that distinguishes it from Gn (190). The tissue expression of Ugn in the species is similar to that seen in mammals, but Rgn expression seems to be restricted to the intestine and the kidney, with highest levels in the latter—hence its name (190).

Interestingly, in experiments where fish are moved from a fresh-water to a salt-water milieu, renal Rgn expression doesn't change significantly but intestinal and renal Ugn expression both increase significantly (120, 180, 190), and the intestinal Rgn expression increases significantly in response to the alteration in water salinity. Both peptides increase in the tissues where their expressions are low (Rgn increases in the intestine, while Ugn increases in the kidney) which implies that the two peptide family members could be playing complementary roles in Na^+ handling. It has been hypothesized that as a consequence of these expression changes there is delayed enteric salt absorption (mediated by Rgn) and accelerated renal salt excretion (mediated by Ugn) (191).

D. Guanylyl Cyclase C

GC-C is A Member of the Family of Natriuretic Peptide Receptors

As detailed above, the natriuretic peptides play a role in the maintenance of Na^+ and volume homeostasis and their main mode of action is through the activation of receptors that belong to a family of receptor guanylyl cyclases (rGC). GC-A and GC-B are the best-described members of this family (27, 28, 79, 122). GC-C was discovered in 1990 through homology cloning, based on sequence similarities to

GC-A and GC-B, and was named C because it was the third family member discovered (164).

GC-C, like the other family members, has a ligand-binding extracellular domain (ECD), a single trans-membrane domain, an intracellular kinase-like regulatory domain and an intracellular catalytic guanylyl cyclase domain. Binding of ligands to the ECD leads to a conformational change that relieves an intramolecular inhibitory effect of the kinase-like domain and allows the catalytic domain to produce cGMP, which acts as a second messenger. The only known ligands for GC-C are the Guanylin family of peptides and the family of heat-stable bacterial toxin (STa) peptides (73, 165). STa is the most potent ligand when administered to T-84 cells, with a K_D for stimulation of cGMP production that is ~10 fold lower than that of Ugn-15 at pH 5.0 (71). The propeptides (proGn and proUgn) are unable to elicit cGMP production by GC-C (71, 82). Activity from these propeptides is only observed after processing to Gn or Ugn (47, 69, 82).

A feature that differentiates GC-C from the other members of the rGC family is a carboxy-terminal extension peptide (CTEP)(42, 167). This CTEP is believed to play a role in trafficking GC-C to the apical membrane of epithelial cells. When this domain is deleted, the receptor is no longer preferentially targeted to the apical membrane of polarized cells, and also no longer responds to Sta or the guanylin family peptides to produce cGMP (42).

In the intestine, GC-C activation and the subsequent increase in intracellular cGMP have three main effects: a) the cystic fibrosis transmembrane conductance regulator (CFTR) is phosphorylated through activation of a specific isoform of cGMP-

dependent protein kinase (PKG II), and this increases its chloride and bicarbonate conductance, b) cGMP inhibits a Na^+/H^+ exchanger (NHE3), perhaps through phosphorylation (though this is unclear, at present) (128); and c) bicarbonate/Cl- co-transporters are activated by an unknown mechanism (168). The combined effect of these three physiological alterations is to block Na^+ uptake from the lumen, promote chloride, bicarbonate, and Na^+ secretion into the lumen, and enhance the osmotic accumulation of water in the lumen. Further data suggest that GC-C activation also affects cell proliferation and apoptosis, from experiments both in cultured cells and in polyps from a mouse model of colon cancer (34, 110).

T-84 Cells are an Immortalized Cell Line that Produces cGMP

T-84 cells are intestinal epithelial cell line that is derived from a human colorectal adenocarcinoma. These cells are immortalized and express high levels of GC-C (45). T-84 cells in culture can be stimulated to produce cGMP in a concentration dependent manner by any of the known GC-C ligands (figure 1.3)(73). This is thought to occur exclusively through GC-C, as the cells neither express any of the other rGCs nor do they produce cGMP in response to other natriuretic peptides outside of the Guanylin Family of peptides (92, 163, and unpublished data of mine).

T-84 cells are useful as a reporter cell line, as they can be used to determine the amount of a Ugn-like peptide in a sample, based on the amount of cGMP they produce when the cells are exposed to the sample. Note, however, that multiple Gn-family peptides are active on these cells, so all samples must be analyzed biochemically (for example by reverse phase HPLC) to determine which peptide is

inducing the response. I used this assay extensively in my early studies as a way to measure Ugn-like peptides in tissue extracts and in plasma (Chapter 2). However, analysis of urine proved problematic for a number of reasons (described in detail in Chapter 3), necessitating the development and validation of a new assay that would work well for urine samples.

E. Prouroguanylin

Uroguanylin versus proUroguanylin

As with Gn, Ugn is first synthesized as a propeptide (86 amino acids) that is subject to proteolytic cleavage (82). 15 amino acid Ugn was the first form identified in the urine of the opossum, and other slightly longer, N-terminally extended forms of the peptide have subsequently been noted (81, 85). However, as I will show in Chapter 2, the predominant form stored in the intestine is actually the propeptide (99, 113). The propeptide is expressed in a rostro-caudal gradient, with highest levels in the duodenum and almost undetectable levels in the colon (113, 162).

One long standing difficulty in the Ugn field has been measuring (and discriminating) Ugn and proUgn in biochemical studies. This has stemmed from the techniques used to assay them. (a) The original method of detection was the T-84 cell bioassay (see figure 1.3), which relies on binding of the peptide to GC-C. ProUgn is unable to stimulate cGMP production by T-84 cells. Therefore, this method is specific to Ugn, and is unable to detect proUgn (82, 114). However, trypsin digestion converts proUgn to Ugn, which can then be measured in the T-84 cell assay. This proteolytic procedure has been used for an indirect assessment of

proUgn by several labs. However, the digestion introduces error to the results if it is not carefully controlled with respect to the stoichiometry of the proUgn-to-Ugn conversion, and the extent to which Ugn itself is degraded during the reaction (82, 1114). (b) A radioimmunoassay (RIA) was subsequently developed, utilizing an antibody directed against a peptide sequence that is common to both Ugn and proUgn. Because both molecules contain the epitope detected by the antibody, the assay cannot differentiate them (24, 139). The assay becomes specific for proUgn and/or Ugn only if it is coupled with an HPLC fractionation that separates the two molecules. However, this labor-intensive method is seldom employed, and many published papers therefore report “Ugn-like immunoreactivity”, without being able to discriminate Ugn from proUgn. (c) When I began my project, one of the first things I did was to help generate a proUgn-specific assay, based on an antibody that is selective for proUgn over Ugn. This assay (described in detail in Chapter 2) uses an electrophoretic Western blot method to separate proUgn from Ugn. (d) I also developed a quantitative binding assay that can be used to measure Ugn without responding to proUgn (Chapter 3). This binding assay has several major advantages over the T-84 cell bioassay: it is much faster to perform, it is more sensitive by a factor of ~100-fold, and it is less sensitive to interference from other constituents of urine or tissue extracts.

Western and Northern blot studies have shown that proUgn expression is limited almost exclusively to the alimentary tract and the kidney (figure 1.4) (134). Using the assay methods described above, I quantitatively analyzed the levels of proUgn and Ugn in these tissues, and in plasma. As will be shown in Chapter 2, I

determined that very little processing of proUgn takes place within tissues. I also demonstrated that intact proUgn circulates at relatively high levels in plasma, whereas levels of circulating Ugn are below the detection limit of my most sensitive assay. Using radiolabeled recombinant proUgn, I also showed that the propeptide circulates intact, and is only converted to Ugn within the renal tubules after filtration at the glomerulus. This is distinct from other typical endocrine axes where the prohormone is processed to the mature peptide at the site of synthesis, and is delivered to the target in active form. This has led me to propose that proUgn is the circulating “endocrine” agent that carries information from the intestine to the kidney.

proUgn Expression in Humans and Rats

Ugn was identified as a 15 amino acid sequence in opossums, but was next found as a 16 amino acid peptide in the urine of humans, with an additional leucine attached at the carboxyl terminus (99). It was subsequently found in the urine of rats in both 15 and 18 amino acid N-terminally extended forms (99). An additional species found by RP-HPLC of human plasma contained 24 amino acids, corresponding to the originally described 16 residue species with an 8 extension at the N-terminus (85).

In 1996, a few years after Ugn’s discovery, a group in Japan observed the existence of two different topological isomers while attempting to synthesize the human 16 amino acid sequence (29). When carefully constructing the peptide with its disulfide bridges in the correct linkage, they found that the order of establishing these linkages would create two distinct species, differentiated by RP-HPLC fractionation (29, 87). The two peptide isomers, named hUgn-A and hUgn-B, also

differed in their ability to stimulate T-84 cells to produce cGMP, with the A conformer being a potent activator and the B conformer being ~100-fold less potent (29, 135). Further analysis revealed that the additional leucine present at the carboxyl terminus of the human form is responsible for steric hindrance to interconversion between these two isomers, allowing them to be isolated as independent species (87). It was later shown that the two human Ugn isomers do transition back and forth, with a half-life of ~2 days. The rat, mouse and opossum forms of Ugn, as well as Gn species (all of which lack the C-terminal leucine), make this transition at a rate of 1 to 2 cycles per second at 37 ° and pH 7.0, making them a racemic mix (87).

Dr. Nicholas Moss in our lab showed that both peptides have effects on the rat kidney, despite h-Ugn-Bs lack of ability to stimulate T-84 cells. However, there is a difference in the natriuresis seen, both in its intensity and its temporal characteristics (135). The B isomer causes greater Na^+ excretion, more rapidly and at a lower dose than does the A isomer (135).

Physiological and Genetic Evidence that Ugn and proUgn Participate in Na^+ Homeostasis

The effects of Ugn and proUgn on the kidney have been studied both in vivo in rats and mice and in isolated perfused rat kidneys. Using an a technique known as the sealed-mouse renal function assay, dose dependent increases in UK^+v, UNa^+v and urine volume were seen when Ugn was infused intravenously (23). Ugn infused into an isolated perfused kidney elicited diuresis, natriuresis and an increase in GFR (57, 76, 139, 186). In whole animals, a limited number of experiments have

shown that when proUgn is infused, there is an increase in Na^+ excretion and urine volume but no change in GFR or UK^+v (76, 136).

The generation of a Ugn knockout mouse by Dr. Mitchell Cohen's group at University of Cincinnati was a major step forward in the investigation of proUgn as the agent responsible for post-prandial natriuresis (118). These mice were developed by substitution of a neomycin resistance gene cassette in for the first exon of the Ugn gene in embryonic stem cells, creating a whole animal knockout. Analysis by both Northern and Western blot showed that neither proUgn protein nor mRNA was present in any of the tissues that are normally positive for Ugn expression in wild type animals.

The baseline phenotype of these animals was relatively normal: animals were viable through adulthood, of a similar body weight to wildtype animals, and capable of reproducing normally. However they did have hypertension, as their mean arterial pressure (MAP) was significantly elevated relative to Ugn+/+ animals. The MAP was not sensitive to the level of salt in the diet: both mutant and wild type animals showed only small changes in MAP in response to large changes in the NaCl content of the food (0.01% vs. 1% vs. 5%), and the small responses of the mutants were indistinguishable from those of the wild type strain (118).

Another prominent defect in these animals is their impaired ability to excrete an acute oral Na^+ load. When challenged with a bolus of NaCl (300mmol) administered by gastric gavage, the Ugn-/- mice showed significantly less cumulative Na^+ excretion than wild-type animals at every time point after 20 min (Figure 1.5, (118)). In contrast, when the same bolus of NaCl was administered

intravenously, mutant and wild type animals excreted it at the same rate (data not shown). In an extension of these studies, the same group analyzed the longer-term effects of changes in oral NaCl in conscious animals (50). Animals were housed in metabolic cages and dietary Na^+ in the chow was switched from 1% NaCl to 5%NaCl. In these circumstances, daily cumulative urinary Na+ excretion over the first 48 hours was significantly higher in the Ugn+/+ mice compared to Ugn-/- animals (Figure 1.5 and reference (50)). By the third 24-hour collection, however, the mutant animals had caught up to the wild type animals. There was no longer a significant difference in Na+ excretion, and both strains were once again balanced with respect to intake and excretion.

The data from these knockout studies support the hypothesis that Ugn and/or proUgn play a role in the handling of oral Na^+ (as suggested by the transient defect in Na^+ balance displayed by the Ugn knockout animals during a diet shift), as well as a potentially distinct role in overall Na^+ homeostasis (as suggested by the chronic hypertension exhibited by these animals that is independent of their level of oral Na+ intake). That the animals' hypertension is not salt sensitive is perhaps not surprising, given that numerous long term Na^+ homeostasis mechanisms remain intact and could come into play during prolonged shifts in Na^+ intake. What is significant is that animals lacking the Ugn-dependent mechanism have impaired Na^+ excretion over the first two days after a switch to high salt, the critical period where other homeostatic control mechanisms have not yet come into balance.

GC-C Knock Out Animals are Still Renally Responsive to Ugn

As described above, GC-C is a member of the group of natriuretic peptide receptors, several of whose other members are highly expressed in the kidney of mammals and play roles in Na^+ regulation. Two different groups have developed GC-C knockout mice, and, as expected, they have lost the intestinal response to STa (127, 166). However, these mice have no overt Na^+-handling phenotype (50), are viable and can reproduce normally.

When Gn and Ugn were infused into GC-C -/- mice, the animals showed a time and dose dependent increase in renal Na^+ excretion that was similar to responses observed in wild type mice (22, 23). Additionally, these renal effects of Ugn appeared to be independent of cGMP as its levels in urine were unchanged during the infusions (50). Related studies in principal cells isolated from human kidneys showed a depolarization in response to Ugn that was independent of GC-C, as no GC-C transcript was detected in these cells by rtPCR (22, 168). These types of studies have provided strong evidence that GC-C is not the only renal receptor for Ugn, and—potentially—may not play any role at all in mediating renal responses to the peptide.

An Alternative Receptor to GC-C May Play These Extra-Intestinal Roles

In light of an absence of a requirement for GC-C in the kidneys for renal effects of Ugn on volume homeostasis, there must be an alternate, cGMP-independent receptor. Several groups have suggested that this renal receptor for Ugn is a pertussis toxin-sensitive G protein (74).

Opossums are again unique from other mammals in that they express an alternate rGC that is stimulated by the guanylin-family of peptides (46). This rGC (termed OK-GC) has ~75% sequence homology to GC-C (117) and is expressed in the digestive, renal, central nervous, reproductive, and immune/lymphoid systems of the opossum (117). No homolog to OK-GC has been found in humans, rats or mice. As opossums are marsupials (in contrast to all other species studied), and are the only known species to express Lgn, these unique features could be related to their unusual reproductive scheme (139).

Pathological States that Result in Changes in Ugn and proUgn

Congestive heart failure (CHF) is a disease state in which compromised cardiac function results in pathological fluid retention (50). In patients with severe CHF, urinary Ugn (24 hour total excretion) is elevated as much as 70 fold over healthy control individuals (24, 141). Based on these results, Ugn could participate in a protective mechanism contributing to reduce blood volume and pressure (24).

Studies on a rat model of nephrotic syndrome revealed elevated levels of urinary Ugn-like activity, which might be expected as the filtration barrier in the kidney is compromised (93). These animals also have a four-fold increase in plasma Ugn immunoreactivity, but the assay used was unable to discriminate between the Ugn and proUgn peptides. Multiple studies have seen similar elevated urinary Ugn-like peptides and plasma proUgn in humans with various forms of renal disease (68, 140).

Differences in proUgn related peptides in tissue compartments involved in Na^+ handling during these different disease conditions suggest that the peptides might play a role in Na^+ homeostasis during pathological states, in addition to their proposed roles under normal physiological conditions. This might allow for proUgn or its metabolites to serve as indicators of disease severity, and (perhaps) as the starting point for the design of therapeutic agents to ameliorate the pathological symptoms in these diseases.

Changes in Ugn and proUgn Expression and/or Secretion Evoked by Orogastric Sodium Loading

Studies in rats, humans and mice have evaluated the effects of dietary Na^+ on Ugn expression (24, 25, 50, 95, 100, 152). These data are summarized in table 1, showing the species, the tissue analyzed and the changes seen. In summary, the studies report no significant change in enteric Ugn expression in response to a high salt stimulus, but some change in renal Ugn expression and a much more significant change in urinary Ugn excretion.

All of these studies lack adequate temporal analysis of changes in Ugn or proUgn levels (either at the mRNA or polypeptide level) following the dietary intervention. In particular, all published studies all focus on late time points following a diet shift (after animals have reestablished an equilibrium between Na^+ intake and Na^+ excretion), whereas the documented defects in Na^+ excretion in the Ugn (-/-) animals occur at early time points presumably before equilibrium has been attained (see figure 1.6 and reference 118). Additionally, some of the studies utilize the RIA assay described above that is not specific for Ugn over proUgn, thus limiting our

ability to discern the essential signaling mechanisms (24, 95, 110, 152). Further studies with better time resolution of sample analysis at critical points in the diet intervention are required to more definitively resolve the role played by Ugn or proUgn in Na^+ homeostasis. This is the major objective of my studies reported in Chapter 4.

F. Hypothesis and Aims

Uroguanylin or Prouroguanylin as an Endocrine Agent?

My dissertation work has addressed four central issues in the Ugn field. (1) It was known that the majority of the proUgn in the body is produced by the intestine, but the conversion of this enteric pool of proUgn to Ugn had never been investigated. Does it occur within the gut itself, within the circulatory system, or within the renal tubules? (2) Some proUgn is also found within the kidney. Is any portion of this intrarenal pool of proUgn processed and stored as Ugn? (3) Does the intestine signal to the kidney through a Ugn-based endocrine axis? In other words, is Ugn (or proUgn) released into the plasma from the gut? Does this circulating peptide account for some or all of the Ugn found in urine? (4) Is the Ugn signaling pathway turned on or off by changes in oral salt intake? In other words, do plasma and/or urinary levels of Ugn or proUgn change in an appropriate way and over an appropriate time frame in response to changes in oral salt intake? The proposed studies to answer these questions serve as critical tests of the hypothesis that Ugn and proUgn participate in an endocrine signaling axis that is mobilized by orogastric

salt intake. I have used biochemical analysis and physiological interventions to address these questions. My studies are divided into three specific aims, as follows.

Aim 1

The objective of Aim 1 was to define the amounts of proUgn and Ugn in the tissue compartments relevant to post-prandial natriuresis. My studies addressed (a) intestinal presence and processing of proUgn; (b) plasma presence and processing of proUgn; and (c) renal presence and processing of proUgn. Direct measurements of peptide levels were coupled with infusion studies that introduced radiolabeled proUgn into the circulation to determine where processing takes place and into what metabolites. These studies are described in Chapter 2.

Aim 2

The objective of Aim 2 was to develop assays that reliably measure proUgn and Ugn independently and with adequate sensitivity in biological samples. A new Western blot-based assay for proUgn is described in Chapter 2. A new assay was developed for Ugn by adapting and validating a commonly used method of competitive receptor binding with a radioligand, as described in Chapter 3.

Aim 3

The objective of Aim 3a was to investigate the relationship between the amount of Na^+ in the diet and the levels of proUgn transcript, proUgn polypeptide and Ugn polypeptide in relevant tissue compartments. This was accomplished by placing animals in metabolic cages and adjusting the amount of Na^+ in their chow, then determining the effects of these manipulations on protein and mRNA levels. The objective of Aim 3b was to investigate whether there is a product-precursor relationship between plasma proUgn and urinary Ugn. These studies are described

in Chapter 2 (vascular infusion of radiolabeled proUgn followed by HPLC analysis of radiolabeled urinary metabolites) and Chapter 4 (vascular infusion of unlabeled proUgn followed by direct measurement of urinary Ugn levels).

Tables

Paper	Animal	Tissue	Protein/mRNA (detection method)	Diet condition	Increase/decrease
Fukae, et.al. 2002 (24)	Rat	Urine	Protein (Non-Specific RIA)	7 day Low (.08% NaCl)	425(HS) vs 128(LS) pmol/day
		Plasma	Protein (Non-Specific RIA)	7 day High (4% NaCl)	No Diff.
		Kidney	RNA (rtPCR)		0.77 (HS) vs 0.32 (LS) UGn/ß-Actin
		SI	RNA (Northern Blot)		7.04 (HS) vs 5.15 (LS) UGn/GAPDH
Carrithers, et.al. 2002 (25)	Rat	Duodenum Jejunum Ileum Colon Kidney	RNA (rtPCR)	4 day Normal (.6% NaCl) compared to 4 day Low (.06% NaCl)	Duo -52% Jej -27% Ile -20% Col -8% Kid No Diff.
				4 day Normal (.6% NaCl) compared to 4 day High (7% NaCl)	Duo No Diff. Jej +5% Ile No Diff. Col No Diff. Kid No Diff.
Kita, et.al. 1999 (100)	Rat	SI (perfused)	Luminal Protein (Non-Specific RIA)	Anesthetized animals intestine was perfused with different molar Na+ solutions	Minor increase (insignificant) at the highest NaCl infusion
Potthast, et.al. 2001 (152)	Mouse	Kidney	RNA (rtPCR)	3 day Normal (.6% NaCl)	No Diff.
				3 day Low (.06% NaCl)	No Diff.
				3 day High (7% NaCl)	No Diff.
				3 day High (1% NaCl H_2O)	75% increase
Elitsur, et.al. 2006 (50)	Mouse	Plasma	proUgn (WB Ab6910)	1% NaCl 1st 3 days then switch to 5% next 3 days	Day 2 No Diff.
					Day 4 low (-40%)
					Day 6 No Diff.
Kinoshita, et.al. 1997 (95)	Human	Urine	Protein (Non-Specific RIA)	Low 7 g/day	95 pmol/day
				High 10g/day	143 pmol/day

Table 1.1 Details from experiments analyzing effects of altered oral Na^+ intake on Ugn and/or proUgn levels in tissues, urine, or plasma. Entries highlighted in light gray were performed with an assay that cannot discriminate Ugn from proUgn.

Figures

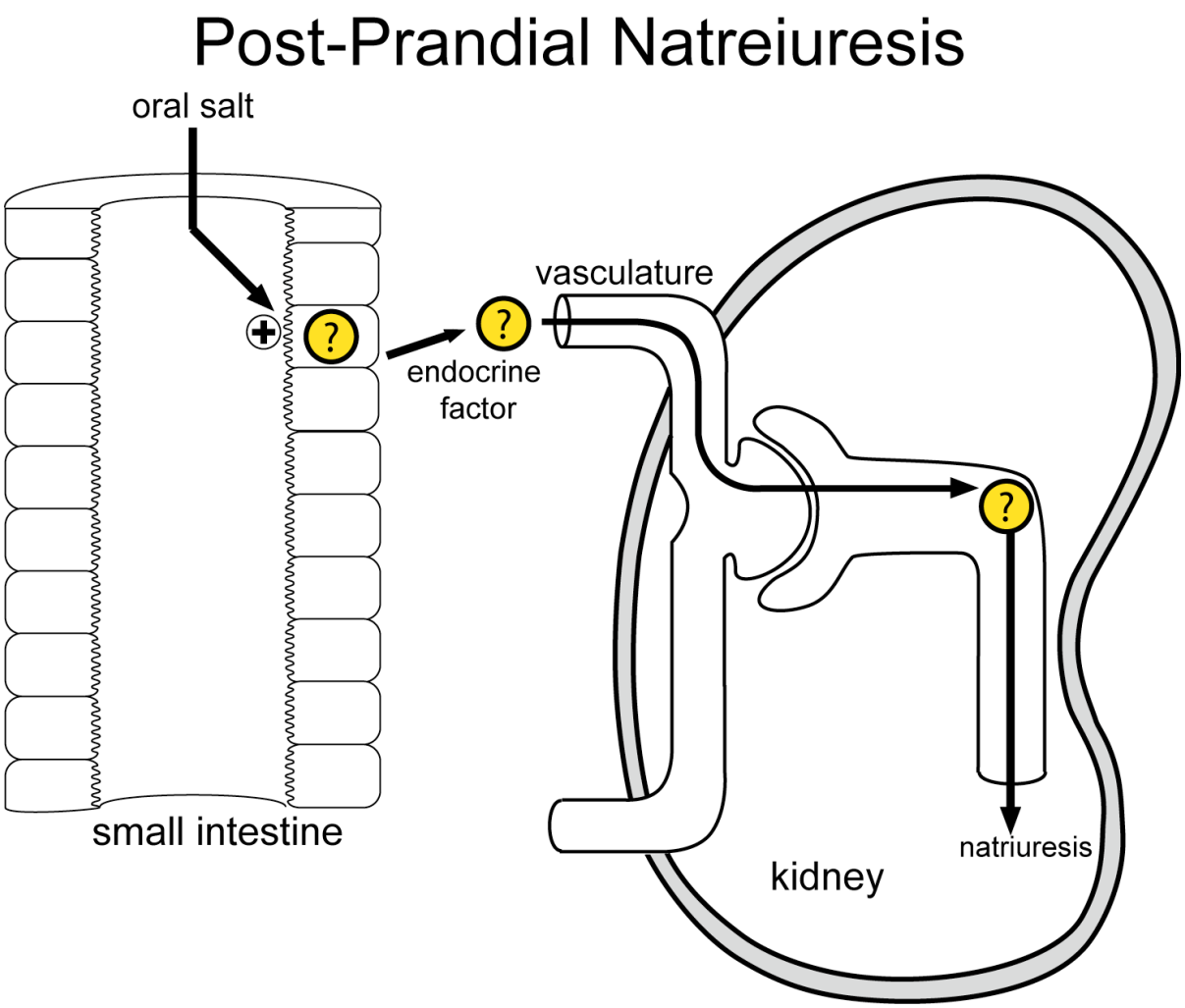

Figure 1.1 Model of Post Prandial Natriuresis Orogastic Na^+ enters the intestine where a undefined sensing mechanism in turn releases a natriuretic endocrine factor into the circulation. It travels via the circulation to the kidney where it is filtered at the glomerulus and has effects on Na^+ excretion in order to maintain balance with the enteric lumenal Na^+ load that is being adsorbed.

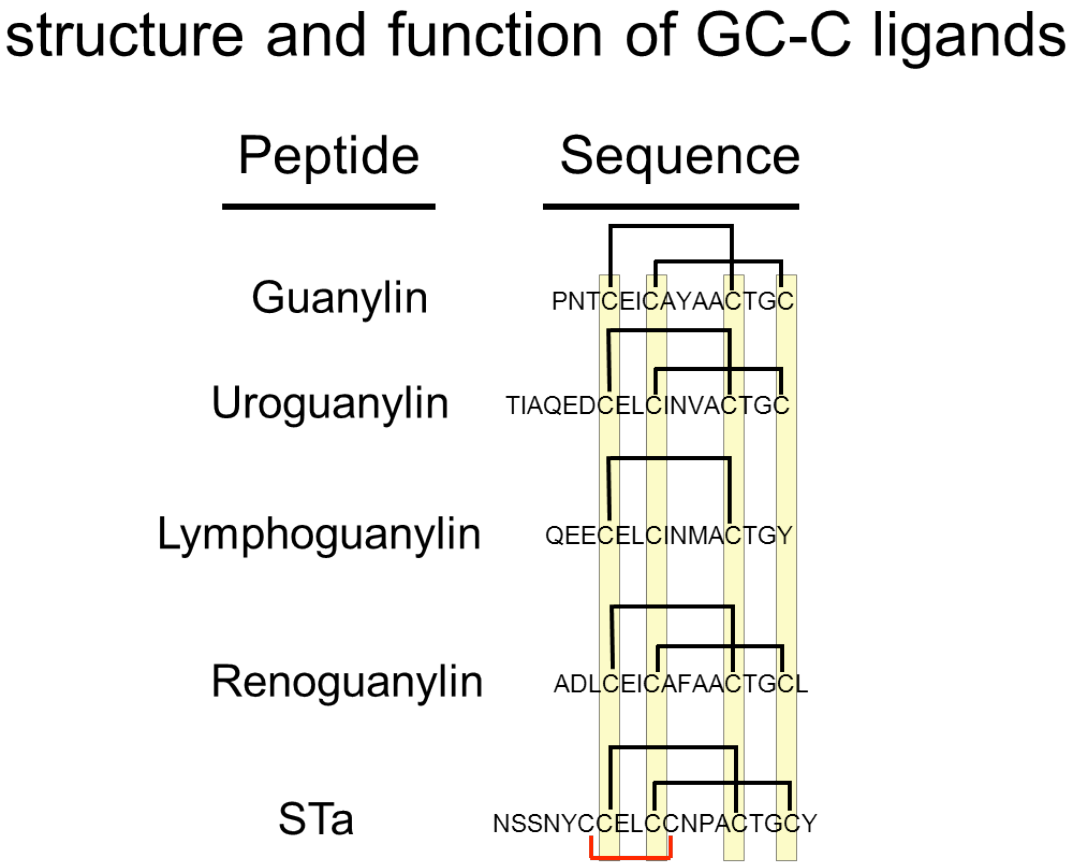

Figure 1.2 Structure of guanylin-family of peptides and the E. Coli enterotoxin Sta Conserved cysteine residues are highlighted in Yellow and shared disulfide bonds are marked with black lines. Additional cysteines and disulfide bond unique to STa is denoted with red lines.

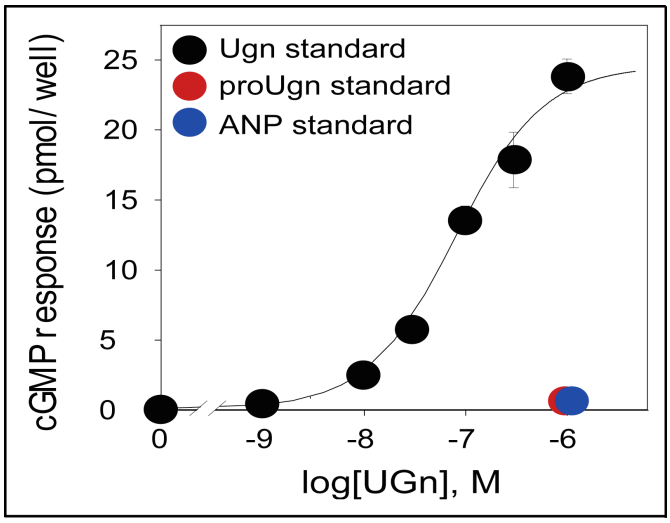

Figure 1.3. T-84 Cell Assay for detection of Ugn. Standard curve showing the concentration response relationship between Ugn administered to T-84 cells and cGMP production in response, to a dilution series of recombinant rat Ugn standard (black circles and line). Blue dot indicates the response from ANP, which potently activates GC-A. Red dot indicates the response from proUgn, which requires processing to activate GC-C.

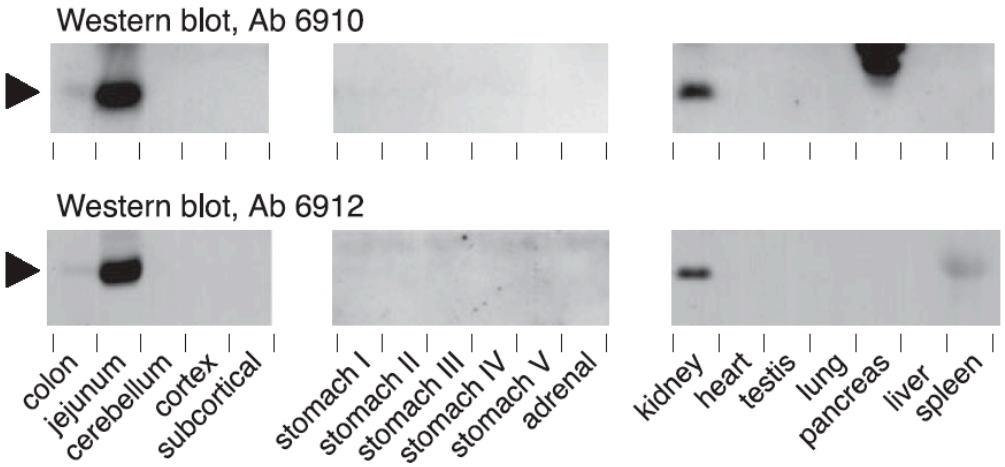

Figure 1.4. Western blot analysis of proUgn expression in a variety of tissues. Brain was divided into three regions: cerebellum, cortex, and subcortex (all of the structures within the forebrain that lie beneath the cortex). Stomach was cut into five approximately equal portions to provide rostral, intermediate, and caudal samples (labeled I–V). Other tissues were removed intact, and extracts were made from the whole organ. Comparable aliquots (60µg protein) from each tissue were tested with two different antibodies (6910 and 6912). The position of the proUgn band is marked by the black arrowheads. Polypeptides in the pancreas and spleen that are detected by only one of the two antibodies cannot represent authentic proUgn, and most likely represent molecules that contain cross-reacting epitopes.

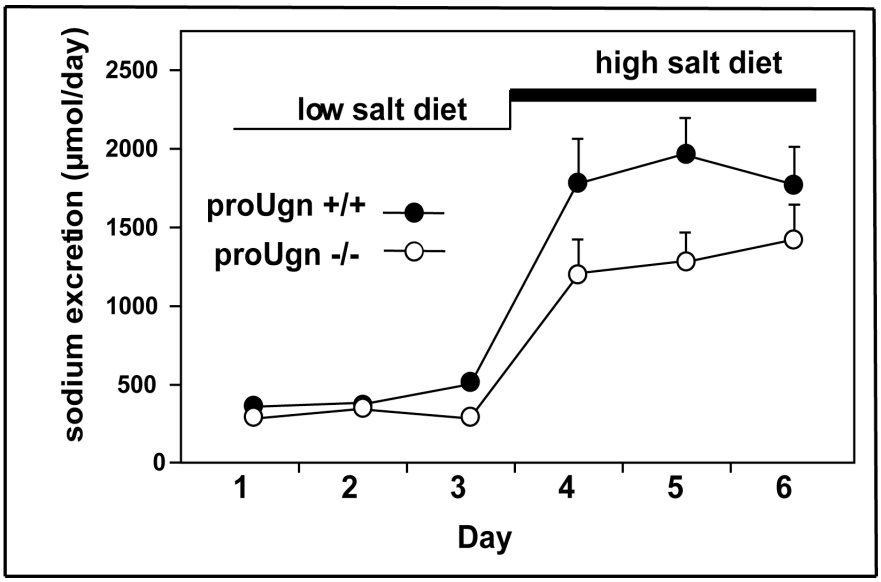

Figure 1.5 Ugn -/- Animal Chronic Response to Oral Salt Data taken from studies performed by Elitsur et.al. 2006 (50). White symbols indicate Na^+ excretion from proUgn knockout mice. Black symbols indicate Na^+ excretion from wild-type mice. The shaded pink area between the curves highlights the time when Na^+ excretion differs between strains in the study.

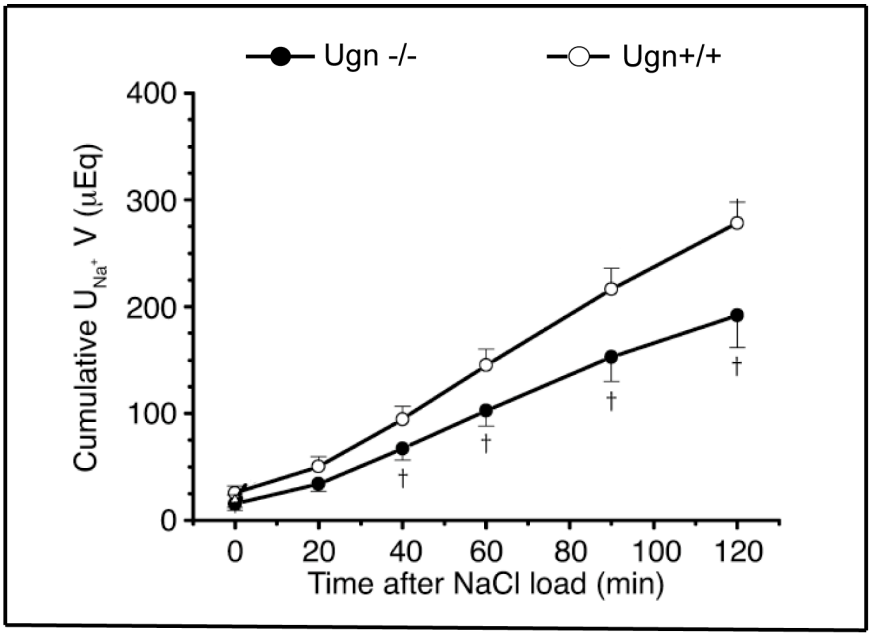

Figure 1.6 Ugn -/- Animal Acute Response to Oral Salt Cumulative Na+ excretion (UNa+V) before and after NaCl administration. Number of animals in each group is shown in parentheses. †P < 0.05 compared with the corresponding time point in the Ugn+/+ group. (Taken from Lorenz JN et.al. The Journal of Clinical Investigation 2003:112;8)(118)

CHAPTER II

Uroguanylin, an Intestinal Natriuretic Peptide, is Delivered to the Kidney as an Unprocessed Propeptide

Nicholas G. Moss*, Robert C. Fellner*, Xun Qian, Sharon J. Yu, Zhiping Li, Masamitsu Nakazato, and Michael F. Goy

And

Circulating Prouroguanylin is Processed to its Active Natriuretic Form Exclusively within the Renal Tubules

Xun Qian*, Nicholas G. Moss*, Robert C. Fellner*, and Michael F. Goy

*Denotes First Authorship, Order is Arbitrary.

Reprinted in part with permission from the Endocrine Society.

Endocrinology 149(9):4486-98, 2008.

and

Endocrinology 149(9):4499-4509, 2008.

A INTRODUCTION

An orally-delivered salt load is excreted faster than an equivalent intravenous salt load (19, 21, 112, 174). Although the mechanisms underlying this "postprandial natriuresis" are not fully understood, an intestinal peptide known as uroguanylin (Ugn) has been identified as a likely participant (63, 65). Perhaps the strongest evidence for this comes from genetic ablation of the uroguanylin gene in mice, which produces chronic hypertension and significantly retards urinary Na^+ excretion after an oral Na^+ load (50, 118). In addition, both Ugn and its propeptide precursor, prouroguanylin (proUgn), circulate in the plasma (53, 85, 95), and—when plasma levels are raised by intravenous infusion of exogenous Ugn—the rate of urinary salt excretion increases (23, 56, 65). Furthermore, the principal site of Ugn expression in the rat intestine is the enterochromaffin (EC) cell (39, 139, 150), an intestinal endocrine cell long known to secrete amines and peptides into the interstitium, and thence into the general circulation (59, 144). Ugn gene expression is regulated in these cells by orally administered salt in the intestine of the intact rat (25), and is also regulated by extracellular hypertonicity in an intestinally derived epithelial cell line (177). Taken together, these observations are consistent with the hypothesis that Ugn functions as the endocrine mediator of an entero-renal hormonal axis that regulates urinary Na^+ excretion in response to dietary Na^+ intake.

To meet the requirements of this hypothesis, however, the renal natriuretic response must be initiated by Ugn that originates from within the intestine. Somewhat surprisingly, this fundamental principle has not yet been established.

Although Northern blot studies have shown that the small intestine is by far the major site for preprouroguanylin mRNA expression (53, 113, 132), detectable amounts of preprouroguanylin mRNA and/or immunoreactive Ugn-like polypeptides have been reported in a variety of other tissues, including the kidney itself, as well as the colon, heart, stomach, lung, pancreas, brain, testis, ovary, oviduct, epididymis, prostate, parotid gland, submandibular gland, nasal mucosa, and gall bladder (52, 53, 81, 89, 106, 107, 108, 110, 113, 124, 126, 132). One caveat to these studies is that the methods employed have either been indirect (RNA-based) or non-quantitative (immunocytochemical), and, where antibodies have been used, they have, for the most part, been unable to discriminate between Ugn and proUgn. Thus, the relative potential of each of these tissues to contribute to plasma pools of Ugn and proUgn remains undefined.

As a further complication, a proUgn-like polypeptide is readily detected in extracts of rat small intestine using standard Western blotting techniques (150, 153), but Ugn itself appears to be present in these extracts only at very low levels (132). Thus, if the intestine is the source of Ugn that is destined for the kidney, it is not clear when and where propeptide processing takes place. Moreover, the Ugn concentrations reported in plasma are also very low, relative to the levels that are required to induce physiological responses in the kidney. Thus, published plasma Ugn levels are in the femtomolar to picomolar range, depending on the species (67, 93, 140), whereas physiological thresholds for renal responses have been established in the nanomolar range by prolonged agonist infusions (56), or have

been based on a bolus injection procedure that produces very high doses of agonist over a very short (non-physiological) time course (22, 77). The “pharmacological” nature of the concentrations employed in these studies has been a source of concern, with respect to the putative endocrine role of Ugn.

To address these issues, we developed a new immunoassay that is specific for proUgn and does not cross-react with free Ugn. We used this assay to quantify proUgn levels in tissues and in plasma, and to determine the effects of gut ablation on the size of the plasma pool. We also measured Ugn levels in parallel, using a quantitative bioassay. Our results demonstrate that the dominant form of the peptide stored in the intestine and secreted into the plasma is proUgn rather than Ugn. To investigate the biological significance of this circulating pool of proUgn, we infused exogenous propeptide intravenously at a “physiological” concentration, and measured the subsequent effects on renal function. The prominent natriuresis evoked by this infusion suggests that some form of post-secretory processing of proUgn must occur, in order to convert the biologically inactive propeptide to its mature, bioactive form.

To investigate potential post-secretory processing mechanisms that could convert circulating proUgn to active metabolite(s), as well as the means by which the propeptide and/or its metabolites are cleared from the plasma, we infused animals intravenously with radiolabeled recombinant proUgn. HPLC analysis of tissue extracts, urine, and plasma from these animals has provided a clear picture of the

relevant mechanisms. Surprisingly, the data show that the propeptide remains in an intact state throughout its time in the circulation. This suggests that processing of circulating proUgn most likely occurs after the propeptide has been delivered to its target organ(s). Our data also reveal that one well-established target organ (the kidney) is able to effectively metabolize proUgn. The resulting peptides, which include Ugn and several other unidentified fragments, are retained within the nephrons and are eliminated in the urine. This is reminiscent of the proposed handling of proUgn in the intestine, where intraluminal digestive enzymes, such as chymotrypsin, are thought to rapidly convert luminally-secreted propeptide into active Ugn (106).

B. MATERIALS AND METHODS

Experimental Animals

Male Wistar or Sprague-Dawley rats (250 - 300 g) were purchased from Charles River Laboratories (Wilmington, MA) and maintained for several days on a 12 hour light/dark cycle in an AALAC-approved facility with continuously available veterinary care and uninterrupted access to water and standard rat chow. All experimental procedures were approved by the Institutional Animal Care and Use Committee at the University of North Carolina at Chapel Hill, and were carried out in accordance with the NIH Guide for the Care and Use of Laboratory Animals.

Bacterially-expressed proUgn Standard

We subcloned the cDNA sequence encoding proUgn into an expression plasmid (pMal-CM, New England Biolabs), downstream from the E. coli maltose binding protein with an intervening thrombin cleavage site. The insert was PCR-amplified from a previously-cloned preproUGn cDNA (23), with an Nde I restriction site added to the forward primer, (5'-CATATGGTCTACATCAAGTACCATGG-3'), and a Hind III restriction site added to the reverse primer (5'-AAGCTTTCAGCAGCCCGTAC-3'). The peptide encoded by the insert (Table 2.1, plasmid pMal-R) lacks the predicted 21 residue N-terminal signal peptide (7, 131), but contains 4 non-native residues that were added to the N terminus to generate the thrombin cleavage site. A similar construct was created using the same forward primer and a different reverse primer (5'-AAGCTTTCAGGTCCTCAAGGCCTTGA-3'), in which both the signal peptide and the last 17 amino acids at the proUgn C-terminus were deleted (Table 2.1, plasmid pMal-CD). The PCR products were ligated into linearized pMal-CM and introduced into E. coli strain DH5a. After single colony isolation and amplification in bacteria, the sequence and orientation of the inserts were confirmed.

Bacterially-expressed fusion proteins were affinity-purified on amylose beads (New England Biolabs, Ipswitch MA) as described by the manufacturer, and cleaved by incubation with thrombin-coated agarose beads (Sigma Chemical Company, St. Louis MO). After cleavage the polypeptide was purified by a two-step chromatographic procedure. Active fractions were again confirmed by Western blotting.

We used four methods to quantify the final yield of recombinant rat proUgn standard (R) after HPLC purification, obtaining comparable results in each case. The first method was by direct protein assay, using a commercially-supplied kit (BioRad, Hercules CA). In addition, we also used the silver stain method (SilverSNAP Stain Kit II, Pierce, Rockford, IL) to compare samples of R side-by-side with standard curves prepared from known amounts of three different commercially-purchased peptides, including (a) 99% pure recombinant human proUgn (BioVendor Laboratory Medicine, Inc., Czech Republic), (b) 99% pure cytochrome C (Sigma Chemical Company, St. Louis, MO), and (c) 99% pure aprotinin (Sigma Chemical Company, St. Louis, MO).

Collection of Plasma and Tissues

Animals were anesthetized (1.6 g urethane/kg body weight, ip). The carotid artery was cannulated with PE 50 tubing for blood withdrawal. After tissue and blood removal, animals were euthanized by anesthetic overdose.

Blood samples were typically obtained from a freshly-anesthetized animal, but, in some cases, were taken both before and 30 min after surgical removal of the small intestine. In this case, extracellular volume was maintained by infusion of isotonic saline through the jugular vein at 30 µl/min/100g body weight. Blood was collected into heparinized tubes (Sigma Chemical Company, St. Louis, MO), centrifuged (16,000 x g for 5 min), and stored frozen at -80° C until used for further analysis.

Individual organs were removed intact, subdivided into smaller pieces as necessary, and rapidly frozen. Prior to freezing, the intestine was cut longitudinally, and rinsed thoroughly with saline to eliminate any contents, and each kidney was flushed intravascularly with 15 ml of saline to ensure that it was free of plasma and ultrafiltrate. All frozen tissues were homogenized in buffer (25 mM HEPES, pH 7.4, containing protease inhibitor cocktail (Sigma Chemical Company, St. Louis, MO) at a ratio of 4 ml buffer/g tissue. Homogenates were centrifuged at 60,000 x g for 30 min at 4° C, and the supernatant fraction was stored at -80° C.

Quantitative T84 Cell Assay for GC-C-stimulating Activity

Plasma and intestinal extracts were bioassayed for Ugn-like activity, based on the method of Currie et al. (40). This assay measures the cyclic GMP responses that are evoked by ligands that activate GC-C (in rats, the known ligands are Ugn and its structurally-related analog guanylin (Gn) (40, 113, 132). Neither proUgn nor proUgn has significant activity in this assay (82, 113, 165).

Typically, a standard curve was also constructed, using known amounts of synthetic rat Ugn (Peptides International, Louisville KY). The responses evoked by the standards were fit using the Michaelis-Menten equation: (pmol cGMP/well) = (Vmax x concentrationUGn)/(EC50 + concentrationUGn). An estimate for the EC50 for rat Ugn was obtained from a previously published study (51), and the value of Vmax was varied to achieve an optimal fit by eye. Standards and unknowns were assayed in duplicate or triplicate. Results for each unknown are reported as pmol Ugn-like activity per well (mean ± sem), as determined by interpolation from the

standard curve, followed by a correction for sample loss during processing, based on the activity recovered from the spiked samples (34 ± 8% recovery, n = 10). No difference in recovery was apparent between spiked gut and spiked plasma samples.

Western Blotting and Quantitative Immunoassay for proUgn

We developed a Western blot-based immunoassay to measure tissue and plasma levels of rat proUgn. This assay employs a standard curve constructed with known amounts of our bacterially-produced recombinant rat proUgn (see above), using either antibody 6910 or 6912 (113, 150) as the primary detection antibody. To perform the assay, the five left-hand lanes of a gradient gel (4 - 12% polyacrylamide, Invitrogen Corporation, Carlsbad CA) were loaded with a dilution series of the recombinant standard (typically spanning the range from 10 - 500 fmol). The remaining lanes were loaded with test samples. After electrophoresis, protein was electroblotted onto 0.2 micron nitrocellulose membrane. The membrane was then incubated for 2 hr with primary antibody (diluted 1:500 in TBS-T), washed and incubated for 1 hr in the dark with infrared-emitting secondary antibody (IRDye 800 Rockland Inc, Gilbertsville PA; diluted 1:2000), and washed in the dark for 1 hr with TBS-T, followed by 20 min with TBS. Immunoreactive proteins were then detected and quantified with an Odyssey infrared gel imaging system (LI-COR Biosciences, Lincoln, NE).

This assay is linear (R^2 = 0.98 ± 0.003, n = 19) up to at least 5 pmol, with a lower detection limit of ~0.01 pmol. The average coefficient of variation for identical

test samples run in the same assay is 11 ± 2% (mean for 11 independent assays, ± SEM). The sensitivity of the assay is adequate for extracts of intestinal tissue, which provide a strong proUgn signal when 50 µg of total protein are run on a gel. The amount of proUgn present in 75 µl of plasma is also well within the range that we can detect with our assay, but analysis of plasma samples required a pre-extraction procedure, using a Superdex 75 10/300 GL size exclusion column (GE Healthcare, Life Sciences, Piscataway, NJ) to separate proUgn from high-abundance plasma proteins that would otherwise have interfered with electrophoresis. The Superdex column was eluted and proUgn-containing fractions were pooled and dialyzed against distilled water, using the 1 kDa cutoff dialysis membrane described above. Dialyzed samples were dried under vacuum, resuspended in boiling SDS sample buffer, and electrophoresed as described above. Recovery of proUgn from the chromatography and dialysis steps was 30 ± 2% (n = 5). Correction for these sample losses has been included in all our plasma calculations.

Production of Isotopically-Labeled Recombinant proUgn

The rat proUgn sequence was subcloned into an expression vector optimized for high yield in vitro translation (pCITE-4a(+), Novagen/EMB Biosciences, Madison, WI). This vector encodes an S-tag peptide and a thrombin cleavage site upstream from the multiple cloning site. The proUgn insert was PCR amplified from a previously-cloned cDNA using a forward primer with an added Nco1 restriction site (5'-TCATGCCATGGTCCAAGTCCAGCTAGAA-3') and a reverse primer with an added Xho I restriction site (5'-TGTACGGGCTGCTGACACTCGAGCACGAGC-3').

These primers were chosen to eliminate both the 21 residue signal peptide and an internal Nco 1 site near the 5' end of the proUgn coding sequence. Additionally, by inserting a methionine residue adjacent to the thrombin cleavage site, this construct enhanced radiolabeling of any peptide fragments that might be cleaved from the amino terminal region of the propeptide. The PCR product was ligated into linearized pCITE-4a(+), and, after single colony isolation and amplification in bacteria, the sequence and orientation of the insert were confirmed. The insert encodes the amino acid sequence

GSMVQVQLESVKKLNELEEKQMSDPQQQKSGLLPDVCYNPALPLDLQPVCASQE AASTFKALRTIATDECELCINVACTGC.

Plasmid DNA was then used as the template for a coupled in vitro transcription/translation reaction (TnT rabbit reticulocyte lysate system, Promega Corp., Madison, WI) in the presence of 35S-cysteine and 35S-methionine (ProMix, Amersham-Pharmacia Biotech/GE Healthcare, Life Sciences, Waukesha, WI). Labeled proUgn was subsequently affinity purified on S-protein-coupled agarose beads (Novagen), and released from the beads by digestion with biotinylated thrombin (Novagen). The thrombin was then bound to streptavidin-agarose beads (Novagen). After removing the beads, the recombinant propeptide in the supernate was applied to a VYDAC 218TP1010 C-18 reverse phase column (The Separations Group Inc. (Grace Vydac), Hesperia, CA). The column was eluted at a flow rate of 1 ml/min, with an immediate step increase to 36% acetonitrile, followed by a linear gradient of acetonitrile from 36% to 45% over 40 min. Two closely eluting peaks of labeled material were identified by liquid scintillation spectroscopy. Two lines of

evidence demonstrate that the later peak corresponds to 35S-proUGn: (a) its retention time (35 - 40 min) was identical to that of native proUgn on this gradient, and (b) the material eluted in this second peak tested positive for full-length proUgn in a Western blot. After HPLC purification, solvents were removed under vacuum, and the recombinant 35S-labeled propeptide was resuspended in phosphate-buffered saline for infusion into anesthetized animals.

Intravenous infusion of labeled, recombinant proUgn

Animals were deprived of food (but not water) overnight, then anesthetized with urethane (1.6 g/kg body weight, ip). To prepare animals for these experiments, surgeries were performed as described prior. Radiolabeled proUgn was then administered as either (a) a bolus injection (5 x 106 cpm) through the jugular vein, or (b) a priming dose (6 x 105 cpm) given by bolus injection followed by a maintenance dose (5 x 106 cpm) added to the infusion solution over a long (60 - 360 min) period. Plasma and urine were collected at intervals, as described in the Results. Plasma samples (heparinized) and urine were stored on ice for the duration of the experiment, then frozen and stored at -80° C prior to analysis by HPLC (see below). At the end of the infusion period, tissues were removed and flash-frozen on dry ice. Note that most tissues were frozen immediately, but kidneys were flushed with 15mls of saline before freezing, to clear radioactive materials from both the intravascular and intratubular compartments. All frozen tissues were homogenized in ice-cold homogenization buffer (4 ml/g tissue), using a motor-driven Potter-Elvehjem homogenizer fitted with a glass pestle. After homogenization, the extracts were

centrifuged at 27,000 x g for 30 min at 4°C in a Ti-50 rotor (Beckman Instruments), and the pellets discarded. Supernatant fractions were stored at -80° C prior to analysis by HPLC (see below). At the end of the experiment, after all tissues and fluids had been collected, animals were euthanized by anesthetic overdose.

HPLC analysis of radiolabeled proUgn metabolites in liver, kidney, plasma, and urine

Tissue, plasma, and urine samples were passed through a 0.2 µm Acrodisc syringe filter (Pall Corporation, Ann Arbor MI), then applied to the C-18 reverse phase column described above, after pre-equilibration with HPLC grade water containing 0.1% trifluoroacetic acid. The column was eluted at a flow rate of 1 ml/min, with a linear gradient of acetonitrile from 2% to 50% over 30 min, followed by a step increase to 100% acetonitrile for 10 min (see figures 2.6 – 2.8). 1 ml samples were collected, dried in a centrifugal vacuum concentrator (Savant SpeedVac, Thermo Electron Corporation, Waltham MA), and dissolved in scintillation fluid (Scintisafe, Fisher Scientific) to determine the retention times and establish the relative amounts of radioactivity incorporated into metabolites.

Inulin and proUgn clearance measurements

FITC-conjugated inulin (Sigma St Louis MO) was dissolved in isotonic saline at a concentration of 40 mg/ml in a boiling water bath and dialyzed against isotonic saline (SpectraPor 6 dialysis membrane, 1000 Da cutoff-limit, Spectrum Laboratories, Rancho Domingo, CA). The dialyzed solution was filtered through a 0.2 micron membrane and then administered to anesthetized Wistar rats as a bolus

injection of 0.5 ml into the jugular vein. Blood samples were collected through the carotid artery cannula into heparanized hematocrit tubes at 0.25, 2, 5, 10, 20, 40, 60, 100, and 120 min following the bolus injection. The procedure was repeated in a separate group of “anephric” rats 5-10 minutes after bilateral ligation of the renal pedicles. The fluorescence intensity obtained from the first plasma sample (30 sec after bolus injection) was set at 100% and subsequent plasma inulin values are expressed as a percentage of this value.

35S-proUGn disappearance curves were generated by a similar procedure in normal and acutely nephrectomized rats, except that the bolus injection contained 5 x106 counts of 35S-proUGn produced by the in vitro reticulocyte expression system described above. Plasma samples were taken at 0.25, 5, 10, 30, 60 , 90, and 120 minutes. Fewer samples were collected than in the inulin experiments, as a greater volume of plasma was needed at each time point for HPLC analysis. A 100 µl aliquot of plasma from each sample was fractionated on a C-18 reverse phase HPLC column to separate 35S-proUGn from other labeled metabolites that might have accumulated in blood over the duration of the experiment. Fractions from the C-18 column were transferred to scintillation vials, dried under vacuum, and reconstituted in Scintiverse (Fisher Scientific, Pittsburgh PA) for liquid scintillation counting. proUgn was estimated as the total counts (blank subtracted) summed across the fractions that coincided with the known retention time for rat proUgn. This always corresponded to a distinct peak of radioactivity (see figure 2.6).

A separate group of 5 rats were cannulated for an infusion of FITC-labeled inulin (Sigma chemical Co, St Louis MO) at a rate of 100µg/min in isotonic saline at

30 µl/min. After 1 hour of equilibration 0.5 ml blood samples were taken from the carotid artery and left renal vein, for analysis of plasma inulin and endogenous (non-radioactive) proUgn concentrations. The renal extraction ratios for each substance were calculated from the arteriovenous concentration differences. Given the well-established renal handling of inulin, the inulin extraction ratio represents the filtration fraction, or the proportion of renal plasma flow that is filtered into the nephrons at that moment. Thus, a comparison of the extraction ratios for proUgn and inulin reveals the extent to which peptide removal by the kidneys corresponds to the amount of peptide filtered into the nephrons.

Renal function studies

An experimental group (8 rats, mean body weight 297±6 g) received an intravenous infusion of recombinant human prouroguanylin (hu-proUgn, BioVendor Laboratory Medicine, Inc., Czech Republic) and a control group (9 rats, mean body weight 309±9 g) received isotonic saline in place of peptide. Animals were anesthetized with sodium pentobarbital (Sigma Chemical Co, St. Louis MO 60 mg/kg body weight ip, dissolved in water at 50 mg/ml). Supplemental doses of anesthetic were provided as needed. Animals breathed spontaneously through a tracheotomy tube (PE240) installed at the start of each experiment. The femoral artery was cannulated with PE 50 tubing for arterial pressure measurement and blood withdrawal. The ureters were exposed through a midline abdominal incision and cannulated with PE10 tubing about 1 cm from each kidney. Urine was collected over 20 minute intervals and the volume was determined gravimetrically. Blood samples

(50 µl) were collected at the mid points of each urine collection. A continuous intravenous infusion of 0.9% NaCl was provided into the left jugular vein at a rate of 10 µl/min/100 g body weight. A portion of this infusion (10 µl/min) was provided through a PE10 cannula connected to a 1 ml syringe. The remainder, provided through a separate cannula, contained 3 mg/ml FITC-conjugated inulin (Sigma Chemical Co. St Louis MO). The inulin infusion solution was pre-dialyzed overnight across a 1 kDa cutoff membrane against isotonic saline (to remove unconjugated FITC and small inulin polymers), then filtered through a 0.2 micron membrane (Steriflip, Millipore Inc. Billerica, MA).

GFR was determined from the clearance of FITC-labeled inulin using the quantitative fluorescence technique described by Lorenz (119). FITC-inulin concentrations in plasma and urine samples were analyzed in 10 ml capillary tubes (Microcap, Clay Adams, Inc.) with an epifluorescence microscope (Zeiss Axioscope) fitted with a CCD camera (Hamamatsu Orca). Metamorph imaging software was used to measure the mean pixel intensity from a central region of each sample over a precisely timed exposure period. Absolute inulin concentrations in plasma and urine were obtained from a standard curve prepared from the infusion solution used in that experiment. Sodium concentrations in plasma and urine were determined by flame photometry (IL Model 943, Instrumentation Laboratory Co., Lexington MA). Blood pressure and heart rate were displayed on an analog monitor (Stoelting Instruments, Wood Dale, IL Model 50110 with pressure transducer Model 56360) and directed to a USB-A/D module (Keithley instruments, Cleveland, OH Model KUSB 3100). A/D output was displayed on a PC using acquisition software

constructed around the DTx_EZ open source system. Data were analyzed with the Prism 5 graphing and analysis program (Graphpad Software, San Diego CA).

Each experiment consisted of seven 20 min clearance periods. After two control periods, rats in the experimental group received recombinant hu-proUgn via the 10 µl/min intravenous infusion line (described above) during the third, fourth, and fifth clearance periods at a rate of 1.66 µg/min/kg body weight (equivalent to 172 pmol/min/kg body weight, or about 50 pmol/min for a 300 g animal). The experiment then continued for two post-infusion clearance periods. Control rats were treated in exactly the same way as the experimental group except no proUgn was infused. At the end of the last collection period, animals were euthanized by anesthetic overdose.

Curve fitting

We used curve fitting procedures in Igor Pro (WaveMetrics, Lake Oswego, OR) and Prism 5 (Graphpad Software, San Diego CA). These procedures use the Levenberg-Marquardt algorithm to iteratively adjust the parameter values of a given function until the weighted sum of the squared residuals ($\chi 2$) is minimized. We used this algorithm to define single, double, and triple exponential functions that would approximate the plasma proUgn and inulin disappearance curves. After each fit was optimized, the resulting $\chi 2$ values were used to calculate Akaike's Information Criterion (AIC) for each function. In each case, the lowest AIC value was observed for the triple exponential function, indicating that it is the preferred model, with the better fit to the data.

C. RESULTS

Extracts of rat intestine contain intact proUgn

A previous study identified an immunoreactive molecule in rat gut extracts whose intestinal expression pattern closely paralleled that of proUgn mRNA, and whose size on an immunoblot approximated the size predicted for the proUgn polypeptide (153). Positive staining with two different anti-proUgn antibodies confirmed that this native polypeptide was structurally related to proUgn, but it remained unclear whether it was proUgn itself, or a large processing fragment derived from proUgn during the production of Ugn. In the present study, therefore, we have used a bacterial expression system to generate a recombinant rat proUgn standard (R) and a truncated version of rat proUgn from which the C-terminal Ugn sequence had been deleted (CΔ); these two standards were then compared to the native proUgn-like molecule on immunoblots, using three different anti-peptide antibodies (6912, 6910, and 1-11). The specificities of the antibodies and the structures of the recombinant standards are presented schematically in Figure 2.1a.

Figure 2.1b shows an immunoblot of an extract of small intestine stained with antibody 6912. As in previous studies, we observed a prominent immunoreactive polypeptide (marked by the black arrowhead) whose apparent molecular weight was consistent with the size predicted for proUgn (~9.4 kDa). This native molecule (N) was just slightly smaller than R, and much larger than CΔ (Figure 2.1c). The slight size discrepancy between N and R (observed on many, but not all, gels) is consistent with the addition of 4 extra N-terminal amino acids to the recombinant protein, as required to generate a thrombin cleavage site in the fusion protein

precursor (see figure 2.1a and Methods). In addition, like R (and unlike CΔ), N was recognized by all three antibodies (figure 2.1d), confirming that it contains the intact C-terminus of proUgn. Thus, based on its size, and its pattern of immunological reactivity, N must correspond to full-length proUgn. Furthermore, as shown in Figure 2.1c, we could not detect proUgn processing fragments (molecules whose size was comparable to CΔ, or smaller), even when we deliberately overloaded the gel with a large excess of gut extract (up to 120 µg of total protein, the limit that can be electrophoresed without serious distortion of the gel).

To look more rigorously for proUgn processing fragments, we used HPLC to enrich our samples before applying them to gels. We first passed a crude gut extract over a sephacryl column and pooled the fractions containing molecules in the 1 - 17 kDa range. This pooled material was concentrated and applied to a C18 reverse phase column to fractionate the peptides of interest. Immunoblots of individual C-18 column fractions are shown in Figures 2.2a and 2.2b. At a moderate sample load, a prominent peak of immunoreactivity was observed in fraction 48 (Figure 2.2a, 1X sample load). This molecule must be full length proUgn, as it co-eluted from the C-18 column with our recombinant proUgn standard (the retention time of R is indicated by the black arrow), had the same molecular weight as R on the gel, and was recognized by all three anti-proUgn antibodies (Figure 2.2b, fraction 48). When we overloaded a gel with material from the same column fractions (Figure 2.2a, 20X sample load), we could still observe the proUgn peak centered in fraction 48 (though it was greatly broadened due to overloading), but, in addition, we could now detect a minor immunoreactive species in fraction 44. We believe that this latter molecule

represents a C-terminally truncated processing fragment of proUgn, as it co-eluted from the C-18 column with our CΔ standard (the retention time of CΔ is indicated by the white arrow), had the same molecular weight as CΔ on the gel, and was recognized by antibodies 6910 and 6912, but not 1-11 (Figure 2.2b, fraction 44). However, the lack of reactivity with antibody 1-11 could also reflect the very small amounts of the candidate molecule in the sample, since antibody 1-11 binds less well to full length rat proUgn than do antibodies 6910 and 6912 (Figure 2.2b, fraction 48). If the CΔ -like molecule is, indeed, a proUgn processing fragment, then its abundance is extremely low, relative to the abundance of full-length proUgn (Figure 2.2a). Furthermore, no other candidate processing fragment was observed in any other HPLC fraction (including the early and late fractions, which were tested but are not shown in the figure).

Quantitation of proUgn expression in the rat gut

Having established that the small intestine contains authentic, full-length proUgn, we then developed an assay to measure the levels of the propeptide in tissue extracts. To ensure that the assay results would reflect the total tissue pool of proUgn, we removed the entire length of the small intestine, transected it at the midpoint, and prepared separate extracts from the proximal and distal halves without discarding any tissue. Using the assay procedure described in the Methods (and shown in Figures 2.3a and 2.3b), we established a specific activity of 12.6 ± 1.0 fmol proUgn/μg protein (n = 21) in proximal extracts, and 10.0 ± 1.0 fmol proUgn/μg protein (n = 17) in distal extracts. This corresponds to a tissue content of 1.32 ± 0.16

nmol proUgn in the proximal half, and 0.98 ± 0.12 nmol proUgn in the distal half, or a total of ~2.3 nmol for the small intestine as a whole (Table 2.2).

Extracts of rat intestine contain relatively little Ugn

To compare the proUgn values reported in Table 2.2 to levels of Ugn in the same regions of intestine, we measured the amount of biologically active peptide in gut extracts, using a well-established T84-cell-based bioassay. This assay is highly selective for Ugn and a related intestinal peptide, guanylin (Gn), but does not recognize proUgn (see Methods).

Initial pilot studies revealed that the amount of Ugn-like bioactivity in gut extracts was near the detection limit of the bioassay. Therefore, to concentrate our samples prior to assay, we passed 1 ml aliquots of each of them over a C18 SepPak, washed the SepPak with water, and used 10% acetonitrile to elute all of the bound activity (Figure 2.3c). The 10% SepPak fraction from each gut extract was then dried, resuspended in a small amount of bioassay medium, and applied to the T84 cells. After SepPak enrichment, all gut-derived samples evoked small, reproducible responses in the cells (Figure 2.3d). By interpolating the responses on a standard curve constructed with known amounts of synthetic Ugn (Figure 2.3d, black bars and inset), we could calculate that each sample contained, on average, 0.52 ± 0.27 pmol of Ugn-like bioactivity. To correct for any losses that might have occurred due to irreversible binding to the SepPak, or to proteolysis at any step during sample processing, we added 30 pmol of Ugn to small frozen pieces of gut tissue, then homogenized these spiked samples and subjected them to the same

processing steps outlined above. On average, 34 ± 8% (n = 10) of the spiked material was recovered. Taking into account this recovery factor, we could then calculate that extracts of proximal small intestine contained, on average, 0.54 ± 0.16 fmol of Ugn-like bioactivity/μg protein (mean ± sem, n = 5; see Table 2.2).

However, not all of the bioactive material in these extracts was necessarily equivalent to Ugn, since T84 cells respond to both Ugn and Gn, and rat jejunum contains both of these peptides (40, 113, 153). To investigate the identity of the molecule(s) responsible for the bioactivity, we SepPak-purified a larger amount of jejunal extract (6 ml), and fractionated this scaled-up preparation by reverse phase HPLC. Column fractions were dried, reconstituted, and bioassayed to establish the elution profile of the biologically active species (Figure 2.4a). One major and one minor peak of activity were evident. The retention time of the major peak (labeled 2 in Figure 2.4a) was identical to that of a synthetic rat Ugn standard (marked by the black arrow), while the retention time of the minor peak (labeled 1 in Figure 2.4a) was very similar to that of a synthetic rat Gn standard (marked by the white arrow). As a further test of the identities of the endogenous bioactive molecules, we examined the pH dependencies of the responses that they evoked in T84 cells, since it has previously been well documented that responses to Ugn are greater at low pH, while responses to Gn are greater at high pH (84). As shown in Figure 2.4b, the responses to peak 2 and authentic rat Ugn were affected identically by pH, whereas the response to peak 1 resembled neither Ugn nor Gn in its pH dependency. Thus, by two criteria (retention time and pH-dependency), the majority of the biological activity present in crude extracts of proximal small intestine is

attributable to authentic Ugn. The identity of the minor peak remains unconfirmed, though it most likely represents a Gn-related peptide. The data presented in Figure 2.4 are thus generally consistent with previous studies showing that rats and mice express higher levels of proUgn than proUgn in the small intestine (both at the mRNA and propeptide levels), and higher levels of proUgn than proUgn in colon (113, 132, 153, 188). It should be noted, however, that this differential pattern of peptide distribution is not observed in other species, such as opossum (53, 116) or human (126).

Furthermore, although Figure 2.4 demonstrates that most of the Ugn-like bioactivity reported in Table 2.2 is indistinguishable from authentic Ugn, this nevertheless represents only a tiny fraction (~4%) of the total uroguanylin-related peptide stored in the tissue. The bulk of the peptide is present in the form of intact proUgn (Table 2.2).

Intact proUgn circulates at much higher levels in rat plasma than does Ugn

The ~23:1 ratio of proUgn to Ugn in the intestine suggests that the intact propeptide might the preferred secretory product. To verify that proUgn is a constituent of rat plasma, we performed Western blots after fractionating plasma on a size exclusion column. This size fractionation step was required to separate proUgn-sized peptides from very abundant higher molecular weight plasma proteins that interfere with electrophoresis. The blots revealed the presence of an ~9.4 kDa proUgn-like immunoreactive polypeptide that eluted between 125 – 150 min (Figure 2.5a). To confirm the identity of this peptide, we compared its properties to those of

intestinal proUgn. The two molecules migrated identically on a high-resolution gradient gel, and both were recognized by all three of the anti-proUgn antibodies (Figure 2.5b). Thus, the plasma molecule was immunologically and electrophoretically identical to the full-length proUgn molecule found in intestinal extracts. Based on its column behavior, proUgn in plasma had a size comparable to that of an ~10 kDa globular protein (Figure 2.5c). Thus, it was not complexed with any high molecular weight protein, such as a plasma binding protein.

To quantify the levels of proUgn in plasma, we analyzed 100 µl samples on a smaller, higher resolution Superdex size exclusion column, which can process multiple samples more efficiently. Arterial plasma was obtained from 21 independent animals. Each sample was individually applied to the column, and the proUgn-containing fractions from each sample were pooled and subjected to the proUgn-specific immunoassay (Figure 2.5d). On the basis of these measurements (including a correction for recovery from the column), we determined that proUgn circulates in plasma at 10.3 ± 1.7 pmol/ml (mean ± sem, n = 21). Assuming a plasma volume of 9 ml for a 300 g rat (149), the estimated circulating pool of proUgn therefore amounts to ~93 pmol, corresponding to ~4% of the total intestinal pool (Table 2.2).

For comparison, we then used the T84 cell bioassay procedure described above to measure Ugn-like bioactivity in plasma. Again, we pre-fractionated each plasma sample on a SepPak before applying it to the reporter cells. However, even when we loaded up to 3 ml of plasma onto the SepPak, we did not recover any signal that could correspond to endogenous Ugn (Figure 2.5e, white bar). By contrast, plasma samples spiked with 30 pmol of Ugn provoked robust responses,

with the same 34% recovery that was observed with gut samples (data not shown). By taking the response to 10-9 M Ugn as the limit of detection for the bioassay (Figure 2.5e, black bars), and factoring in the appropriate volumes and the recovery factor, we calculate that the upper limit for the plasma concentration of Ugn is 0.25 pmol/ml. Thus, the plasma concentration of Ugn is less than 2.5% of the plasma concentration of proUgn (Table 2.2). In fact, the percentage is probably much lower, since sensitive radioimmunoassay measurements have established a circulating level of 0.003 pmol/ml for Ugn in human plasma (97). (Note that the published assays of Ugn levels in rat plasma report only “total Ugn-like” immunoreactivity, without separating Ugn from proUgn (67, 93)—see the Discussion for further elaboration of this point).

The intestine is the likely source of circulating proUgn

We then used our gel-based proUgn assay to quantify propeptide levels in colon and kidney, for comparison to the levels in small intestine. The results are shown in Table 2.2. The total proUgn content of the small intestine is approximately 10 times greater than that of the kidney, and approximately 85 times greater than that of the colon. Thus, although our results do not rule out the possibility that some of the other tissues that we tested may contain levels of proUgn that fall below the detection limit of our gel-based assay, it is, nevertheless, reasonable to consider only the intestine and the kidney as plausible tissue sources of the high levels of proUgn observed in plasma, with small intestine being the best candidate.

Direct evidence for intestinal secretion of proUgn

To more directly investigate the hypothesis that circulating proUgn is derived from the intestine, we used our proUgn assay to measure the level of propeptide in the venous outflow of the intestine (portal vein plasma) relative to that in the systemic circulation (carotid artery plasma). In paired measurements, portal plasma contained almost twice as much proUgn as did systemic plasma obtained at the same time from the same animal (portal levels were 177 ± 16% of arterial levels; n = 20, p = 0.002, paired t-test), providing strong evidence that the intestine is a source of circulating proUgn. In contrast, the kidney does not appear to play a significant role in maintaining the plasma pool. Paired measurements of proUgn levels in the renal vein and the renal artery revealed that there was significantly less proUgn in the venous outflow from the kidney than was present in the arterial input to the kidney (renal vein levels were 63 ± 5% of renal artery levels; n = 8, p = 0.02, paired t-test). Thus, the net contribution of the kidney is to remove proUgn from the plasma, rather than to supply the propeptide to the plasma.

As a final test of the origin of circulating proUgn, we measured levels in systemic plasma before and after complete resection of the small intestine. At 30 min after resection, proUgn levels were reduced to 27 ± 6% of the pre-resection level (n = 3, p = 0.01, paired t-test), whereas in control animals maintained for 30 min under identical conditions, but with no intestinal resection, plasma proUgn levels remained constant (levels at 30 min were 104 ± 2% of the “zero time” control; n = 3). These effects of resection, coupled with the regional plasma measurements

described above, indicate that most (and very likely all) of the proUgn in the circulation is derived from the gut.

During infusion of radiolabeled proUgn, radioactivity accumulates in liver, kidney and urine

After 60 min of continuous infusion with labeled propeptide, only two tissues (kidney and liver) accumulated significant amounts of radioactivity (Figure 2.6a, white bars). The specific activity of labeled material in the kidney was ~10 times higher than that in liver (Figure 2.6a, black bars), and the concentration of radioactivity in urine was ~10 times higher than that in plasma (Figure 2.6b), consistent with the idea that the kidney plays a dominant role in clearing the propeptide from the circulation, as would be expected for a peptide of this size.

Circulating proUgn is rapidly removed from the plasma by renal clearance

To further explore the role of the kidney in proUgn clearance, we measured the rate of disappearance of labeled propeptide from plasma after bolus infusion into control and anephric animals (the latter produced by ligating the renal pedicles 5 min prior to infusion). This type of infusion is equivalent to a classical pulse-chase procedure because, as demonstrated in our companion publication, significant amounts of endogenous, nonradioactive proUgn are continuously released from the intestine into the circulation in both intact and anephric animals. Plasma samples obtained at specific times after the bolus infusion were fractionated by reverse phase HPLC (Figure 2.7a, control animals; Figure 2.7b, anephric animals). At every time point, the radioactivity eluted from the reverse phase column as a single, well-

defined peak, whose chromatographic behavior was indistinguishable from that of authentic proUgn (retention times of HPLC standards are given in figure 2.7c, and marked by the arrows in Figures 2.7a and b). The amplitude of this peak decreased progressively over time in both types of animal. To evaluate this quantitatively, we integrated the area of the peak for each sample, and plotted this value as a function of time after infusion (Figure 2.7d). In control animals, proUgn was cleared quickly from the circulation, with an overall plasma half-life of 49 sec (Figure 2.7d, white symbols). This disappearance curve was best fit by a triple exponential function (Table 2.3), suggesting that infused propeptide exits the circulation by a minimum of three independent routes. At least one of these routes must involve the kidney, since complete nephrectomy increased proUgn's plasma dwell time by a factor of 7, giving a new overall plasma half-life of 351 sec (Figure 2.7d, black symbols). Furthermore, although the time-course of propeptide disappearance was again best fit by a triple exponential function, the fit in the nephrectomized animals appeared to lack the slowest clearance component that was normally observed in control animals, and instead included an ultra-slow process ($t > 300$ min – see Table 2.3) that was difficult to observe under control conditions, due to the exceedingly low levels of proUgn present in the plasma at all time points after 30 min when the kidneys were functional.

We also performed experiments to measure the rate of disappearance of FITC-labeled inulin after bolus infusions into control and anephric animals (Figure 2.7e). Inulin has long been used as a filtration marker in renal clearance studies, because it is biologically inert, not metabolized by any tissue, freely filtered by the

kidney, and neither absorbed nor secreted by the renal tubules. The similar effect of nephrectomy on the time constants for proUgn and inulin disappearance (Table 2.3) suggests that the two molecules are handled in a similar way; i.e., that the kidney provides a prominent route for clearance of both molecules under normal circumstances. This is supported by measurements of the renal extraction of inulin and native proUgn. Based on the concentration difference between arterial and renal venous blood the renal extraction of inulin from arterial blood was 26.6+3.5% compared to 29.9+5.0% for proUgn (mean ± sem, n = 5). These values are not different, and suggest that that the renal clearance of proUgn is a filtration-dependent phenomenon that parallels inulin clearance.

Note, however, that proUgn was eliminated from the circulation slightly more effectively than inulin—both in the presence and the absence of the kidneys (compare the inulin curves in Figure 2.7d to the superimposed proUgn curves, shown in grey and reproduced from Figure 2.7c). Thus, at least one clearance mechanism acts on proUgn that does not act on inulin.

Circulating proUgn is not metabolized within the vascular compartment

The HPLC traces in Figure 2.7a reveal that essentially all of the radioactivity in plasma was accounted for by intact proUgn at each time point after bolus injection; this remained true even when plasma clearance was greatly retarded by removing the kidneys (Figure 2.7b). If there had been significant conversion of proUgn to Ugn in the plasma, a radioactive peak should have appeared in the chromatogram at 42 – 43 min (the retention time of authentic Ugn). Any such

metabolite would have been heavily 35S-labeled, as it would contain the 4 cysteine residues that are found at the C-terminus of the propeptide (Figure 2.7c). Furthermore, because we added an extra (non-native) methionine residue to the N-terminus of our recombinant construct, we would also have detected any processing fragments derived from this portion of the molecule. Given the precursor/product relationship between proUgn and any such metabolites, the levels of the latter should have risen as levels of the former fell. However, no fragments of any sort were observed in any of the chromatograms at any time point, arguing strongly that plasma and endothelial proteases did not process proUgn while it was circulating within the vasculature. Furthermore, within the time frame of these bolus infusion experiments, any proUgn metabolites that were generated in tissues were not returned to the plasma in detectable amounts.

For comparison to the results obtained with the radiolabeled recombinant propeptide, we also investigated the plasma stability of native proUgn. For these experiments, we generated 2 µl aliquots from a freshly-drawn sample of plasma, and added 500 fmol of native rat proUgn to each. We then incubated the aliquots at 37° C for varying amounts of time, terminating any potential ongoing proteolytic activity at each specified time point by adding SDS sample buffer and immediately boiling the sample. SDS-denatured samples were then applied to polyacrylamide gels, and the relative proUgn content was determined by Western blotting followed by quantitative densitometry. We observed no significant degradation of proUgn, even after 60 min of incubation (more than 70 times longer than the plasma half-life that is normally observed in the intact animal): the propeptide content at 60 min was 92 ±

7% of the control level measured in samples that had been immediately boiled in SDS without any incubation at 37° C (mean ± sem, n = 4).

Circulating proUgn is metabolized by the kidney, and specific metabolites are excreted in the urine

As shown above (Figure 2.6a), a significant amount of labeled material accumulated in the kidney during prolonged intravenous infusion with radioactive proUgn. When analyzed by HPLC, however, kidney extracts actually contained very little intact proUgn (Figure 2.8a). Instead, label was principally associated with two large HPLC peaks eluting at positions corresponding to free cysteine (peak 1) and free methionine (peak 2).

To evaluate the possibility that the absence of significant amounts of intact proUgn in kidney extracts was due to post-homogenization proteolysis of the propeptide, we spiked a homogenized sample with a known amount of native proUgn and measured the recovery of intact propeptide after prolonged incubation. This was similar to the plasma stability studies described above, except that we also included our standard protease inhibitor cocktail and performed the incubation at 4° C, to parallel the way in which the radioactive samples had been processed. After 60 min, we recovered essentially all (92.6 ± 2.6%, mean ± range, n = 2) of the spiked native material in intact form, indicating that proteolysis was not a significant factor in the radiolabeling studies.

In striking contrast to the limited spectrum of labeled metabolites observed in kidney homogenates, radioactivity recovered in the urine was distributed among a wide variety of molecular species (Figure 2.8b), including cysteine (peak 1),

methionine (peak 2), a small amount of material whose retention time matches that of intact proUgn (peak 6), and three additional metabolites (peaks 3, 4, and 5—note that peak 3 partially overlaps the methionine peak). One of these metabolites (peak 5) had a retention time identical to that of an authentic rat UGn15 standard. The other metabolites (peaks 3 and 4) are as-yet unidentified. However we believe it is likely that they correspond to UGn13 and UGn14, since these alternative proUgn cleavage products were both previously identified (along with UGn15) as prominent bioactive components of opossum urine (83). It is difficult, however, to rigorously compare the previously published and current results on a peak-by-peak basis, since substantial differences in pH, ion pairing reagent, and gradient elution profile will have affected the relative retention times of the individual molecules.

The fact that urinary peptide metabolites of proUgn do not gain access to the circulation was further confirmed in samples of blood taken contemporaneously from carotid artery and renal vein after 1-2 hours of continuous intravenous 35S-proUGn infusion (Figure 2.9a). Consistent with the prolonged nature of this infusion protocol, both plasma samples showed a predominant proUgn peak (peak 6). In addition, and unlike the bolus infusion studies previously presented in Figure 2.7, modest cysteine- and methionine-like peaks were also detectible (peaks 1 and 2). Presumably, these were generated within the kidney during the processing of proUgn, and then returned to the plasma. As would be predicted by this hypothesis, the renal vein contained a significantly higher proportion of the labeled amino acids, relative to intact proUgn, than did the systemic circulation (Figure 2.9b). It is particularly noteworthy, however, that neither the venous nor the arterial blood

sample contained any metabolite of proUgn other than free cysteine and free methionine. Thus, even over prolonged time periods, circulating proUgn does not serve as a source of circulating Ugn.

Infused proUgn stimulates renal sodium excretion

The data presented to this point demonstrate that, relative to Ugn, proUgn is by far the dominant molecular species stored in the intestine and circulating in the plasma. This indicates that secretion of proUgn, rather than Ugn, is the likely endocrine response of the intestine to salt intake. Might the presumably inactive propeptide somehow be capable of triggering physiological responses in the kidney? To investigate this question, we infused a commercially available recombinant human form of the propeptide (hu-proUgn) into anesthetized rats, and evaluated its effects on renal function (note that our recombinant rat propeptide was not available in sufficient quantities for these studies).

In control animals, Na^+ excretion, urine flow, glomerular filtration rate (GFR), blood pressure, heart rate, and potassium excretion did not change significantly over the course of the experiment (Figures 2.10a – 2.10h, white symbols). In contrast, intravenous infusion of 100 µg/kg body weight of hu-proUgn over 60 min increased total urinary Na^+ excretion by ~70% (Figure 2.10a, black symbols), fractional Na^+ excretion by ~50% (Figure 7b, black symbols), and urine flow by ~20% (Figure 2.10c, black symbols). These natriuretic and diuretic responses had a relatively slow onset and long duration, outlasting the application of the peptide by more than 40 min, and were not accompanied by changes in GFR, mean arterial pressure, or

heart rate (Figure 2.10d, e, and f, black symbols). Potassium excretion was also stimulated slightly by propeptide infusion, but the kaliuresis developed very slowly, and the statistical significance of the response was marginal (Figure 2.10g and h, black symbols).

Preliminary quantitative studies revealed that our infusion protocol produced a 3.2 ± 0.36-fold increase in plasma proUgn levels (mean ± range, n = 2). Thus, the renal responses observed in Figure 2.10 were evoked by peptide infusions that fell within a “physiological” range. The absence of hemodynamic effects of proUgn suggests a direct tubular effect of the peptide on Na^+ excretion, and this is confirmed by the significant increase in fractional Na^+ excretion during and after peptide infusion. The prolonged time course of the natriuretic response to hu-proUgn in our studies is comparable to the prolonged responses evoked by Ugn in the isolated perfused kidney (56, 65, 161) or the intact mouse (22, 23). However, the kaliuretic responses to propeptide infusion are much less pronounced than those observed in previous studies with Ugn.

D. DISCUSSION

A number of observations (summarized in the Introduction) have led to the hypothesis that Ugn serves as the endocrine mediator of an entero-renal signaling pathway that enhances renal salt excretion following oral salt intake (56, 65). Most studies investigating this hypothesis have focused on Ugn itself. We provide evidence that the Ugn precursor, proUgn, plays a previously under-appreciated role in the entero-renal natriuretic axis. The underpinnings of this idea are provided by

two key observations, both presented above. First, nearly all of the Ugn that is stored within the small intestine is in the form of intact proUgn (Figures 2.1, 2.2, and 2.3, and Table 2.2). This observation is consistent with the fact that none of the potential mono- and dibasic cleavage sites in rat proUgn matches the consensus sequence for cleavage by conventional prohormone convertases (48). Second, plasma levels of proUgn are also very high (Figure 2.5d and Table 2.2), while circulating Ugn levels are so low that they fall below the limit of detection of our assay (Figure 2.5e and Table 2.2).

The Ugn and proUgn measurements given in Table 2.2 can be compared to previously-published radioimmunoassay (RIA) values for both tissue and plasma pools of “Like-like immunoreactivity” (67, 68, 93, 95, 97, 139, 140). In particular, the proUgn levels determined with our newly developed assay are substantially higher than those published previously. However, the RIA procedures used in all prior studies have employed antibodies directed exclusively against the C-terminal amino acid sequence that defines Ugn. This introduces several complications. First, any such antibody will recognize both Ugn and proUgn (Figure 2.1a), and thus, unless the two target molecules are separated before performing the measurement, the assay will reflect the contributions of both. Second, even after separation of proUgn from Ugn, the concentration of proUgn cannot be measured accurately, since the standard curve is established with Ugn and, in general, anti-Ugn antibodies crossreact poorly with intact proUgn. Recognizing this problem, some studies have proteolytically converted proUgn to free Ugn before performing the assay (139)—

but, even so, the results provide only a lower limit for proUgn levels because it is not possible to assess the stoichiometry of the conversion.

Our new gel-based proUgn assay eliminates these problems, because it detects proUgn directly, does not crossreact with Ugn, requires no proteolysis, and is based on an authentic rat proUgn standard. We have used this assay to quantify proUgn levels in the plasma, small intestine, colon, and kidney of the rat (Table 2.2).

The tissue proUgn values obtained in our current studies are consistent with tissue levels that have been established for other mammalian GI peptides, such as secretin and cholecystokinin, which range from 50 - 500 pmol/g wet weight (calculated as the sum of all the known forms of these peptides, both processed and unprocessed, that reside in the small intestine) (157).

As a general rule, peptide hormones are synthesized as inactive propeptide precursors, and converted to smaller, biologically-active peptides by specific proteolytic cleavages (44, 180). For typical peptide hormones, the most abundant intracellular storage form is the mature, processed peptide. For example, only 5% of gastrin and 20% of cholecystokinin are found in the small intestine in propeptide form (184). However, a few peptide hormones, such as ANP and angiotensin, are stored almost exclusively as inactive propeptides (26, 122, 157). In such cases, processing occurs as a post-secretory event, mediated by ectoproteases located at the site of secretion or within the vasculature.

Radiolabel infusion studies reveal that Ugn falls into yet a third category. Like ANP and angiotensin, Ugn is stored within tissues primarily in propeptide form, and significant quantities of the intact propeptide are released into the plasma.

However—in contrast to proANP and angiotensinogen—circulating proUgn is not processed intravascularly (Figures 2.7a, 2.7b, and 2.9a). Rather, it is cleared from plasma by the kidney (Figure 2.7d), and processed intrarenally (Figure 2.8b). With the exception of free cysteine and free methionine, the renal metabolites are not returned to the general circulation (Figure 2.9a), but rather are excreted in the urine (Figure 2.8b).

In addition, a sampling of published values for the circulating levels of a variety of peptide hormones (13, 31, 32, 114, 184) reveals that, while our estimate of the plasma proUgn concentration is significantly higher than the levels observed for peptides that are processed either prior to or coincident with secretion (e.g. gastrin, cholecystokinin, atrial natriuretic peptide, and B-type natriuretic peptide), it is nevertheless well below the levels established for two circulating propeptides that are only converted to mature peptides subsequent to secretion (angiotensinogen, the precursor for angiotensin II, and T-kininogen, a rat-specific propeptide that is the precursor for ile-ser-bradykinin). Thus, there is biological precedent for the idea that plasma levels of unprocessed propeptides can be very high. Our data also suggest that the intestine must maintain a very high rate of proUgn synthesis and secretion in order to generate such a large, steady-state plasma pool of propeptide in the face of the rapid plasma clearance processes that are observed in figure 2.7.

In addition to high levels of proUgn, our measurements also demonstrate comparatively low levels of Ugn, both in gut extracts and in plasma. The bioassay technique that we used to measure Ugn is not as sensitive as an RIA or a Western blot. Nevertheless, it was adequate to detect a small pool of biologically active Ugn

in extracts of proximal small intestine (Figure 2.3c and d), which, upon quantification (Table 2.2), revealed a proUgn-to-Ugn ratio on the order of 23:1. The assay was not, however, sufficiently sensitive to detect bioactive Ugn in plasma, even when the plasma sample was scaled up to 3 ml (representing nearly one-third of the plasma in an individual animal). Thus, we can only set an upper limit on the level of Ugn in plasma (Table 2.2), and establish a minimal proUgn-to-Ugn ratio of 40:1.

One strikingly consistent feature of these measurements is that proUgn levels are very much higher than Ugn levels, both in gut extracts and in plasma (indeed, the slightly different proUgn-to-Ugn ratios in the two compartments may only reflect the potential sources of error in our measurements) and in the ratios of radiolabeled proUgn infused to the radioactivity associated with the Ugn-like peak from the urine. In terms of an endocrine (tissue-to-tissue) signaling role, this therefore suggests that circulating proUgn might be functionally more important than circulating Ugn. This concept can only be valid, however, if circulating proUgn is capable of eliciting appropriate responses from the target tissue. To investigate this latter possibility, we infused recombinant hu-proUgn into anesthetized rats and measured their renal function. As shown in figure 2.10, both Na^+ and fluid excretion were significantly elevated in response to the propeptide.

Direct plasma measurements demonstrated that our cold–peptide infusion protocol produced an approximately 3-fold increase in plasma proUgn levels. This can be contrasted with previously-published studies of Ugn, in which the peptide had to be infused at supra-physiological levels, in order to evoke renal responses (22,

56). Thus, in contrast to Ugn, proUgn appears to act at levels that are appropriate for an entero-renal signaling molecule.

Our experiments do not identify the intrarenal site where proUgn processing occurs. Two distinct possibilities can be considered. First, the propeptide could pass intact across the glomerular filtration barrier, for processing within the tubular lumen by proteases residing in the epithelial brush border of the proximal tubules. Alternatively, the propeptide could be absorbed from the plasma into tubular epithelial cells by basolateral endocytosis, then processed within vacuoles for apical secretion (in processed form) into the tubular lumen. Although our data do not unequivocally discriminate between these models, several lines of evidence provide strong support for the former over the latter. First, as shown in Figure 2.5, proUgn circulates in plasma as a free 9.4 kDa peptide, uncomplexed with a carrier protein, and is thus small enough to be readily filterable. This predicts that, at a minimum, approximately 30% of the propeptide entering the kidney at any time will be delivered to the tubular lumen in intact form by filtration. This was confirmed by the equivalence between renal extraction ratios close to 30% for both proUgn and inulin, a classical marker of renal function that is cleared exclusively by glomerular filtration. Second, the time course of clearance of plasma proUgn (Figure 2.7d) was very similar to that of inulin, which reinforces the idea that the renal clearance of proUgn is due to filtration rather than secretion. Third, we observed intense radioactive labeling of proximal tubule profiles after intravenous infusion of labeled proUgn (not shown), but the tissue content of radioactivity associated with those profiles was comprised almost exclusively of free amino acids (Figure 2.8a) rather than the larger

peptide metabolites that are found in urine (Figure 2.8b). All of these results are more consistent with intratubular processing than with transcytotic intracellular processing.

This “target organ-mediated” model for propeptide processing is unusual, and it is worth considering why it might be of particular utility in the case of Ugn and proUgn. (a) Ugn, like all GC-C agonists, is highly dependent on disulfide-mediated folding for activity, and, if unfolded, will preferentially refold in an inactive conformation (86). There is, however, an “intramolecular chaperone” domain at the N-terminus of the prosequence that specifies the correct disulfide pairing during synthesis, and permits correct refolding of the C-terminus after oxidation (87). Thus, the increased stability and oxidation-resistance of full-length proUgn over Ugn provides one rationale for favoring the propeptide as the circulating form. (b) When Ugn is retained within the prosequence it has little or no biological activity on GC-C-expressing cells. Consequently, minimizing the level of free Ugn in the plasma will limit potential extra-renal systemic actions (for example, activation of GC-C receptors in the pancreas (106, 108), the reproductive organs (89), and the liver (109)). (c) Embedding Ugn within the prosequence may protect it from plasma, endothelial, and tissue ectoproteases. (d) The EC cells that synthesize proUgn have long been known to release their previously-identified secretory products (serotonin and substance P) both apically, into the intestinal lumen, and basolaterally into the circulation (1, 17, 18). This raises the interesting possibility that the cleavage products of proUgn that are produced in the lumen of the gut may be distinct from those produced in the lumen of the proximal tubule.

It is appropriate to acknowledge that the biochemical experiments do not rule out the possibility that proUgn may be converted to Ugn in tissues that were not studied—although, if this occurs, any Ugn-mediated effects must be strictly local, since no measurable amount of Ugn was returned to the plasma even during our longest infusion studies. In addition, it is well-documented that small amounts of Ugn do, indeed, circulate in plasma (53, 85, 95), and this might become quantitatively more important at certain times of day or in response to specific environmental stimuli. Thus, we must leave open the possibility that a more conventional Based-based endocrine pathway may operate in parallel with the propeptide-based mechanism that we have described here.

Final Thoughts

In summary, the biochemical and physiological studies presented above, in combination with the pulse-chase studies of infused proUgn suggest a unique model for proUgn processing. Not only does processing appear to be primarily a post-secretory event, but, to our knowledge, it is unique among endocrine mechanisms identified to date, as it also occurs only after the circulating propeptide has reached (and been sequestered within) one of its principal target organs, the renal tubules. We propose, therefore, that the N-terminal prosequence may serve as a specialized delivery vehicle that shields Ugn—either preventing its destruction or minimizing its physiological actions—during its passage from the gut to the kidney.

Tables

plasmid	encoded propeptide sequence
pMal-R	GSHMVYIKYHGFQVQLESVKKLNELEEKQMSDPQQQKSGLLP DVCYNPALPLDLQPVCASQEAASTFKALRTIATDECELCINVAC TGC
pMal-CD	GSHMVYIKYHGFQVQLESVKKLNELEEKQMSDPQQQKSGLLP DVCYNPALPLDLQPVCASQEAASTFKALRT

Table 2.1 proUgn Constructs Used in This Study

	proUgn		Ugn-like bioactivity	
	fmol/μg protein (n)	pmol/animal (n)	fmol/μg protein (n)	pmol/animal (n)
small intestine, proximal half	12.6 ± 1.0 (21)	1322 ± 160 (21)	≤ 0.54 ± 0.16 (5)[B]	56.8 ± 17 (5)
small intestine, distal half	10.0 ± 1.0 (17)	978 ± 122 (21)		
small intestine, total	11.3 ± 1.0 (21)	2300 ± 262 (21)		
kidney	2.1 ± 0.3 (12)	247 ± 27 (6)		
colon	1.1 ± 0.3 (5)	27 ± 7 (5)		
	pmol/ml	estimated pmol/animal[A]	pmol/ml	
arterial plasma	10.3 ± 1.7 (21)	~93 (21)	Below Detection Threshold (5) (<0.25)[C]	

Table 2.2 proUgn and Ugn Levels of Tissues and Plasma

[A] Based on an estimated plasma volume of 9 ml for a typical 300 g animal

[B] This represents an upper limit, since a portion (~20%) of the bioactivity is chromatographically distinct from authentic Ugn

[C] This represents an upper limit, calculated on the basis of the detection limit of the assay

	proUgn		inulin	
	control	anephric	control	anephric
t_{fast} (sec)	27	77	49	66
$t_{intermediate}$ (sec)	260	389	210	355
t_{slow} (sec)	4474	BDT[A]	1604	BDT[A]
$t_{ultraslow}$ (sec)	BDT[A]	21296	BDT[A]	13259

Table 2.3 Time Constants (t) for the Clearance of proUgn and Inulin in Control and Anephric Animals. These values were determined by fitting the plasma disappearance curves for each solute to a triple exponential decay function (see the Methods for details). For control animals, we used the equation:

$$\% \text{ remaining} = amp_{residual} + amp_{fast}\, e^{(-t/\tau_{fast})} + amp_{medium}\, e^{(-t/\tau_{medium})} + amp_{slow}\, e^{(-t/\tau_{slow})}.$$

For anephric animals, we assumed that removal of the kidneys eliminated the slow clearance mechanism, which revealed an ultraslow process that could only be observed in the absence of renal activity. In this case, we used the equation:

$$\% \text{ remaining} = amp_{residual} + amp_{fast}\, e^{(-t/\tau_{fast})} + amp_{medium}\, e^{(-t/\tau_{medium})} + amp_{ultraslow}\, e^{(-t/\tau_{ultraslow})}.$$

[A] BDT = Below Detection Threshold

Figures

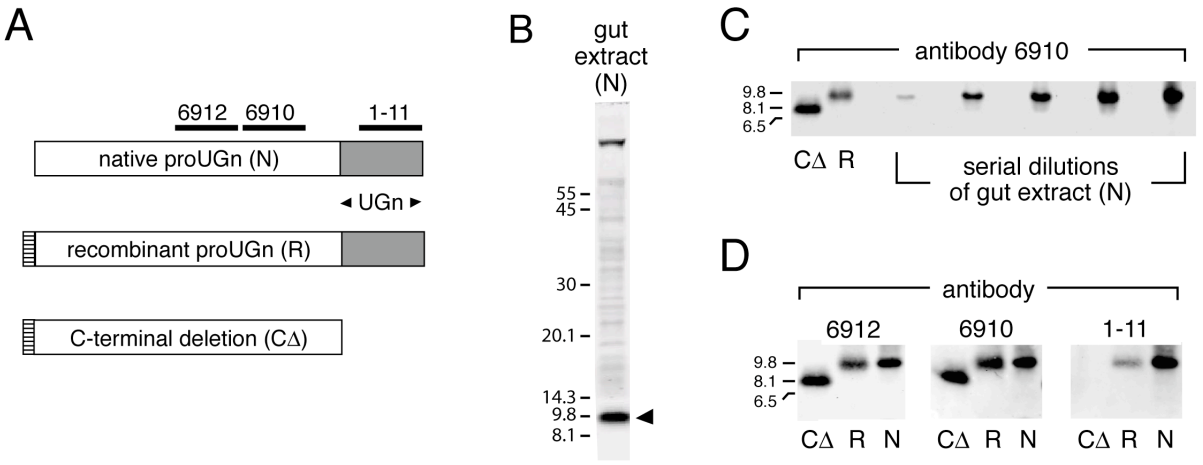

Figure 2.1. Biochemical Confirmation that Gut Extracts Contain Authentic proUgn. A) Depiction of native rat proUgn (N), showing domains targeted by three independent anti-peptide antibodies. Recombinant constructs are aligned beneath the proUgn schematic. R is identical to authentic rat proUgn, except that 4 extra, non-native residues were added to its N-terminus to generate a thrombin cleavage site. CΔ is identical to R, except that 17 residues were deleted from its C-terminus. **B)** An extract of small intestine immunoblotted with antibody 6912. The arrowhead marks the putative proUgn band. The scale gives molecular weights of standards, in kDa. **C)** Side-by-side comparison of CΔ, R, and N. A dilution series of gut extract containing N was loaded in adjacent lanes of the gel, from left to right, to investigate the possible presence of low molecular weight proUgn processing fragments. **D)** A single gel was loaded with samples of CΔ, R, and N, and then cut into three pieces, each of which was probed with a different antibody, as indicated.

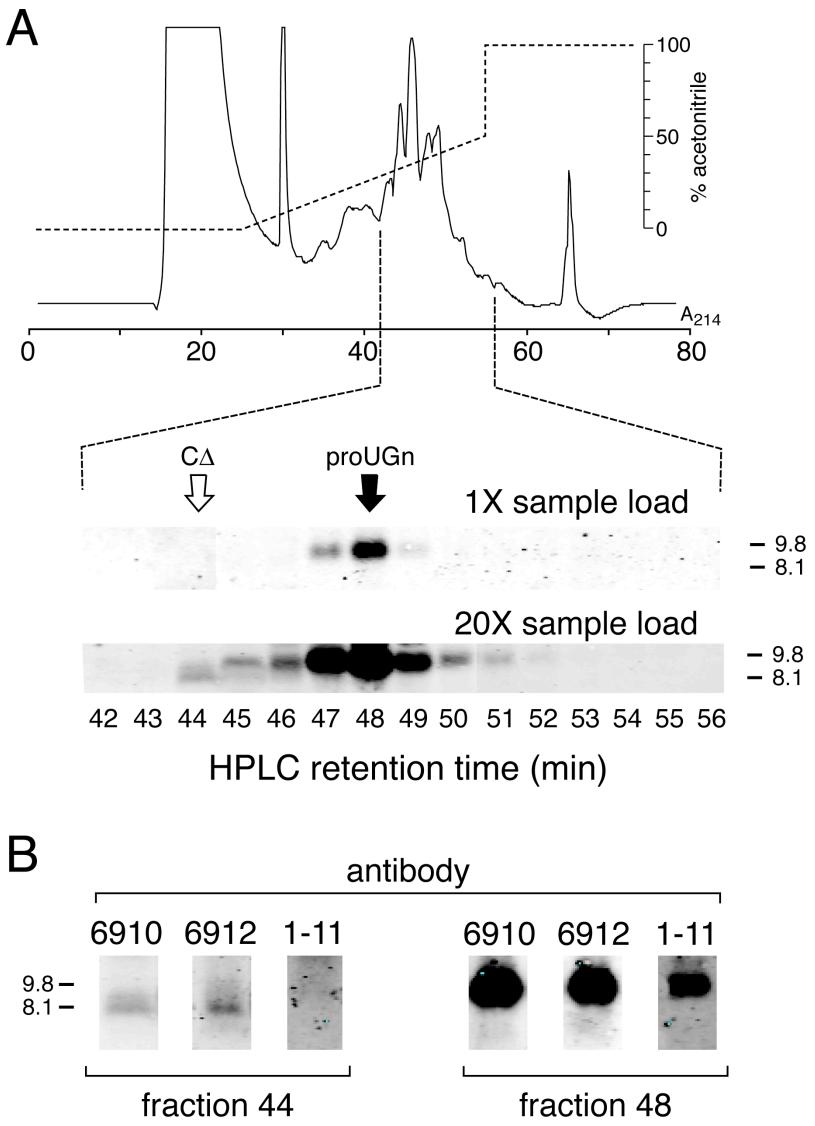

Figure 2.2. C-18 Reverse Phase HPLC Analysis of the Native proUgn-like Immunoreactivity Present in Rat Jejunum. A) Half of the material from a single jejunum was pre-enriched on a sephacryl column, then loaded onto a C-18 column. The elution gradient is shown by the upper dashed line, and the UV profile by the solid trace. A Western blot was performed with antibody 6912 on 25% of each fraction. Only the fractions eluting between 42 and 56 minutes contained immunoreactive polypeptides of appropriate sizes (less than 12 kDa). For simplicity, only these fractions are shown in the figure. The retention times of two recombinant standards (R and CΔ), as determined in separate column runs, are indicated by the black and white arrows, respectively. The structures of these standards are given in figure 1a. **B)** Fractions eluting at 44 and 48 min from the C-18 reverse phase column (in panel (a)) were analyzed by Western blotting, in parallel with R and CΔ. Blots were probed with three different antibodies (6912, 6910, 1-11), as indicated. Each lane was loaded with 25% of the indicated fraction. Only the 3 – 12 kDa regions of the blots are shown.

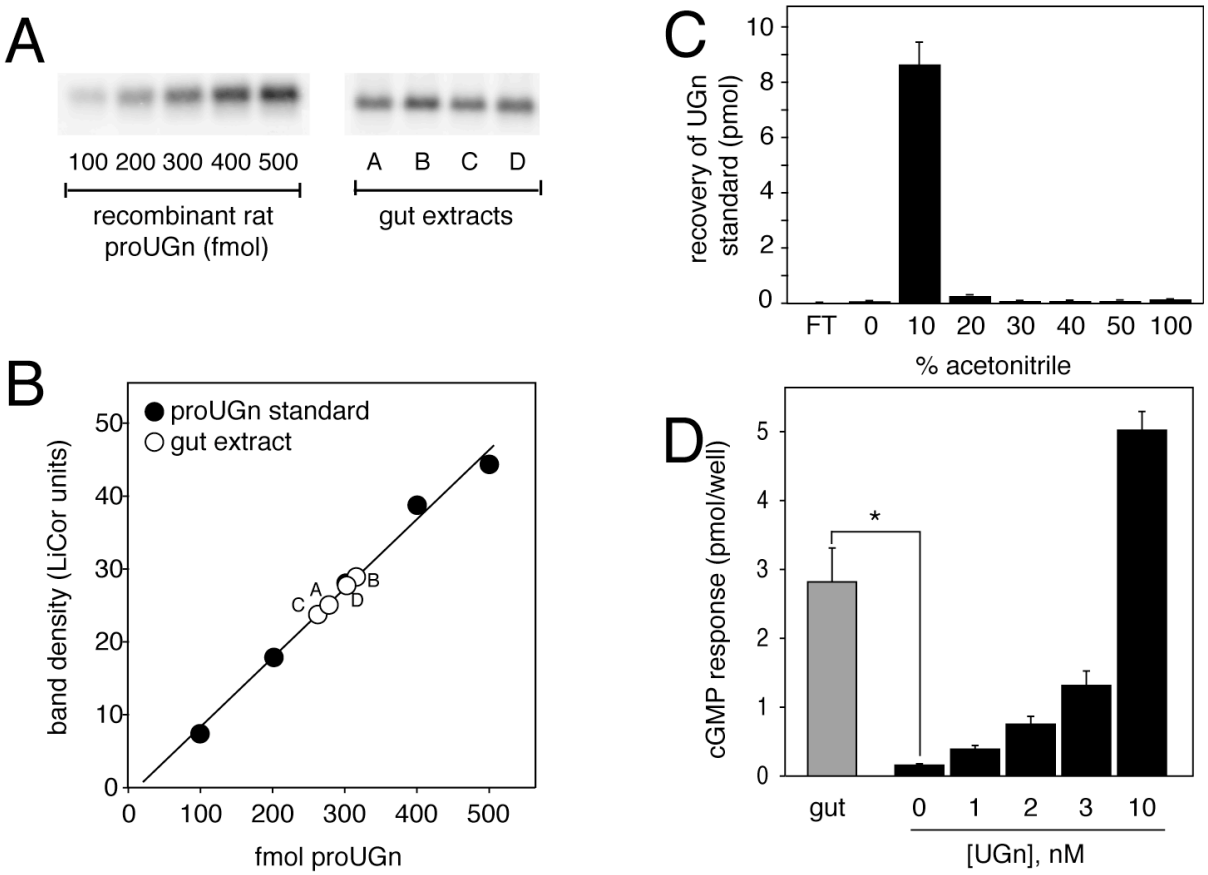

Figure 2.3. ProUgn and Ugn Levels in Extracts of Rat Small Intestine. A) Western blot assay for proUgn, including a standard curve constructed with known quantities of recombinant rat proUgn and samples of gut extract (A – D). A number of similar assays were performed to obtain the values presented in Table 2. **B)** Numerical values derived from the blots in panel (a). **C)** SepPak elution profile of an authentic Ugn sample. After applying the peptide to the SepPak, the flow through (FT) was collected, followed by sequential elution with increasingly-hydrophobic solvent. Peptide recovery in each fraction was measured with the T84 cell bioassay (see Methods). Bioactivity eluted from the SepPak in the 10% acetonitrile fraction. The native bioactivity in gut extracts elutes with an identical profile (data not shown). **D)** Averaged responses of T-84 cells to Ugn extracted from 1 ml jejunal extract (gray bar, mean ± sem, n = 5), after SepPak pre-purification as in panel (c). Responses to gut samples are compared to responses obtained with known amounts of synthetic Ugn (black bars). The inset shows the responses to a full range of synthetic Ugn standards, as performed in a typical assay. Ugn concentrations in the biological samples are determined by interpolation on this standard curve (see Methods).

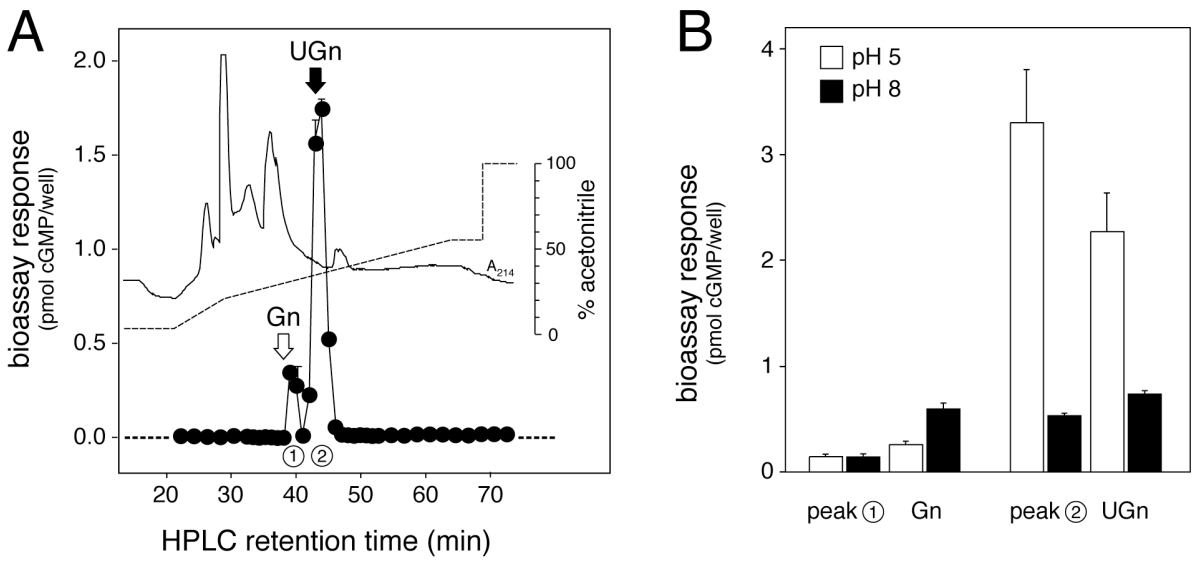

Figure 2.4. HPLC and Bioassay Analysis of Ugn-like Bioactivity From Proximal Small Intestine. A) Extracts were prepared independently from four separate animals, and a 1.5 ml aliquot was withdrawn from each. These aliquots were individually purified on C-18 SepPaks, as in figure 3c, then each was applied to a C-18 reverse phase column and eluted with a gradient of acetonitrile, as indicated by the dashed line. UV absorbance is given by the solid trace. One ml fractions were collected, and either assayed individually or combined in pairs (as indicated) using the T84 cell bioassay. The symbols plot the average of the duplicates, and the error bars give the range (in most cases, the error bars are hidden beneath the symbol). The black and white arrows indicate the retention times of synthetic Ugn and Gn standards. This experiment was repeated a second time with very similar results (data not shown). **B)** Aliquots of material in peak 1 (eluting at 39 min) and peak 2 (eluting at 43 min) were assayed at pH 5 (white bars) and pH 8 (black bars), side-by-side with authentic Gn and Ugn standards.

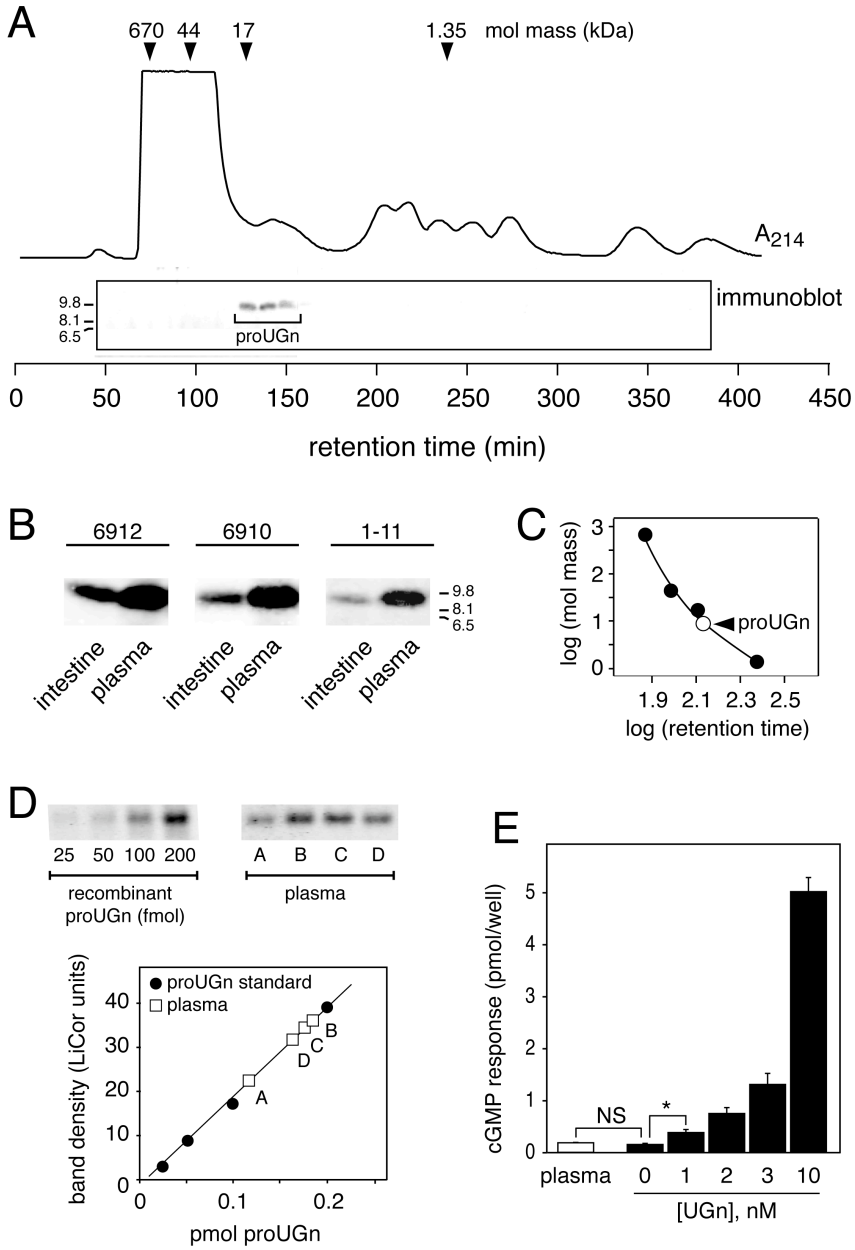

Figure 2.5. Authentic, Full-length proUgn Circulates in Plasma. A) Chromatography of rat plasma on a sephacryl S-100 HR column. Retention times and molecular weights of standards used to calibrate the column are indicated at the top of the panel. The solid trace shows the UV absorption profile. An immunoblot was performed with antibody 6912 on each fraction eluting between 45 and 380 min. **B)** Samples of partially-purified plasma proUgn are compared to samples of partially-purified intestinal proUgn the same gel, probed with multiple antibodies. **C)** Log-log plot of molecular weight vs retention time for proUgn compared to standards run on the same column (taken from panel (a)). **D)** Quantitative assay for plasma proUgn, performed as in figure 3. Plasma was partially purified on a size exclusion column prior to the assay. **E)** Quantitative assay for plasma Ugn, performed on 3 ml samples of plasma (white bar, mean ± sem, n = 5), as in figure 3.

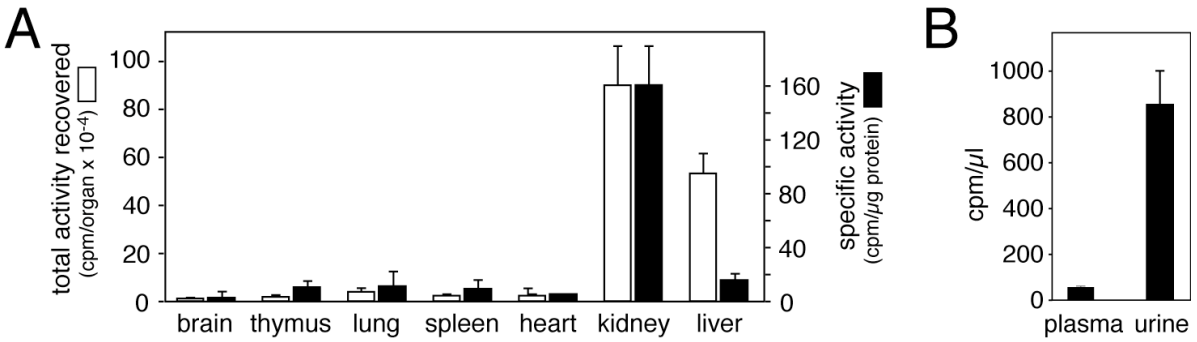

Figure 2.6. Distribution of Radiolabel in Tissues and Fluid Compartments at the End of a 60 Min Steady Intravascular Infusion of ^{35}S-proUGn. A) The bulk of the recovered radioactivity (cpm/organ) was found in kidney and liver (white bars). However, specific activity of labeling (cpm/µg protein) in the kidney is far greater than in any other tissue (black bars). Data report the mean ± sem for 3 independent determinations. **B)** Radioactivity was substantially more concentrated in urine than in plasma (mean ± sem, n = 3).

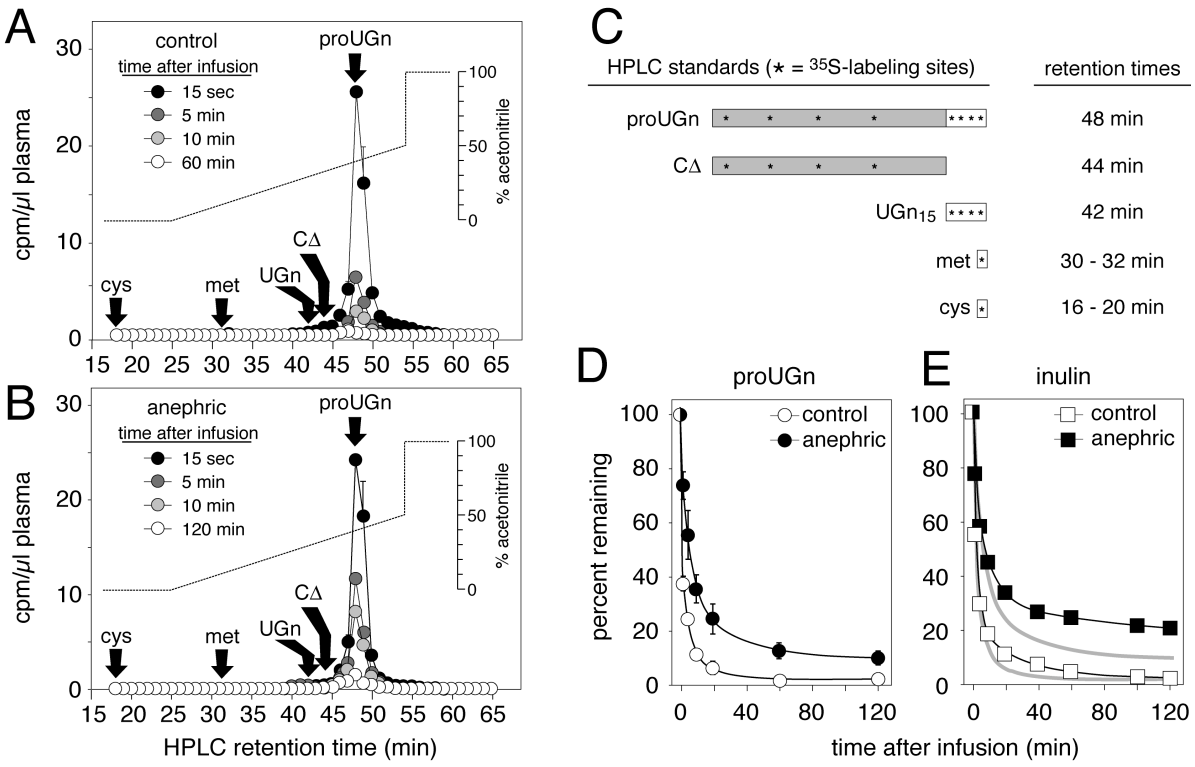

Figure 2.7 A Bolus Dose of ^{35}S-proUgn Was Cleared Rapidly From the Plasma of a Normal Animal, and Much More Slowly After Renal Ablation. A) Representative HPLC analysis of plasma samples obtained from a control animal. Radioactive material eluted in each fraction was measured in a scintillation counter, and is expressed as cpm recovered per µl of plasma applied to the column (mean ± sem for replicate column runs, n = 3). The dotted line shows the gradient of acetonitrile that was used to elute the column. **B)** Representative HPLC analyses of plasma samples obtained from an anephric animal, as in panel (**C)** Schematic depiction (not to scale) of cysteine, methionine, Ugn_{15}, proUGnD17, and proUgn standards, along with their observed retention times on the C-18 column. The retention times are also marked by arrows in panels (a) and (b). The asterisks indicate the approximate positions of cysteine and methionine residues that would be radioactively labeled in the parent molecule and its metabolites. **D)** The plasma level of radioactive proUgn is plotted as a function of time after a bolus infusion into control animals (white symbols) and anephric animals (black symbols). At each time point, the amount of proUgn in the plasma was determined by integrating the radioactivity in the proUgn peak. To correct for animal-to-animal differences in total blood volume and proUgn specific activities, the proUgn levels for each animal were normalized to the amount present at that animal's earliest (15 sec) time point. The solid lines represent the best fit of a triple exponential function to the data (see Methods). **E)** Inulin disappearance curves, obtained under the same conditions as the proUgn disappearance curves shown in panel (c). The grey curves (for proUgn) are reproduced from panel (c) for reference.

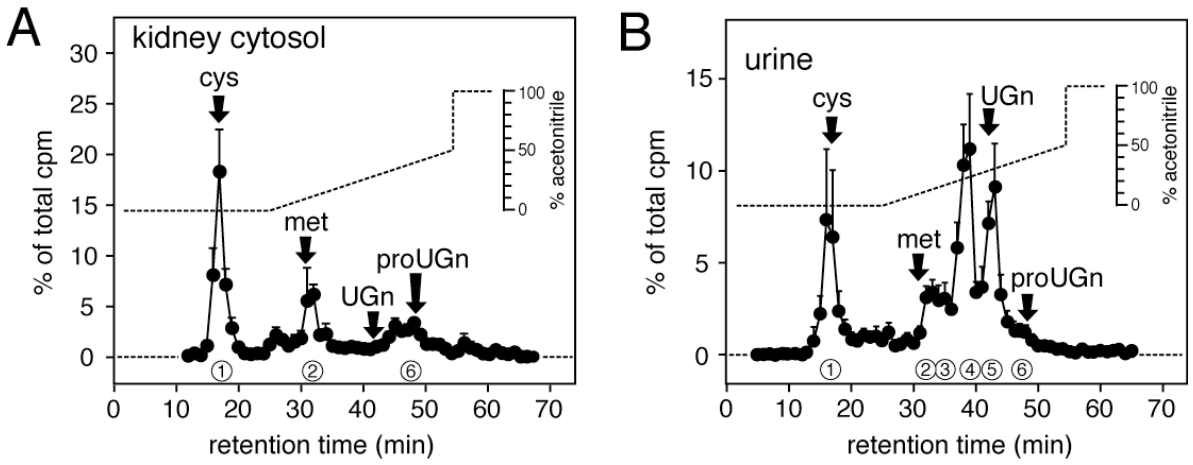

Figure 2.8 Metabolites Accumulating in Kidney and Urine During Prolonged Infusion of Radiolabeled proUgn. A) HPLC analysis of the 27,000 x g supernatant fraction (cytosol) obtained from kidney homogenates. Material was applied to a C-18 reverse phase column and eluted with a gradient of acetonitrile (dashed line). Radioactivity eluting in each fraction was measured in a scintillation counter, and is expressed as a percentage of the total radioactivity recovered (mean ± sem, n = 4). Retention times of cysteine, methionine, Ugn, and proUgn standards are marked by the arrows. **B)** HPLC analysis of urine (mean ± sem, n = 7), performed as described for panel (a). Retention times of cysteine, methionine, Ugn, and proUgn standards are marked by the arrows. Peaks numbered 3 and 4 represent unidentified metabolites. See text for details.

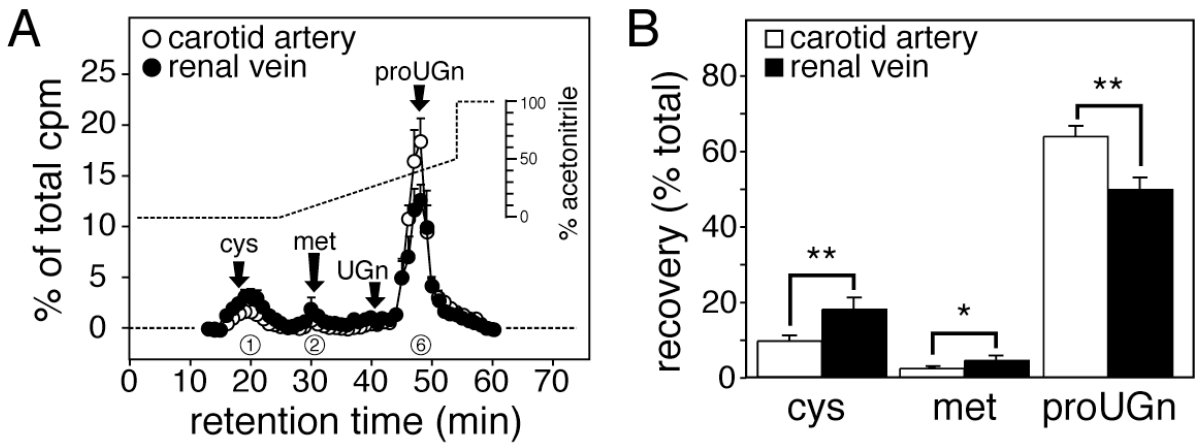

Figure 2.9 During Prolonged Infusion of Radiolabeled proUgn, the Kidney Extracted the Propeptide from the Plasma, While Secreting Radiolabeled Amino Acids Back Into the Circulation. A) HPLC profile of radioactive metabolites in systemic plasma, collected from the carotid artery (open symbols), compared to plasma collected from the renal vein (filled symbols), as in figure 2. **B)** Relative recoveries of cysteine, methionine, and proUgn. Compared to the systemic circulation (open bars), the renal vein (filled bars) contains a significantly higher proportion of metabolites, and lower proportion of intact proUgn (mean ± sem, n = 6, ** = $p < 0.01$, * = $p < 0.05$). This is consistent with the loss of some proUgn due to renal extraction, coupled with the return of some cysteine and methionine to the circulation after digestion of the extracted proUgn.

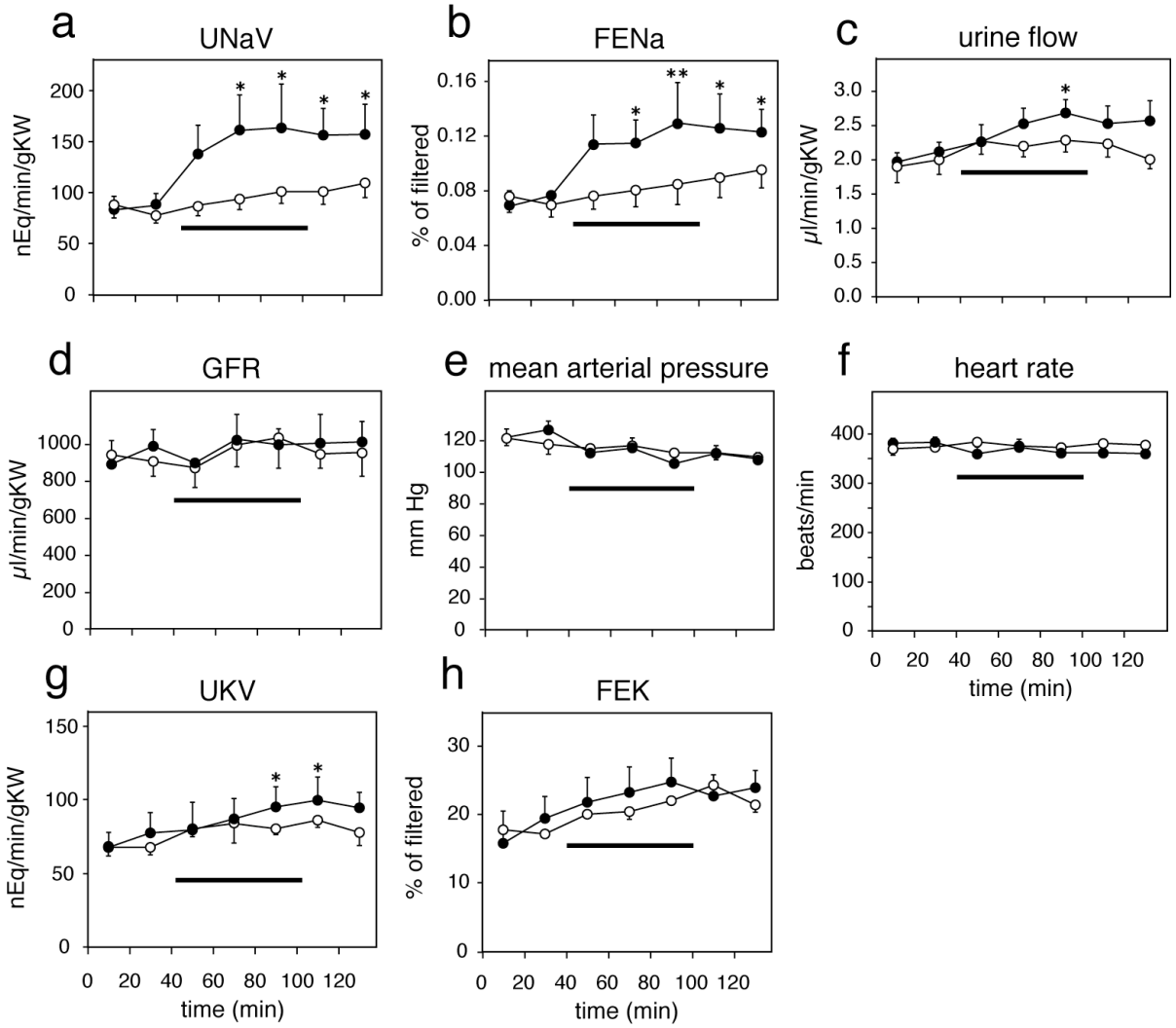

Figure 2.10 Infused hu-proUgn is Natriuretic and Diuretic in Rat Renal Clearance Studies. Horizontal bars indicate the duration of hu-proUgn infusion (100 µg/kg body weight over 60 min) in the experimental group (filled circles, n=8). Control rats (open circles, n=9) received isotonic saline in place of proUgn. Asterisks indicate a significant difference between the associated data point and the first clearance period, as determined by 1 way ANOVA with repeated measures, followed by the Bonferonni method for post hoc testing (* = $p < 0.05$, ** = $p < 0.01$).

CHAPTER III

DEVELOPMENT AND VALIDATION OF QUANTITATIVE ASSAY FOR THE ASSESSMENT OF UGN IN BIOLOGICAL SAMPLES

A. Introduction

To test the role of Ugn in the context of post-prandial natriuresis, a sound assay technique is required for the quantification of Ugn in various types of tissue samples. Two methods have been used extensively in the past, but both have shortcomings that render them inappropriate for my proposed Aim 3 studies.

The first method is an RIA technique that was developed by the Nakazato laboratory in Japan. This sensitive method has been used to quantify urinary peptide levels in rats in response to changes in dietary Na^+ (24, 111) and both plasma and urinary peptide levels in humans with renal disease (141). The drawbacks of this method are that 1) the reagents have not been made publicly available (and the lab that developed them is, in fact, no longer working in the field of Ugn research), and 2) neither a Ugn RIA kit, nor a high affinity Ugn antibody, is available commercially that would allow me to develop a comparable in-house assay.

The second method is the previously described bioassay technique that measures Ugn-evoked cGMP synthesis in the T-84 reporter cell line. There are also problems with using this method for the proposed studies; 1) Even simple biological samples (urine) must undergo a purification/enrichment step, due to the presence of interfering substances (for example, endogenous cGMP that is already present in the sample). 2) Large sample sizes are necessary, due to the relatively low sensitivity of the assay. 3) The assay has many steps that allow for the possibility of systemic errors, increasing the variability in the results.

I did employ the T84 cell assay in my initial efforts to quantify Ugn in tissue samples, such as plasma, intestinal extracts and kidney extracts (134, 154).

However, I quickly found that the protein content or some other aspect of the samples disrupted the production of cGMP by T-84 cells, putatively through oncotic pressure that negatively affected the cells tonicity and/or inhibited ligand binding to or the enzymatic activity of GC-C. Urine, though it has relatively low protein content, was particularly problematic for another reason, due to its high and variable level of endogenous cGMP. In my initial studies, this contaminating cGMP gave “false positive” values that I erroneously attributed to the presence of Ugn in my samples.

The common remedy for interfering compounds in biological samples is to enrich and purify Ugn away from the other constituents in these samples. HPLC methods utilizing properties such as size and affinity are commonly used for this, but there is inevitable loss of sample during processing that decreases the sensitivity of the assay and can be variable. More importantly, this loss during purification increases the volume required for analysis. For the greatest accuracy using the T-84 whole-cell/cGMP based assay, samples were assayed in triplicate and each data point required at least 600µl of urine even before purification. Even then, this volume usually just produces a barely-detectable signal. For reference, the urine samples that I was collecting for my diet studies were on the order of 1-2mls and the samples from acute studies where peptides were infused produced samples of ~200µl. Thus, the limited sensitivity of the assay and the relatively small volume of urine in each sample posed a significant problem.

In addition to this enrichment step, there are other steps in the T-84 whole-cell/cGMP assay that lead to intra-sample variability. The first step is to grow the T-84 cells to confluency in a 24-well culture plate, which is subject to plating and

growth conditions that can affect consistency of cell density between wells and/or platings. Next is the extraction and de-acidification of the cell supernate containing the cGMP that can also lead to intra- and inter-sample variability. Finally the cGMP RIA itself has an intrinsic variability of ±5% for the same sample in replicate (165).

In an effort to remedy these shortcomings, I explored the possibility of a competitive binding displacement assay. This assay is a modification of a previously described radio-receptor binding assay (78). My adaptation is based on competitive binding between Ugn and ^{125}I -labeled Y-Ugn at GC-C receptors in isolated T84 cell membrane preparations. Concentrations of Ugn in urine samples are calculated from a standard curve generated with pure synthetic rat Ugn. Figure 3.1 illustrates this difference where panel A shows how T-84 cells grown to confluence are incubated with ~200µl of a test solution to elicit cGMP production. Panel B from Figure 3.1 shows how the competitive binding reaction is allowed to take place in sample solutions as small as 20µl.

As described in detail in Chapter 1, GC-C is a member of a family of membrane bound guanylyl cyclases that are glycoprotein receptors consisting of multiple domains. GC-C has a ligand-binding ECD (extracellular domain), a single trans-membrane domain, a kinase-like domain and a catalytic guanylyl cyclase domain (74). Binding of ligands to the ECD leads to a conformational change that activates the intracellular catalytic domain to produce cGMP, which acts as a second messenger. The only known ligands for GC-C are the Guanylin family of peptides that are endogenous to mammals and then the family of heat-stable bacterial toxin (ST) peptides with Ugn being the only family member in the urine of most mammals

(73, 165). STa is more potent when administered to T-84 cells with a K_D ~10 fold lower for stimulation of cGMP production when compared to similar concentrations of Ugn-15 at pH 5.0 (73).

Previous studies using ^{125}I-Y-STa as a ligand have reported that there are two distinct binding affinities for GC-C to this radioligand: a high affinity binding and a low affinity binding of the receptor with disassociation constants (K_D) of 3.1 x10^{-12} and 2.2 x 10^{-9} respectively (36, 43). The studies also show that >95% of the binding at a radioligand concentration of 2.9nM is due to the low affinity receptor. Shifts towards a ratio favoring binding to the high affinity receptor do not happen until the radioligand is in the picomolar range (36, 42). Additionally, the studies demonstrate a binding-dependent shift of affinity of STa for receptors, and a correlation of the occupancy of the lowest affinity state of these sites with cyclase activation, suggesting that catalytic activity may be required for this shift (42).

Receptor-ligand binding experiments can be complicated by such factors as the presence of a single or multiple classes of receptors, or cooperativity for binding. Assumptions that must be made and factors that must be determined include: Is the binding reversible? Is there a homogeneous or heterogeneous receptor population? Does ligand binding increase the affinity of the receptor for more ligand (cooperativity)? Statistical analysis of results using variations of the Cheng–Prusoff equation that account for these factors can help define the nature of the binding relationship, based on the adequateness of fit to the data (143). Additionally, determining the correct formula to describe the binding relationship will allow for accurate interpolation of Ugn levels present in unknown samples.

B. Methods and Materials

Peptides Used

The radioligand for these binding studies was prepared from N-tyrosyl rat Ugn (Y-Ugn) obtained from Bachem Inc (Torrance CA). huUgnA and huUgnB were obtained from a commercial supplier (Bachem, Torrance CA). Synthetic rat Ugn and rat Guanylin (Gn) were purchased from Peptides International (Boston, Ma.). STa was obtained from Sigma (St. Louis, Mo.). Recombinant rat proUgn was provided by Ironwoods Pharmaceutical Inc.

Radiolabeled Tyrosinated Ugn Production and Purification

Radiolabeled Ugn trace was produced by iodinating the tyrosine residue at the end of a synthetic rat Uroguanylin-15 with an additional non-native tyrosine added at the N terminus (Y-T-D-E-C-E-L-C-I-N-V-A-C-T-G-C-OH (Disulfide bonds between Cys4 and Cys12/Cys7 and Cys15))(Bachem, USA) with ^{125}I. Iodination was performed by first activating the ^{125}I in pre-coated iodination tubes (Pierce), then transferring the activated ^{125}I to the Y-Ugn peptide solution for incubation, quenching the reaction with an abundance of free tyrosine and finally separating the peptide from the free tyrosine with a PD-Midi Trap Sephadex G-10 (GE Healthcare, Piscataway N.J.,USA) size exclusion cartridge. This semi purified ^{125}I-Y-Ugn product was then applied to a VYDAC 218TP1010 C-18 reverse phase column (Grace Vydac, Hesperia, CA), and eluted with a 0–60% linear gradient of acetonitrile over 35 min at 1 ml/min flow rate. One minute (1ml) fractions were collected and the peak of radioactivity was detected in the fraction eluting from the column at 28 minutes,

corresponding to 47% acetonitrile. This is two minutes later and 5% acetonitrile more that synthetic Ugn-15 without the tyrosine (26 minutes at 42% Acn). This purified ^{125}I-Y-Ugn was stored at 4º C. The 59-day half-life of ^{125}I limits use of the ^{125}I-Y-Ugn to approximately 8 weeks from synthesis.

Binding Assay Membrane Bound Receptor Preparation

T-84 cells were cultured on tissue culture plastic flasks in DMEM/F12 supplemented with antibiotics and 10% fetal bovine serum. Upon attaining confluency, cells were harvested by scraping in ice-cold homogenization buffer (50mMTris, 10mM NaCl, 5mM MgCl, 2.5mM $CaCl_2$). The cells were then homogenized in a glass tissue grinder (Radnoti, Monrovia, CA. USA) and centrifuged at 100,000 × *g* for 50 min at 4 °C. The supernatant was discarded and the pellet resuspended in Hanks buffered salt solution (HBSS, Invitrogen, USA, pH 7.0) then centrifuged at 2000 × *g* for 5 min at 4 °C to pellet the nuclear material and membrane aggregates. The membranes retained in the supernatant were assayed for protein concentration by the Bradford method (BioRad, Hercules, Ca. USA) and aliquoted for storage at −80 °C in HBSS until time of use.

Sample Preparation

When necessary, samples were dialyzed against diH_2O before further processing, using SpectrPor®500-M.W. cutoff dialysis membrane (Spectrum Laboratories Inc., Rancho Domingo, Ca.). Control experiments showed 100% recovery from the dialysis procedure. Plasma and kidney extracts were applied to a

VYDAC 218TP1010 C-18 reverse phase column [The Separations Group Inc. (Grace Vydac), Hesperia, CA], and eluted with a 2–55% linear gradient of acetonitrile (.01%TFA) over 30 min at 1 ml/min. Each biological sample (dialyzed, HPLC fractionated or not) was then reduced to dryness (Savant SpeedVac, Thermo Electron Corporation, Waltham MA) and re-dissolved in 100µl assay buffer (1 nM ^{125}I-Y-Ugn in HBSS minus $NaHCO_3$, 20 mM Sodium Citrate, 0.75% bovine serum albumin [Sigma, St. Louis, Mo, USA]). I then assessed and adjusted the pH of each sample using a miniaturized glass microelectrode (Microelectrodes Inc., Bedford, N.H.) and NaOH or HCl accordingly. Most samples were assayed at a standard pH of 4.5, but in some experiments the pH was systematically adjusted over a range to define the binding optimum.

Binding Reaction

Prepared samples were then incubated in replicate in polypropylene tubes with 20µl of T84 cell membranes (15–25µg protein). After 1 h of incubation at 25 °C, samples were diluted in 1ml of ice cold rinse buffer, pipetted up and down, rapidly filtered through Whatman GF/C glass microfiber filters presoaked in distilled water and then quickly rinsed twice with 5 ml of ice cold rinse buffer consisting of 50mM Tris-HCl at pH 7.0. Bound radioligand (retained by the filter) was quantified with a gamma counter (Packard Cobra, PerkinElmer Life and Analytical Sciences Inc., Waltham, Ma, USA). Ugn concentrations in sample solutions were calculated by interpolation on a standard curve computed from a dilution series of synthetic rat Ugn standard incubated in parallel with the unknowns. Non-specific binding was

determined by incubating T84 cell membranes with ^{125}I-Y-Ugn and 10^{-5} M unlabeled Y-Ugn in place of Ugn standards or unknowns.

Statistical Analysis

Values are expressed as a mean ±SEM. GraphPad Prism 5.0 (LaJolla, Ca.) was used for analysis of binding kinetics data. All formulas used in the software are derived from the Cheng-Prusoff equation (137, 143).

Experimental Animals

Rat experiments were performed on Sprague Dawley rats obtained from a commercial supplier (Harlan laboratories, Dublin VA).

Mouse experiments were performed on BL6 wild-type mice and congenic Ugn knockout mice that were backcrossed >10 generations into the BL6 line. These animals were obtained from Dr. Mitchell Cohen at Cincinnati Children's Hospital Medical Center.

All animals were maintained on a 12 hour light/dark cycle in an AALAC-approved facility with continuously available veterinary care and uninterrupted access to water and standard rat chow. All experimental procedures were approved by the Institutional Animal Care and Use Committee at the University of North Carolina at Chapel Hill, and were carried out in accordance with the NIH Guide for the Care and Use of Laboratory Animals.

C. Results

Computation of ^{125}I Iodinated Y-Ugn concentration

The HPLC purified probe produced had ~130,000 CPMs/µl. The specific activity of ^{125}I is 2.19 x 10^{6} Ci/mole or 4.5 x 10^{-7} moles/Ci. One Ci is equal to 2.2 x 10^{12} DPM, and the Packard Cobra gamma counter used for assessment of radioactivity present in samples is estimated to have a counting efficiency of 40%. Therefore, 1 CPM is equal to 2.5 DPM. Based on this I estimate I produced a stock solution of 3.25 x 10^{-7} M. Using this estimate, and published data for the optimal concentrations for the high affinity binding vs low affinity binding, I determined that I should use the radioligand in experiments at 750 CPM/µl, or a concentration of ~1 x 10^{-9} M ^{125}I -Y-Ugn. To confirm this, I performed a saturation binding experiment to determine the K_D of the binding relationship using my ligand and the T84 cell membrane preparation as prepared in our laboratory.

Determination of K_D and Optimal Assay Conditions

Increasing concentrations of radioligand were incubated with a static amount membranes/receptors in the presence and absence of cold ligand (10^{-5}M Y-Ugn). Specific binding was computed as the difference between total binding and non-specific binding in the presence of a saturating amount of unlabeled Y-Ugn. The results are illustrated in Figure 3.2 by a logarithmic line of best fit with an R^2 = .96. Statistical analysis with GraphPad Prism determined the K_D to be 1.5 x 10^{-9} ± 4.0 x 10^{-10} and maximal binding to be 275 CPMs/µg membrane protein. The cooperativity seen by other groups with regards to binding of STa to GC-C seems to not be

present in this data. This could be due to differences in the ligand or as previous publications hypothesized this dual affinity could be due to enzymatic activity which might not be preserved in my membrane vesicle preparations

The next receptor-ligand relationship parameter relevant for optimizing the assay was the time it takes for the binding reaction to come to equilibrium. This was done by determining specific binding at a variety of different time points. The results in Figure 3.3 show that the reaction comes to equilibrium at 120 minutes, with 87% of max specific binding at 60 minutes and 97% of max specific binding by 90 minutes. Non-specific binding only increased from 59 CPM at 10 minutes incubation to 150 CPM at 240 minutes. The curve was fit to the data using GraphPad Prism and had an R^2 value of .998. Based on this study, I optimized my protocol by incubating samples for 70 minutes, which allows for near-maximal binding. Under these conditions, small differences in incubation times of samples will have negligible effects on the results.

To show that the ligand receptor binding relationship is reversible I attempted to determine an off-rate. In this experiment I incubated membranes with a fixed concentration of radioligand in the presence and absence of a blocking concentration of cold peptide for 90 minutes and then diluted the reaction 90-fold. For practical limitations, I could not dilute the binding reaction any more than this, nor did I have a way to immobilize the receptor to rinse the free ligand away. The graph in Figure 3.4 shows that when the ligand concentration is reduced, the specific binding drops to a new equilibrium level over the course of 70 minutes. The new level is approximately 50% of initial level. This illustrates that the ligand binding is

reversible, a key concern when determining if this binding relationship is useful for a competitive binding assay.

Next I performed an experiment to determine the pH optimum for the binding assay. I wanted to perform the reaction at an acidic pH if possible, because previous studies using whole cell T-84 assays had shown that the affinity of GC-C for Ugn increases at acidic pH (<6) while the affinity for Gn increases at basic pH (>7). Thus, the assay would be most specific for Ugn at acidic pH, and the specificity would decrease as the pH increased. Note that the ability to vary the pH dramatically in the whole cell assay was limited by the lysis of the cells at pH less than 5.0. The results in Figure 3.5 show that, contrary to the cell lysis and destruction in the whole cell assay that prohibits enzymatic production of cGMP at lower pH conditions, this low pH increases the affinity of the ligand for the receptor in a simple binding situation. These results show the optimal pH for the assay was in the range of 3.8 - 4.8. I decided to use a standard pH of 4.5. To achieve this, a sample buffer of 4.5 was combined with the standard 7.0 pH membrane vesicle preparations, and all buffers had the $NaHCO_3$ (pKa = 10.3) omitted to shift the pH of combined buffers to a more acidic range. Figure 3.5 shows that there is a relatively stable plateau with little variation in binding between pH 4.0 and 4.8.

As another consideration, I noticed in my early assays that the Ugn peptide tends to adhere hydrophobically to plastic tubes. For example, a simple experiment with radiolabel showed that transfer from one tube to the next resulted in >10% loss due to nonspecific binding to the tube. I also noticed that excess amounts of unlabeled Y-Ugn (added to some tubes for non-specific binding determinations)

would partially prevent this loss, presumably by occupying the hydrophobic binding sites on the plastic. I then tested to see if bovine serum albumin (BSA) added to the sample buffer could inhibit non-specific binding in the same fashion, and found that concentrations above 0.7% BSA fully inhibited this binding. Additionally I had to determine if BSA would affect the binding of Y-Ugn to GC-C. The results showed that BSA in the buffer has little effect on total binding, but acts to strongly inhibit non-specific binding (presumably to the tubes, and also possibly to the membranes), and therefore gives a better signal due to reduced background. Based on these results, I add .75% BSA to my assay buffer before any cold or radiolabeled peptides are added so that they will remain in solution and not bind to the tube.

Concentration Dependent Radioligand Displacement by Ugn

In order to quantify Ugn in bio-samples, Ugn must displace the radioligand from the receptor in a concentration dependent manner that can be accurately modeled with an equation that allows interpolation of unknown values on a standard curve. Furthermore it must be statistically shown that the formula used for interpolation of values is appropriate for the binding relationship. The major considerations are 1) is it a single receptor system, 2) is there cooperatively in binding and 3) do the Y-Ugn radioligand and endogenous Ugn have the same affinity for the receptor? I used synthetic rat Ugn-15 for my standard, in anticipation that the affinities of Ugn-15 and Y-Ugn-15 for the receptor might be the same. The results shown in Figure 3.6 the amount of radioactivity bound when competing with different concentrations of synthetic rat Ugn-15. The statistical model that best fit the

data was a system with a homologous receptor, no cooperatively for binding and a slightly different affinity of the receptor for the two ligands. The curve of best fit had an R^2 = .9985 and this computed to a Ki = 1.042 x 10^{-9} ± .328 x 10^{-9} (95% C.I.).

Assessment of Uroguanylin Family Peptides

The T-84 whole cell based assay detects Guanylin family peptides with varying degrees of sensitivity, commonly thought to reflect differential affinities of the ligands for the receptor. This could also, however, be due to differential ability to stimulate enzymatic production of cGMP after binding to the GC-C receptor. A competitive binding assay would be able to measure the ligand-receptor binding affinities directly for the different peptides. Ugn is synthesized as a propeptide (proUgn) that has a very low affinity for GC-C (82, 113, 165), but after processing in relevant tissue compartments in the rat to the 15 amino acid (16 in human) the mature form is able to bind GC-C with high specificity (40, 113). Figure 3.7 illustrates that Ugn has a 1000 fold greater affinity for GC-C than does proUgn.

Additionally, previous studies have shown that the Ugn peptide shifts back and forth between two distinct conformations, termed Ugn-A and Ugn-B (87). For the rat isoforms of Ugn, this reaction occurs at a rate of 1–2 cycles per sec at 37° C at neutral pH (57), and therefore any sample of rat Ugn is a racemic mix of the two forms. In the human isoform (h-Ugn-16), the extra leucine residue on the C-terminus inhibits the conformational change, and extends the half-life of the separate conformers to 48 hours (29, 101). Additionally, the two conformations have different properties on a reverse phase HPLC column, and therefore can be isolated from each other. In the whole T-48 cell assay employed previously it had been observed

that these two different topoisomers have differential ability to elicit cGMP production (29). They also have different physiological effects when infused into animals (135). When I assayed the human Ugn-A and Ugn-B using the competitive binding assay, I observed (Figure 3.8) that Ugn-A had a three-fold greater affinity for the receptor than the racemic mix of synthetic rat Ugns, but Ugn-B had a ten fold lower affinity than the racemic rat mix. These results are consistent with previous studies of mine using whole cells.

The Ugn related peptide Guanylin is also produced in the small intestine and has been found in the plasma as a propeptide but is not found in the urine of most mammalian species (99). This is due to its susceptibility to proteolytic cleavage (33, 51). A single experiment found a Gn-like peptide in the urine of opossum when 8 liters of starting material was enriched. The concentration was estimated to be 10^{-10}M Gn (83). It is therefore important to know if Gn in levels that might be present in urine samples could contribute to the displacement of radioligand when attempting to quantify Ugn. Figure 3.9 shows that at pH 4.5 Gn has a Ki = 1.7×10^{-7}, and must be present at levels higher than 10^{-8} M to elicit a response. This is much higher than the 10^{-10} M that past investigations have detected (83). Additionally, differences in affinity between the two molecules is such that when samples are diluted to put Ugn in an appropriate range for the assay, Gn at known levels would be well below the threshold for detection.

The molecule that has the greatest potency for stimulating cGMP production by GC-C in T-84 cells is the heat stable toxin from enteric *E. coli* (STa). STa is ~10 fold more potent than Ugn-15 at pH 5.0. When I assayed STa for radioligand

displacement from GC-C/membranes, it had approximately the same Ki and therefore the same affinity for the receptor as the synthetic rat Ugn-15 standard (Figure 3.10). Previous studies have suggested that initiation of catalytic activity by GC-C has a cooperative effect on further STa binding to the receptor, and therefore the lack of catalytic activity in the membrane preparations (in the absence of GTP, which is required as the substrate for cGMP synthesis) could render the affinity the same as Ugn-15.

Optimization of Conditions for Biological Samples

The method utilized for analysis of biological samples is to dry them to complete dryness and resuspend them in an equal volume or less of sample buffer, in order to increase sensitivity of Ugn detection while minimizing the loss due to purification or enrichment steps. With the receptor binding competition assay being dependent on pH, each individual sample must be assessed for proper pH. Trials of different buffer compositions determined that a buffering salt with a pK_a near the range of the desired pH was optimal. The buffer that I use is made with Hank's Balanced Salt Solution and sodium citrate added. Citrate has a pK_a of 4.8, so this is ideal. However, HBSS can optionally contain $NaHCO_3$, which has a pK_a of 10.3. Empirically I observed that physiologic samples in buffer without $NaHCO_3$ were easier to pH properly with minimal addition of acid and base, reducing changes in volume and thus Ugn concentration. A test was done on the buffer with and without $NaHCO_3$ to determine if it had an effect on binding. The absence of NaHCO3 had no statistically significant effect on the specific binding of Y-Ugn to the membrane preparations.

Assessment of Urinary Ugn with Binding Assay

The ability of the proposed assay to accurately quantify Ugn in biological samples requires that these biological samples not alter the ligand-receptor binding relationship in any way. To investigate this, I used the assay to quantify a serial dilution of a urine sample. The results reported in Figure 3.11 show the radioligand displacement signal from full strength urine plotted on the line of best fit for the Ugn-15 standard displacement curve (orange circle). This sample was estimated to be ~10^{-8} M Ugn. When I plotted the radioligand binding for each urine dilution, dividing this interpolated [Ugn] by the dilution factor the values fell precisely on the curve of best fit for the Ugn-15 standard. This demonstrates that the "unknown" that is being detected by the assay has exactly the same affinity for the receptor as does the authentic rat Ugn standard.

To further ensure that some component of the urine was not altering the Y-Ugn-GC-C binding relationship, I prepared a dilution series of Ugn-15 standards in normal-strength urine by resuspending dried urine in one half of its original volume of sample buffer and combining aliquots with equal volumes of the Ugn-15 standards at twice their desired concentrations. Therefore the signal observed for each sample should reflect the sum of the [Ugn-15 standard] and the [Urinary Ugn]. Any deviation would imply enhancement or diminishing of the radioligand binding by urine constituents in a manner that was independent of the Ugn present in the sample. The results in Figure 3.11 show that when the concentration of neat urine is determined and then added to the concentration of Ugn-15 in the urine spiked samples, the curve (blue symbols) values fall right on the curve of best fit for [Ugn].

Assessment of Urinary Ugn From a Ugn-/- Mouse

An additional effort was made to determine that no constituents of urine other than Ugn are responsible for radioligand displacement by utilizing urine from knockout mice that have the gene coding for Ugn disabled. Rats and mice have the same sequence for mature Ugn-15, and both being from the same subfamily, *Murinae*, it would be expected that their urine composition would be very similar. Urine was collected from wild type and knockout animals, dried to dryness and a serial dilution of each was assessed in the binding assay. As can be seen in Figure 3.12, wild type mouse urine is able to displace radioligand binding in a concentration dependent manner, exactly the same as I previously observed with rat urine. However the urine from the Ugn-/- mouse had no effect on binding.

Protocol Modifications to Compensate for Experimental Urine Properties

The receptor binding competition assay depends on a fixed affinity of the receptor for radioligand Ugn in the sample. Any alterations in this relationship can give a false signal, negative or positive (if the radioligand affinity is increased of decreased, respectively). Additionally, sample characteristics, or treatment of samples during processing or sample collection, might cause precipitation of the radioligand that would confound the assay by changing the concentration of free ligand available for binding.

In this regard, the urine samples generated during physiological studies (including those from animals undergoing peptide infusions, Gut Tie-off experiments and diet studies) could potentially contain exogenous molecules and properties not

normal to basal urine. During Gut Tie-off experiments, for example, animals are infused with a 10% mannitol solution in order to maintain GFR. During many studies, animals are also infused with FITC-conjugated inulin for clearance determinations.

I tested the effects of mannitol on the ligand-receptor relationship by adding concentrations of mannitol that would be expected in the urine after infusion into the circulation of anesthetized animals. I found that mannitol does in fact affect the relationship, inhibiting radioligand binding. Therefore, I tested the ability to dialyze away the mannitol by spiking a rat urine sample with a known amount of synthetic Ugn and ±mannitol, then dialyzing, drying and comparing. I observed that accurate quantification of Ugn in the urine was restored after 2 hours of dialysis with 500MW-cutoff membrane against diH_2O with no loss of Ugn in the sample, as its size is ~1.7kDa.

Assessment of Ugn in Plasma and Kidney Extract

The receptor binding competition assay was used to assess the amount of Ugn in plasma and tissue extracts to ascertain if the increased sensitivity would allow for detection in tissues where Ugn had previously not been found. Neat samples of plasma and kidney extract were analyzed and did inhibit binding but not in a concentration dependent manner as was seen with urine. Sample were purified across a C-18 reverse phase column and single 1ml/minute fractions were collected. Samples from fractions in the range where Ugn is known to elute were dried, suspended in assay buffer and pH adjusted. Enigmatically some fractions adjacent to where Ugn was expected to elute from the column displayed enhanced binding of radioligand, more CPMs bound than with no competitor present. No inhibition to

binding was detected where Ugn elutes from the column. Additional kidney extracts were analyzed that had been spiked with synthetic rat Ugn before HPLC processing and sample preparation, at amounts equal to an extract concentration of 10^{-9}M Ugn. These fractions gave comparable binding to equal molarity Ugn standard therefore Ugn in urine and plasma is likely below the detection threshold of this assay, ~2 x 10^{-10} M Ugn.

D. Discussion

These studies detail the development of a novel assay technique for quantifying Ugn in biological samples. The results of these studies confirm that this assay can be used to address specific questions regarding the role of Ugn in post-prandial natriuresis that were previously unanswerable. Results indicate that this Ugn assay can be used to determine peptide levels in smaller sample sizes and with greater sensitivity than prior assays. The sensitivity is almost two orders of magnitude greater than the previous T84 cell method for quantification of Ugn.

In addition to being more sensitive, it is more accurate for the different peptide family members. The previous assay was dependent on the catalyzed synthesis of cGMP via GC-C and it is not known whether the different ligands have the same potency in stimulating this synthesis at a comparable level of binding.

The results presented here indicate that because the observed K_D of the two of ligands, Ugn and STa, are approximately equal, that the receptor occupancy at a given concentration is hypothesized to be the same. This would lead to the

conclusion that the ability of STa to elicit greater production of cGMP via GC-C than Ugn at a comparable concentration is not due to affinity for the receptor but due to increased catalytic activity when bound. This differential catalytic activity could also apply to other guanylin family members, and is significant because it means that the previously utilized whole cell T-84/cGMP assay may not have been accurate if a different peptide family member was being used as the standard for quantification.

Statistical analysis of the kinetics of the binding of the radiolabeled Y-Ugn to the T-84 membrane preparations and in competition with pure synthetic Ugn indicates that there is a single class of receptors, GC-C as confirmed by earlier work with GC-C knockout animals (96). The results indicate that the tyrosinated Ugn has a slightly greater affinity for the receptor than the synthetic Ugn-15 as illustrated by its lower K_D.

A number of specific experiments were performed to evaluate whether this assay would allow me to accurately determine Ugn levels in urine (and other biological samples). The key points are:

- The radioligand displacement by rat urine and wild type mouse urine dilutes the same as it does for synthetic Ugn standard
- Urine from a Ugn knockout mouse fails to inhibit radioligand binding
- There is stability in the amount of binding displacement between pH 4.0 and 4.7
- Exogenous factors (inulin and mannitol) have no effect on binding or can be dialyzed away with no change in signal
- Plasma and kidney extract Ugn content is below detection threshold

By applying a variation of the Cheng-Prusoff equation to the radioligand displacement resulting from a concentration response curve of synthetic rat Ugn, an accurate measuring tool has been developed to quantify Ugn in biological samples. This tool can be used to investigate questions that previously were intractable, and has allowed me to address previously undefined aspects of the role of Ugn in Na^+ and fluid homeostasis, which will be illustrated in Chapter 4.

Figures

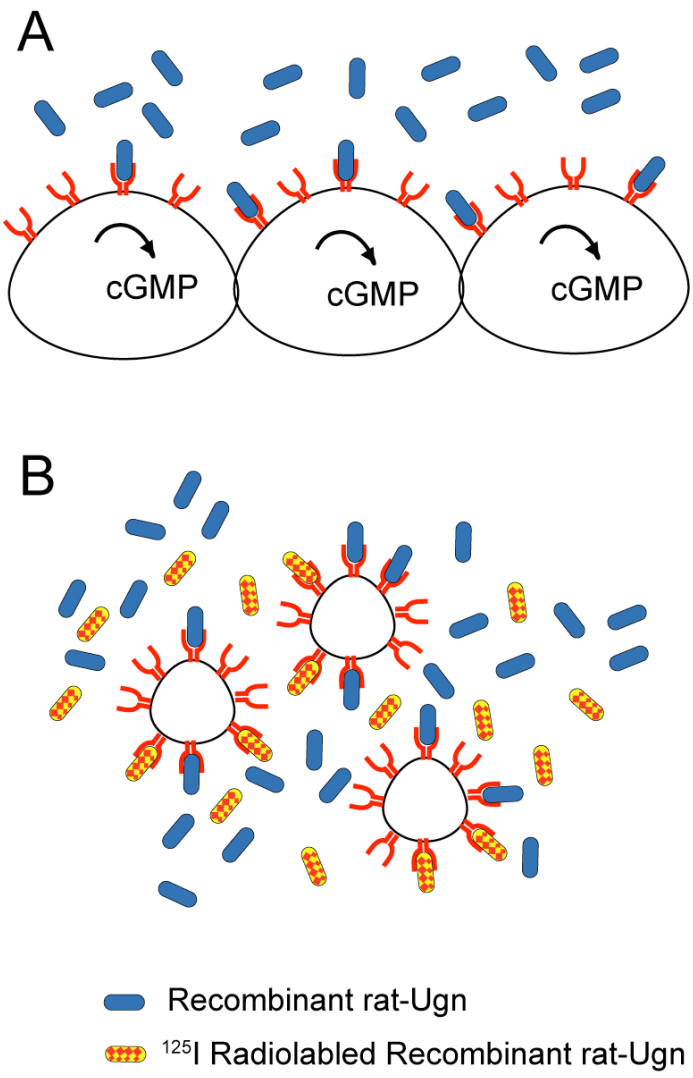

Figure 3.1 Graphic of T-84 Cell Assay vs Membrane Binding Assay. A) Illustrates binding of Ugn (blue oval) to GC-C (red receptor) in whole T-84 cells to catalyze cGMP production in a concentration dependent manner. **B)** Illustrates competition between Ugn and ^{125}I-radiolabeled Y-Ugn for binding to GC-C in T-84 cell membrane homogenates.

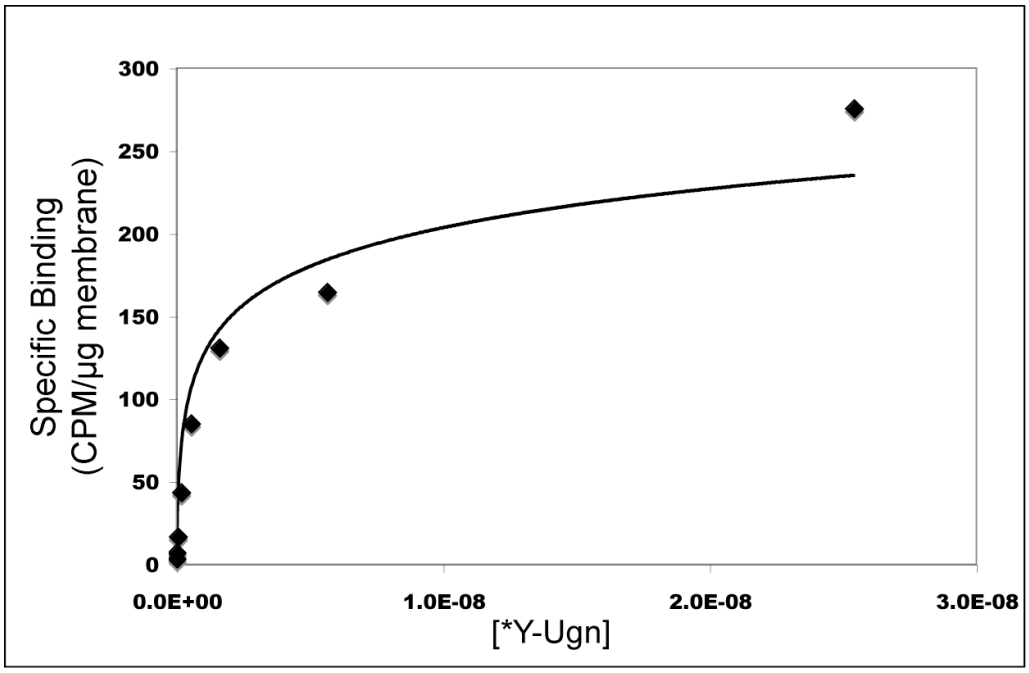

Figure 3.2 Specific Binding Curve. Graph of specific binding to GC-C at various radioligand concentrations. All radioligand concentration were used on an equal amount of membranes. K_D was determined to be 1.5 x 10^{-9} +- 4 x 10^{-10} and maximal binding to be 275 CPMs/µg membrane protein. R2 = 0.964, Mean±SEM.

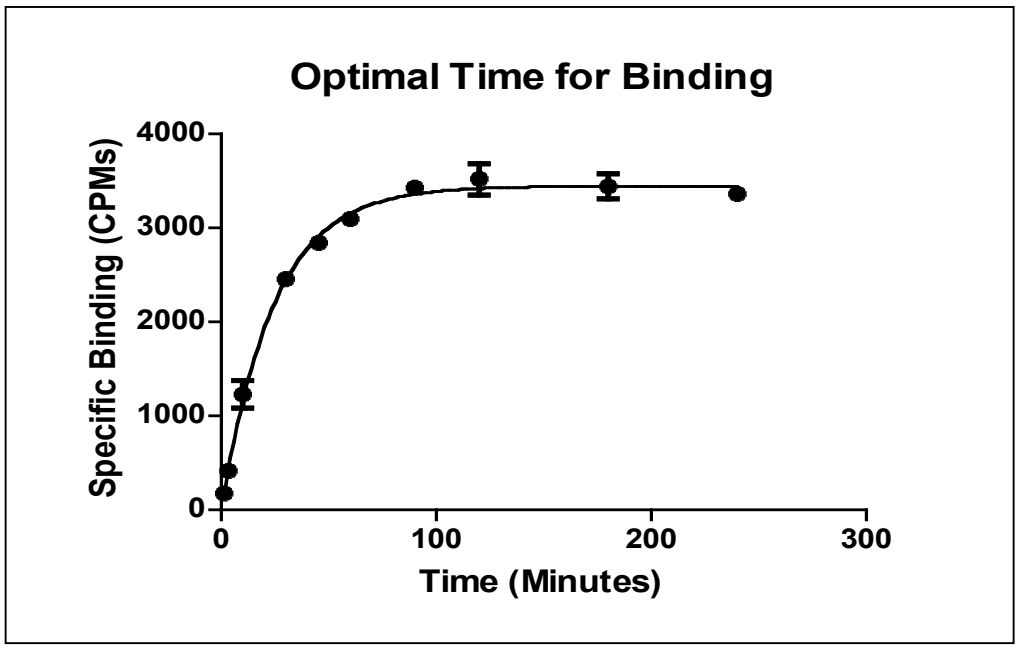

Figure 3.3 Association Rate Binding Curve. Graph of the amount of specific binding (CPMs) when membranes are incubated with 10-9 M ^{125}I -Y-Ugn for various lengths of time, R^2 = 0.998, Mean±SEM.

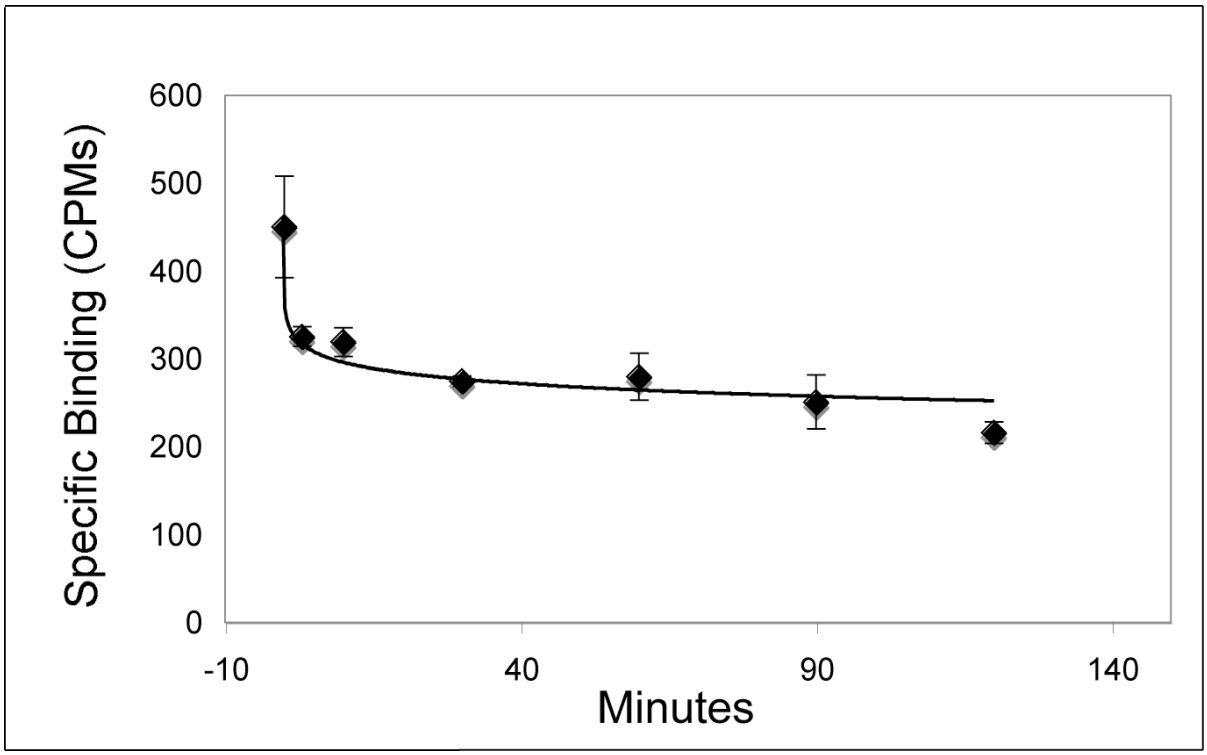

Figure 3.4 Disassociation Rate Binding Curve. Graph of specific binding (CPMs) when maximally bound ligand was diluted 90-fold for various lengths of time. R^2= 0.974, Mean±SEM.

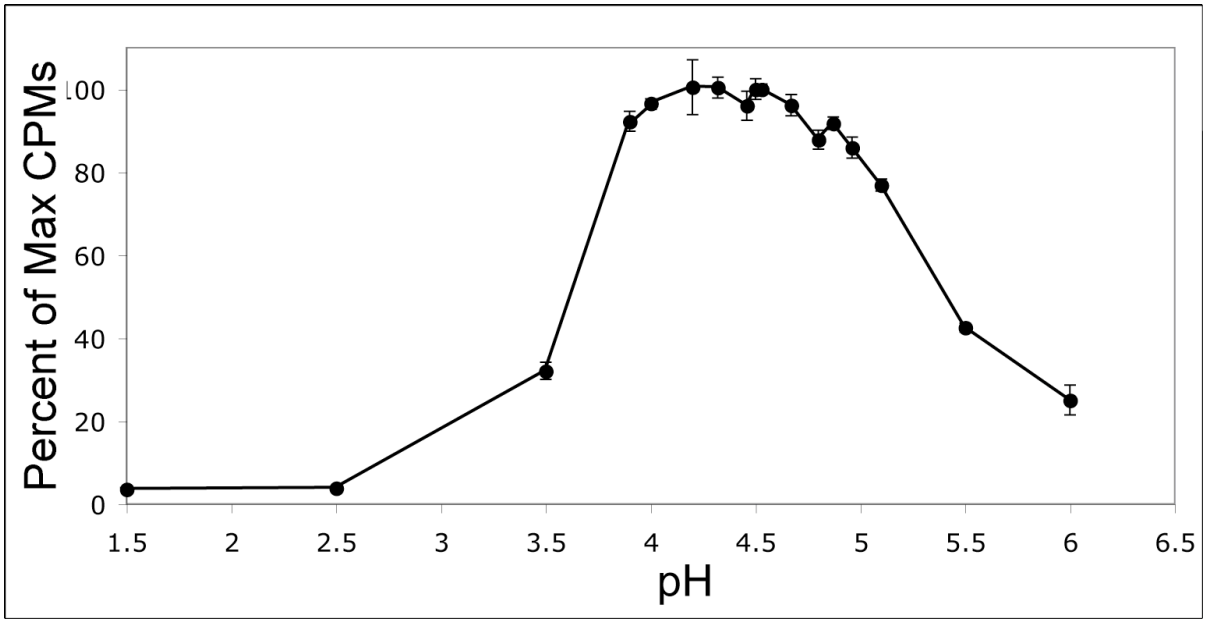

Figure 3.5 Association Curve at Various pHs. Graph of specific binding (percent of max CPMs bound) when membranes were incubated with 10-9 M ^{125}I -Y-Ugn at various pHs. n=3 values are Mean±SEM.

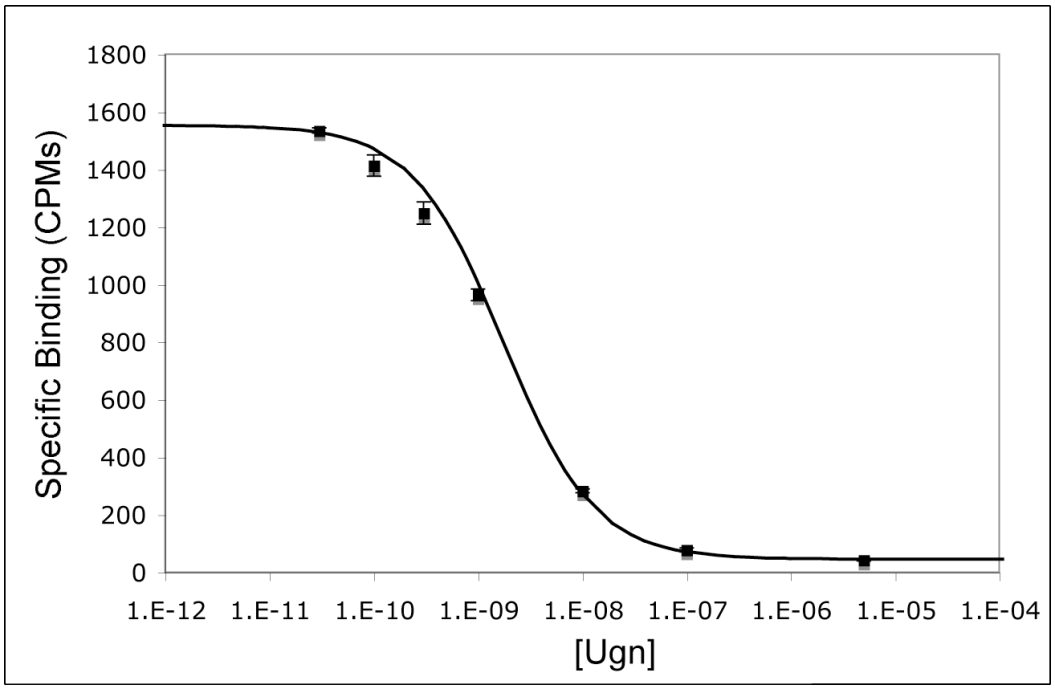

Figure 3.6 Radioligand Displacement by Recombinant Rat Ugn. Graph of specific binding (CPMs) when membranes were incubated with various concentrations of recombinant rat Ugn-15 for 70 minutes. R^2 = 0.9985 n=3 values are Mean±SEM.

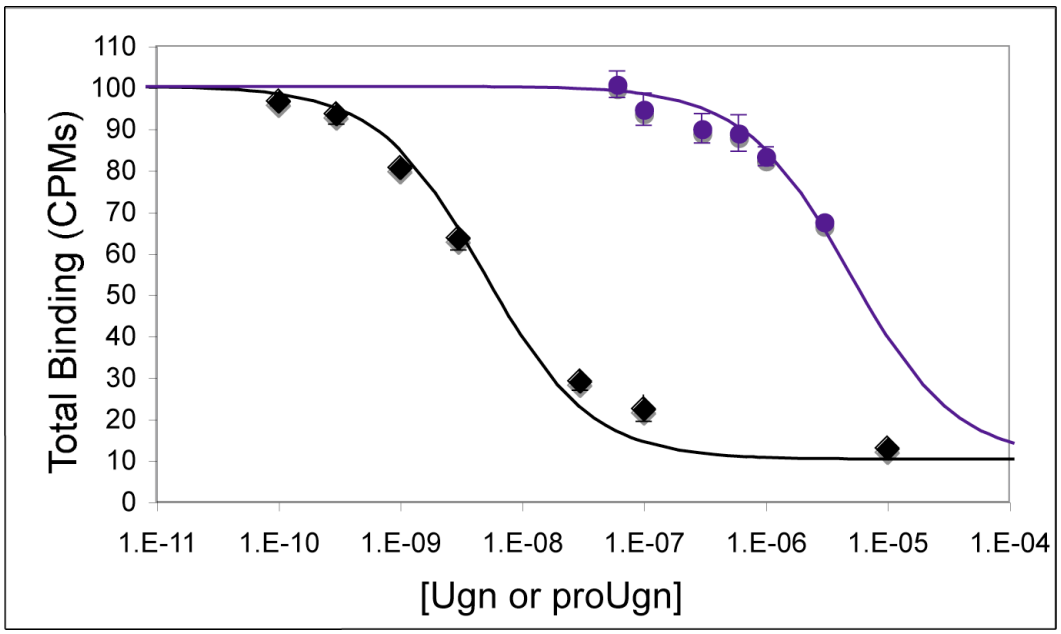

Figure 3.7 Radioligand Displacement by Recombinant Rat proUgn. Graph of total binding (CPMs) when membranes were incubated with various concentrations of recombinant rat Ugn (black line and diamonds) or recombinant rat proUgn (Purple line and circles) for 70 minutes. R^2 = 0.9677 n=3 values are Mean±SEM.

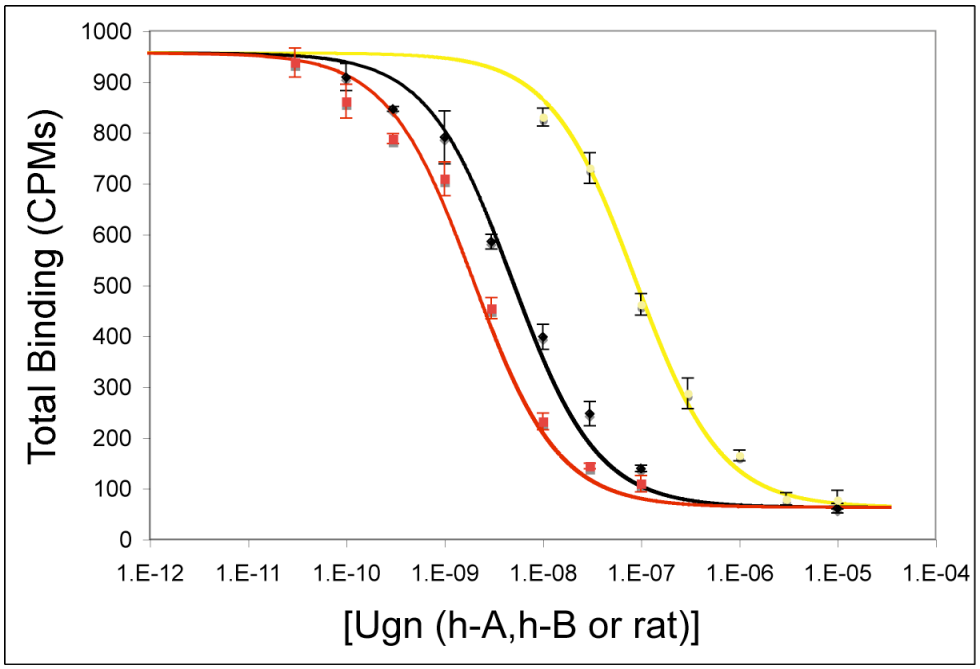

Figure 3.8 Radioligand Displacement by Recombinant Human Ugn-A and Ugn-B. Graph of total binding (CPMs) when membranes were incubated with various concentrations of recombinant rat Ugn (black line and diamonds) or recombinant human Ugn-A (Red line and squares) or human Ugn-B (Yellow line and circles) for 70 minutes. Ugn-A R^2 = 0.9686 Ugn-B R^2 = 0.9892, n=3 values are Mean±SEM.

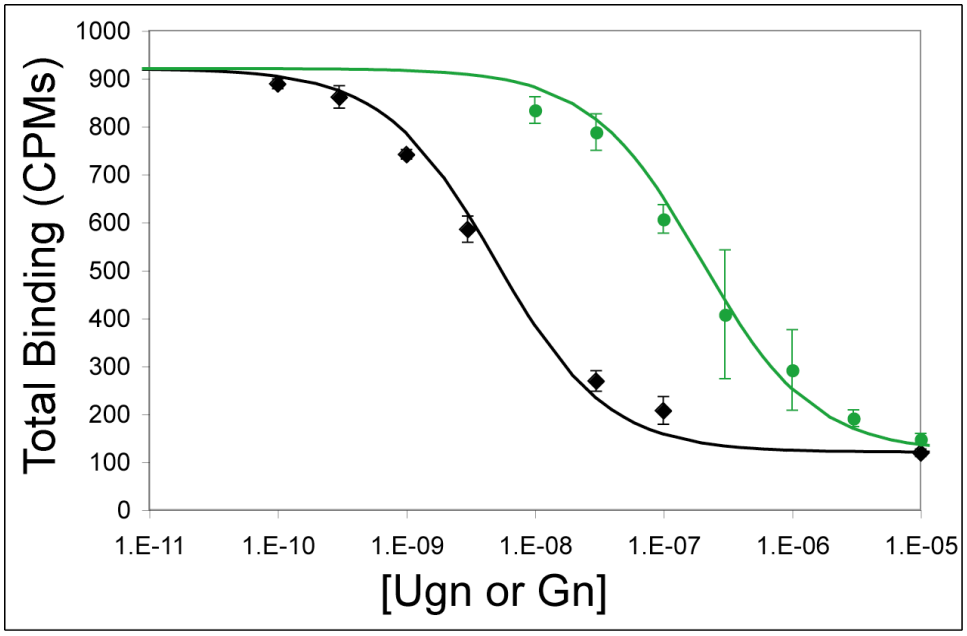

Figure 3.9 Radioligand Displacement by Recombinant Rat Gn. Graph of total binding (CPMs) when membranes were incubated with various concentrations of recombinant rat Ugn (black line and diamonds) or of recombinant rat Guanylin (green line and circles) for 70 minutes. Gn has a Ki = 1.7 x 10^{-7} R^2 = 0.9587 n=3 values are Mean±SEM.

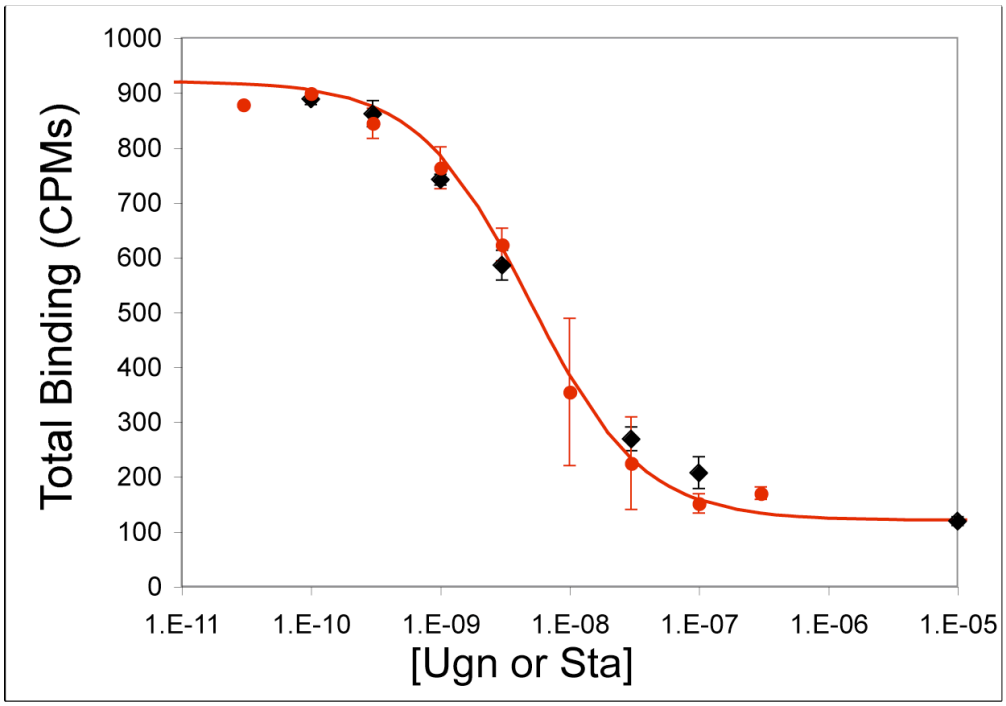

Figure 3.10 Radioligand Displacement by *E. Coli* Sta. Graph of total binding (CPMs) when membranes were incubated with various concentrations of recombinant rat Ugn (black line and diamonds) or *E. coli* heat stable toxin (red line and circles) for 70 minutes. R^2 = 0.9834, n=3 values are Mean±SEM.

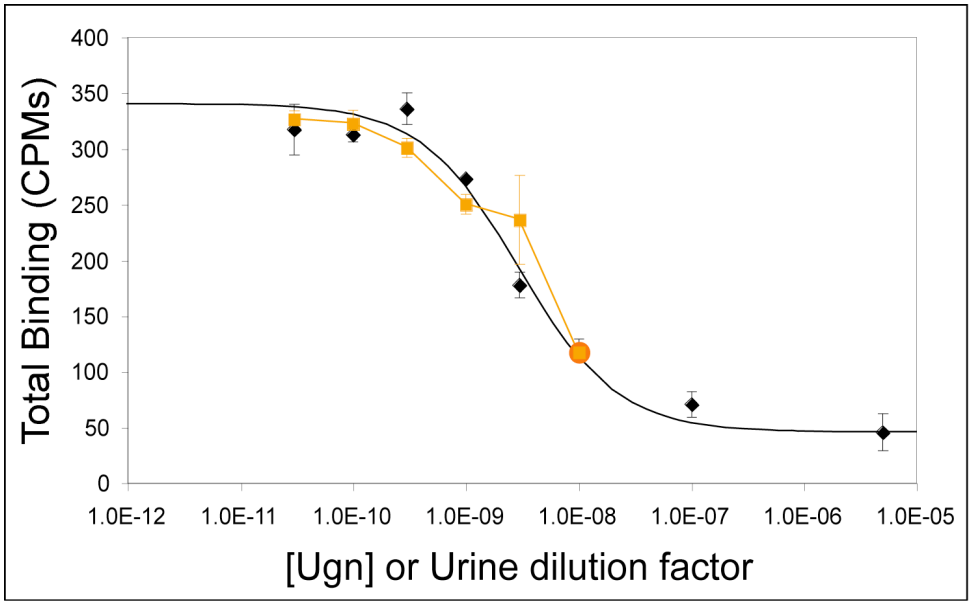

Figure 3.11 Radioligand Displacement by Rat Urine. Graph of total binding (CPMs) when membranes were incubated with various concentrations of recombinant rat Ugn (black line and diamonds) or a dilution series of rat urine (light orange line and squares) for 70 minutes. Orange circle indicates interpolation of "Ugn" in the sample that the dilution series of the urine "[Ugn]" was based on. R^2 = 0.9699, n=3 values are Mean±SEM.

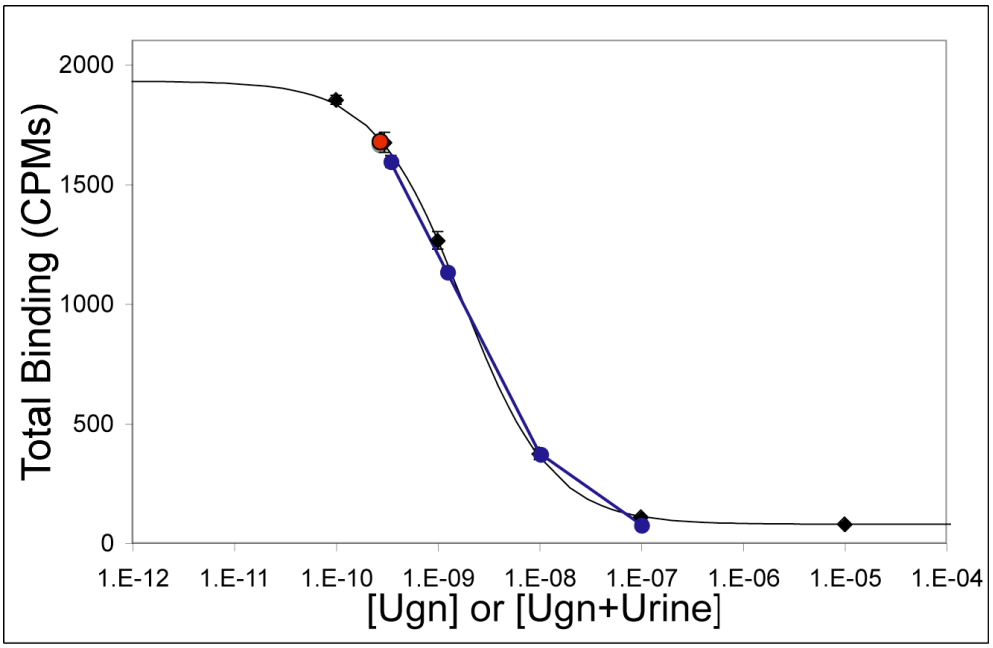

Figure 3.12 Radioligand Displacement by Rat Urine. Graph of total binding (CPMs) when membranes were incubated with various concentrations of recombinant rat Ugn (black line and diamonds) or a various concentrations of recombinant rat Ugn in rat urine (blue line and circles) for 70 minutes. Red circle indicates interpolation of "Ugn" in the urine sample that was added to the recombinant Ugn. R^2 = 0.9819, n=3 values are Mean±SEM.

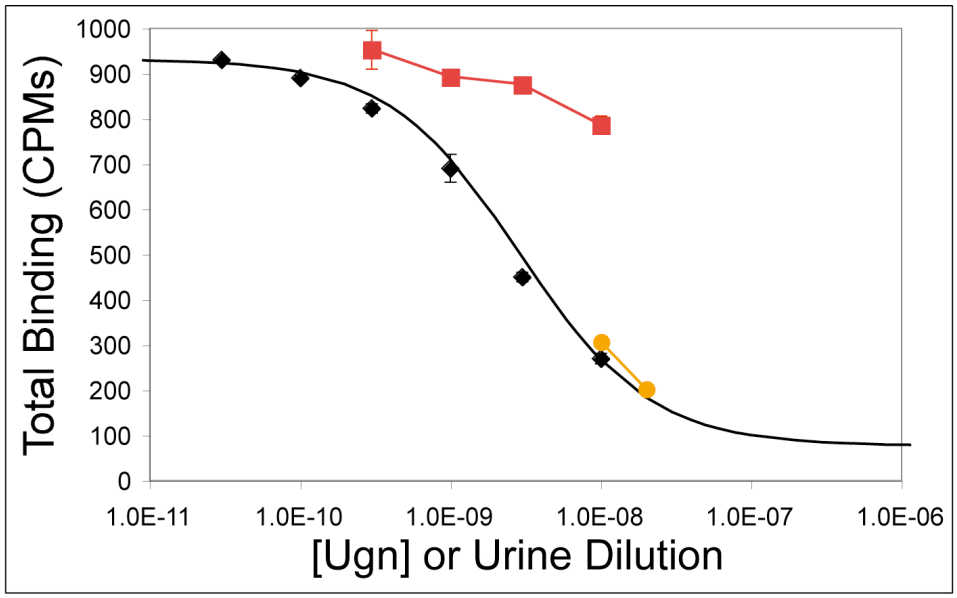

Figure 3.13 Radioligand Displacement by Ugn-/- Mouse Urine. Graph of total binding (CPMs) when membranes were incubated with various concentrations of recombinant rat Ugn (black line and diamonds) or a dilution series of mouse Ugn+/+ urine (light orange line and squares) or a dilution series of mouse Ugn+/+ urine (light orange line and circles) or a dilution series of mouse Ugn-/- urine (red line and squares) for 70 minutes. n=3 values are Mean±SEM.

CHAPTER IV

INTESTINAL PROUROGUANYLIN PLAYS A ROLE IN VOLUME HOMEOSTASIS, POSSIBLY A DIRECT RESPONES TO ORAL SODIUM

A. Introduction and Hypothesis

The Roles of proUgn and Ugn in Post-Prandial Natriuresis

The central hypothesis that has guided work in the Ugn field over the past 15 years is that the polypeptide product of the proUgn gene is 1) generated within the intestine, 2) released from the intestine in response to oral Na^+ intake, and 3) participates in the post-prandial natriuresis (PPN) that occurs in the kidney after oral Na^+ intake. Evidence presented thus far in this thesis is generally consistent with this hypothesis. The Ugn gene encodes a propeptide (proUgn) that is produced and stored in the intestine and secreted into the bloodstream. As shown below (Figure 4.5), essentially all (~90%) of this circulating proUgn is supplied by the intestine. Evidence presented in Chapter 2 demonstrates that circulating proUgn is filtered by the kidney where it is completely broken down into smaller metabolites (including Ugn) that can induce natriuresis by an as-yet undefined mechanism (134, 154). However, the situation is complicated by the fact that the kidney also makes proUgn (Chapter 2). Although the kidney does not release its proUgn into the circulation (Nicholas Moss, unpublished data), the locally produced propeptide could nevertheless play a paracrine or exocrine role within the kidney to regulate Na+ excretion. Therefore, to rigorously implicate Ugn and proUgn in the hypothesized entero-renal endocrine pathway that initiates PPN, changes in circulating proUgn and urinary Ugn are predicted to be linked to dietary intake of Na^+. Furthermore, it is important to show that the changes in peptide levels induced by dietary Na^+ are adequate to stimulate a natriuretic response commensurate with their postulated function. Using the proUgn assay described in Chapter 2 and the Ugn assay

described in Chapter 3, it is possible to investigate two key questions that are corollaries of the central hypothesis: a) Does intake of dietary Na^+ directly affect circulating proUgn and urinary Ugn levels? b) Are changes in urinary Ugn levels induced by salt diet the direct result of changes in plasma proUgn concentration?

Changes in Ugn and proUgn due to Sodium

In the introductory chapter, Table 1.1 presents the results from studies in which Ugn-related peptide levels were measured in tissue, plasma, and urine before and after adjustments in dietary Na^+ (24, 25, 50, 95, 100, 152). These data do not strongly support a entero-renal link that is mediated by Ugn or proUgn. Expression of proUgn mRNA in the intestine and plasma proUgn polypeptide levels do not been consistently change in response to increased salt intake, as published results on this issue are contradictory and fragmentary. For example, one study demonstrated an increase in intestinal mRNA due to changes of Na^+ in the water but not in the food (23), while another study reported no change in intestinal mRNA in response to chronically increased Na^+ in the food but a 2-fold increase eight hours after gavage of a oral Na^+ bolus (25), and a third study noted a 30% increase in enteric Ugn mRNA expression by Northern blot in response to a sustained high Na^+ diet (50). Changes in plasma proUgn and/or Ugn levels in response to dietary Na^+ have also been noted, but these results, too, are debatable.

A problematic aspect of these past studies is the lack of a sensitive assay that is specific for Ugn. To date, studies analyzing changes in this system due to alteration in dietary Na^+ have reported their results in terms of “Ugn-related peptides”. The radioimmunoassay commonly used to determine these values utilizes

an antibody directed towards Ugn. As described in Chapter 1, Ugn defines the C-terminus of the propeptide and its sequence is shared among multiple peptide species generated from the proUgn gene (Ugn-15, Ugn-18, Ugn-24 and proUgn) (81, 101, 108). The solution to this problem is HPLC purification of Ugn from each biological sample, but this reduces sensitivity and requires large sample sizes.

The most comprehensive study, by Fukae et.al.(67), looked at changes in gene expression and polypeptide levels in animals on a 5% Na^+ diet, relative to those in animals maintained on a control diet. Samples were taken at day 7 on each diet, so the experimental animals were in a state that would be considered salt-adapted. Fukae et al. saw a greater than 3-fold increase in urinary "Ugn-related peptides" but no change in plasma "Ugn-related peptides". Expression of the proUgn gene in the kidney and the intestine both apparently increased in relation to a housekeeping gene, but no statistical significance was noted for these responses.

Only two studies have looked at a time period short enough to be considered an acute response; one study was performed by Dr. Mitchell Cohens' group (50) and the other by Carrithers et.al. (25). These results are in slight disagreement with each other with regards to a short-term intestinal response to high salt. The Carrithers study saw a 2-fold increase in intestinal Ugn mRNA when animals that were being fed a low Na^+ diet were given a gavage of a bolus of NaCl. This is simply mRNA message though and not expression or secretion.

Cohen's group took a plasma sample from mice 24 hours after a switch from normal to high salt diet. Western blot analysis showed a 40% decrease in circulating proUgn. This is not the expected response for a signaling molecule that activates

salt excretion in response to salt ingestion. Another study by this group with the same protocol, Ugn-/- mice showed that these mice had an impaired renal response to abrupt increases in dietary Na^+ content, transiently excreting less Na^+ in the urine than wild-type animals during the first two days after switching to high salt chow (50). The combination of these experiments—a deficient natriuretic response from proUgn-/- animals to a salt load, but no increase in plasma proUgn in wild-type animals subjected to the same salt load—leads to an alternate hypothesis: that intestinal proUgn is irrelevant, and proUgn produced locally within the kidney (see Chapter 2) is responsible for regulating post-prandial salt excretion.

Circadian proUgn Expression and Excretion

Excretion of Ugn in the urine has a circadian rhythm. During a study of patients with heart failure, Carrithers et.al. (24) noted that healthy humans excrete more Ugn in the urine during the 6 hour daylight period from 8am to 2pm than from the other 3 periods. This cycle is more pronounced in males than females (24).

Another experiment looking at intestinal tissue from mice that were sacrificed at six evenly spaced times throughout a 24 hour period showed highest mRNA levels in the periods of darkness (when the animals are awake and active) (152) Interestingly, expression was elevated first in the ileum, followed by an increase in the jejunum with a phase delay of 2 hours. This is contrary to what is expected if luminal content of Na^+ (ingested during the animals' waking hours) is the trigger for increased expression, as the jejunum is proximal to the ileum.

Receptor or Signaling Mechanism of proUgn in the Kidney

proUgn is known to act through GC-C in the intestine via Ugn, but less is known about the mechanism that mediates Ugn's actions in the kidney. In addition, there is uncertainty about where Ugn acts in the kidney. Some reports allude to effects in the proximal tubule (94), while others emphasize effects in the collecting duct (26, 27, 30).

A number of lines of evidence argue that GC-C is not the primary receptor responsible for Ugn's actions in the kidney. 1) When the gene for GC-C is disabled in mice, the intestinal effects of Ugn are severely compromised, but the animals are still renally responsive to infusions of Ugn (22, 98). 2) Human Ugn occurs in two semi-stable isomeric forms (A and B). The B form increases Na^+ excretion when infused into rats, even though it is almost completely incapable of activating GC-C (135). 3) Functional biochemical measurements and RT-PCR analyses show that GC-C expression is negligible in the rat kidney (Qian et al, submitted), even though isolated rat kidneys respond well to Ugn infusions (57, 67, 139). 4) In vitro responses to Ugn have been observed in renal cell lines that fail to express GC-C (74,170).

Thus, GC-C appears to be unnecessary for the renal effects of Ugn. Therefore, it seems probable that Ugn acts on an alternate, cGMP-independent receptor in the kidney. Several groups have suggested that this renal receptor for Ugn is a pertussis toxin-sensitive G protein (22, 74, 129).

Prior studies with Ugn/proUgn infusions

The effects of Ugn on the kidney have been studied extensively. Ugn has been tested in rats and mice both in vivo and in isolated perfused kidneys. Dose dependent increases in UK^+V, UNa^+V and urine volume were seen following bolus intravenous injections of Ugn to conscious animals, using a technique known as the sealed-mouse renal function assay (23). In an isolated perfused kidney preparation, Ugn infusion elicited diuresis, natriuresis and an increase in GFR (56, 108, 187). Ugn can both depolarize and hyperpolarize membranes at high and low concentrations, respectively, in isolated collecting duct principal cells (172).

In contrast, investigation into the renal effects of proUgn is limited. The natriuretic effects of proUgn have been reported by our research group (112, 136) and by Greenberg et al. in abstract from a meeting that has not been published (76). In all of these studies proUgn increased Na^+ excretion and urine volume without affecting GFR and with very small increases (or in some cases decreases) in UK^+v or FEK.

The Ugn infusion studies raise a critical question about physiological relevance, as the doses of peptide required to elicit natriuretic responses in rats and mice exceed reasonable physiological levels (56). One plausible rationale for the apparent low potency of Ugn-15 is that an alternate metabolite derived from proUgn may be the true mediator of the entero-renal natriuretic pathway. In this case, the renal phenotype of the Ugn knockout mouse would reflect the loss of the alternate metabolite, rather than the loss of Ugn *per se*. This hypothesis is strongly supported by a previous report from our laboratory showing that human proUgn is more

natriuretic than Ugn when the two are infused intravenously at equivalent doses (136). Consistent with this concept, my infusion studies with radiolabeled recombinant proUgn (reported in Chapter 2, Figure 2.8b) suggest the production of at least one alternative proUgn digestion product within the renal tubules. Although the structure and biological activity of this novel peptide are not yet known, it is an intriguing candidate for future studies.

Responses to Oral Na^+ are impaired in proUgn Knockout Animals

The creation of a proUgn/Ugn knockout mouse was a major step forward in the investigation of proUgn and/or Ugn as the agent(s) responsible for post-prandial natriuresis (118). The knockout animals are hypertensive, suggesting a prominent role for one or both of these peptides in volume homeostasis, with a significant impact on blood pressure control (118). The animals' hypertension is considered salt-insensitive, as the difference in blood pressure is approximately the same between the proUgn-+/+ and proUgn-/- mice on low, normal and high salt chow. In addition, when the knockout animals are challenged with an oral salt load, they are not able to excrete to excrete it as fast as wild type animals (50). This defect (shown graphically in Figure 1.4 of the Introduction to this thesis) is the strongest evidence to date that proUgn plays a role in PPN..

The aim of the studies presented in this chapter is to provide direct evidence that the proUgn/Ugn signaling pathway is responsive to changes in oral Na^+ intake. I tested the hypothesis that a change in salt intake would produce a change in circulating proUgn levels, which in turn would lead to a change in urinary Ugn excretion. I predicted that these responses would be bi-directional (i.e. that

increases or decreases in salt intake would lead to corresponding increases or decreases in peptide levels). I focused on proUgn in plasma, because my initial studies (Chapter 2) revealed that it is orders of magnitude more abundant in plasma than Ugn (which is below the limit of detection of my most sensitive assay). Previous studies from our lab have shown that circulating proUgn is derived primarily (and perhaps exclusively) from the intestine, consistent with the PPN hypothesis (105). I focused on Ugn in the urine, because my initial pulse-chase tracer studies showed that infused proUgn is converted to Ugn and other metabolites within the kidney, and excreted exclusively in processed form (Chapter 2). Furthermore, a number of laboratories have shown that Ugn is abundant in the urine produced by a healthy kidney, whereas proUgn is detectable only in urine produced by failing kidneys (68, 124). As a further investigation of the hypothesis that urinary Ugn is derived from circulating proUgn, I used the quantitative assays described in Chapters 2 and 3 to measure the stoichiometric relationship between proUgn infused into the plasma and Ugn recovered in the urine.

B. Methods and Materials

Animals Used

All experiments were performed on Sprague Dawley rats (Harlan laboratories, Dublin VA). Animals were maintained on a 12 hour light/dark cycle (on/off at 8am/pm) in an AALAC-approved facility with continuously available veterinary care and uninterrupted access to water and standard rat chow. All experimental procedures were approved by the Institutional Animal Care and Use Committee at

the University of North Carolina at Chapel Hill, and were carried out in accordance with the NIH Guide for the Care and Use of Laboratory Animals.

Sodium Diet Studies

In all diet studies, animals were housed individually in metabolic cages (Techniplast, Milan, Italy) with access to deionized water and food ad libitum. The rats were acclimated to the cages at least 2 days before study. The diet consisted of either low salt chow (LS) (0.02% Na^+ Cat #TD.90228), normal salt chow (NS) (0.26% Na^+ Cat #TD.90229) or high salt chow (HS) (3.1% Na^+ Cat #TD.92012) (Harlan Teklad, Madison, WI) for various times (see Figure 4.1). Food and water intake and feces excreted were measured gravimetrically every 6 hours. Urine was collected under mineral oil to limit evaporation. Urine was collected every 6 hours and the volume was determined gravimetrically. Urine samples were frozen at the time of collection and stored at -80°C for future analysis. Arterial plasma was sampled via an indwelling carotid artery cannula from a subset of animals. Na+ and K+ concentrations in plasma and urine were measured by flame emission photometry (Model 943, Instrumentation Laboratory Co., Lexington MA). Animals were sacrificed at various time points during the study (days marked with black dots in Figure 1) to obtain plasma and tissue samples for analysis. The time of sacrifice for each group was 4am. The method of sacrifice was urethane anesthesia (Sigma-Aldrich, St. Louis Mo. USA) followed by midline incision of the peritoneal cavity. Each animal was exsanguinated, and blood was collected into heparinized tubes. Kidney and duodenum were flushed with ice cold saline, minced and stored in

RNAlater (Ambien Inc., Carlsbad Ca. USA) for 24 hours at room temperature, then stored short term at 4°c prior to PCR analysis.

Installation of Indwelling Carotid Artery Cannula

Rats were anesthetized with sodium pentobarbital (60 mg/kg, ip) and prepared for aseptic surgery with 80% EtOH and 10% topical povidone-Iodine (Novaplus, Irving Tx, USA). A sterile subcutaneous port (PMINA-CBAS-C30 Soloport; Instech Solomon, Plymouth Meeting, Pennsylvania, USA) was implanted in the neck. The attached polyurethane heparin coated catheter was tunneled over the right shoulder into the neck region and cannulated into the exposed carotid artery. After surgery, the animals received intramuscular injections of buprenorphine HCl (Carpuject, 0.3 mg/ml; Hospira Inc., Lake Forest Il. USA) every 12 hours for 60 hours. The catheters were flushed daily with 200µL of Heparin Lock Flush (100 USP Units/ml)(Hospira Inc., Lake Forest Il. USA). The area of the port was disinfected with 90% ethanol before puncture. Blood samples were collected into heparinized tubes, centrifuged and plasma was separated from the red blood cells, aliquoted and frozen at -80°C for later analysis.

RT-PCR amplifications

Random hexamer-primed cDNA was prepared from isolated RNA, using the SuperScript® III First-Strand Synthesis System (Invitrogen, Carlsbad CA), according to the supplier's protocol. Subsequent RT-PCR analysis employed primer pairs and probes (Table 1) synthesized by the Animal Clinical Chemistry and Gene Expression Core of the UNC Department of Laboratory Medicine and Pathology (directed by Dr.

H. Kim). Each sample included a fluorescent probe with a reporter dye (fluorescein) at the 5' end and a quencher dye (tetramethylrhodamine) at the 3' end, as indicated in Table 1. Amplifications were performed in duplicate in a 96-well plate in the ABI Prism 7700 sequence detector (PE Biosystems) for 40 thermal cycles (15 sec at 94°C and 1 min at 60°C), as described by Kim et al. (94). Fluorescence was continuously measured in each well, and the fractional cycle at which each sample crossed a fluorescence threshold, CT, was determined using software provided by the manufacturer. CT values were not corrected for differences in amplification efficiency, because efficiencies were consistently close to 1.9 (note: a 100% efficient reaction that doubles with each cycle has an efficiency of 2.0).

Measurement of proUgn in plasma and urine

ProUgn concentrations in plasma and urine were measured with the quantitative Western blot assay described in Chapter 2. Though proUgn is undetectable in the urine, results from Chapter 2 show that proUgn is filtered at the glomerulus and ends up in the urine. In the absence of direct measurements (the gold standard), a reliable estimate of GFR is required for calculations of peptide conversion ratios, and to correlate estimated tubule concentrations with physiologic responses. Technical limitations of my study prohibited direct determination of GFR. Prior studies with conscious rats have reported GFR in the range of ~0.85 ml/min/100g bw (124) or 2.5 ml/min for a 260g rat (5). GFR has a circadian component in mammals. For example, humans show a 33% reduction in GFR while sleeping (105, 185). Results from studies in rats cite a 0.9 ml/min reduction in GFR

while animals are sleeping, consistent with the 33% reductions in humans. This would give an estimated sleeping GFR of 1.75ml/min for a 300g rat. (151)

Measurement of Ugn in urine

This assay of Ugn in urine is a modification of a previously described radio-receptor binding assay (78). Our assay is based on competitive binding between Ugn and ^{125}I -labeled Y-Ugn at GC-C receptors in an isolated T-84 cell membrane preparation. Concentrations of Ugn in urine samples are calculated from a standard curve generated with rat. The assay is highly specific for guanylin family peptides, which are limited to Ugn in urine (51). The details of this assay are presented in Chapter 3.

Analysis of Data from Metabolic Balance

Ugn excretion rates are expressed as fmol/min. Urine Ugn concentrations are expressed as pmol/ml, which approximates the concentration of Ugn within terminal nephron segments and may be correlated with biological activity. Net excreted amount of Ugn for each rat was calculated by subtracting Ugn excretion in the control collection period from excreted amounts during the infusion and post infusion collection periods, and is expressed as pmol/kg BW.

Graphing and statistical testing were performed with the Prism 5.3 graphing and analysis program (Graphpad Software, San Diego, CA) and Excel (Microsoft, Remond Wa.). Paired t-tests were used for comparison of urinary Ugn excretion, water consumption, and food consumption. Group comparisons for circadian changes in plasma proUgn were made with one-way analysis of variance (ANOVA)

using diet interventions as column variables and times of day for plasma or urine collection as row variables. Comparisons were also made with two-way ANOVA to determine which variable was responsible for any variation seen in the data.

In the absence of direct measurements, a reliable estimate of GFR is required to calculate peptide conversion ratios, and to correlate estimated tubule concentrations with physiologic responses. Technical limitations of my study prohibited direct determination of GFR. Prior studies with conscious rats have reported GFR in the range of ~0.85 ml/min/100g bw (124, 177) or 2.5 ml/min for a 260g rat (5). GFR has a circadian component in mammals. For example, humans show a 33% reduction in GFR while sleeping (105, 185). Results from studies in rats cite a .9 ml/min reduction in GFR while animals are sleeping, consistent with the 33% reductions in humans. This would give an estimated sleeping GFR of 1.75ml/min for a 300g rat. (151)

Peptides Used

Rat Ugn for use in intravenous infusion experiments and as a standard in Ugn binding assays was purchased from commercial suppliers (Anaspec Inc, San Jose CA and Peptides International Inc, Louisville KY). The radioligand for binding studies was prepared from N-tyrosyl rat Ugn (Y-Ugn, Bachem Inc. Torrance CA). Y-Ugn was labeled with ^{125}I using precoated iodination tubes according to the manufacturer's instructions (Thermo Scientific, Rockford, IL) then purified by reverse phase HPLC before use. Recombinant rat proUgn (provided by Ironwoods Pharmaceutical Inc.) was produced as a His-tagged trxA fusion protein from plasmid pTM203 in an Origami (DE3) bacterial expression system. The fusion protein was purified by

immobilized metal ion affinity chromatography, and proUgn was released by cleavage with PreScission protease.

Peptide Infusion Protocols

Rats were anesthetized with sodium pentobarbital (60 mg/kg, ip) and prepared for clearance experiments with a PE240 cannula in the trachea, one PE50 and two PE 10 cannulae in a jugular vein, a PE50 cannula in the left femoral artery and a PE10 cannula in each ureter. Rats received an initial volume expansion (infusion of isotonic saline amounting to 6% of body weight over 60 min) followed by an intravenous maintenance infusion of isotonic saline at 10 µl/min/100g BW for the remainder of the experiment. 10 µl/min of the maintenance infusion was provided through a PE10 cannula to deliver peptide infusions; the balance was administered via the PE50 cannula. Supplemental anesthetic was provided as required through the second PE10 intravenous cannula. Blood samples were obtained from the femoral artery cannula, which was otherwise connected to a pressure transducer system for measurement of arterial pressure (Model 50110, Stoelting Instruments Wood Dale, IL). Arterial pressure was digitized with an A/D converter (Keithley instruments, Cleveland, OH Model KUSB 3100) for display and storage on a personal computer running open layers data acquisition software (Dtx_Ez, Data Translation Inc). 20 min urine collections were started 1 hr after the volume expansion period. Renal excretory responses to intravenous infusions were determined for proUgn and Ugn at a dose of 10 nmol/kg This dose is based on our previous studies, which showed human Ugn-A to be natriuretic at a doses between 20 and 50 nmol/kg BW (135) and human proUgn to be natriuretic at a dose of 10

nmol/kg BW (36). Urine Ugn concentrations were measured in all urine collections, while proUgn concentrations were measured in urine only from rats receiving proUgn infusions. Plasma proUgn was measured before the start of proUgn infusions and at the completion of the 60 min infusion period.

Analysis of Data from Peptide Infusion Studies

Basal Ugn excretion rates are expressed in fmol/min. Net excreted amount of Ugn for each rat was calculated by subtracting Ugn excretion in the control collection period from excreted amounts during the infusion and post infusion collection periods and expressed as pmol/kg BW.

Results from both kidneys in each collection period were averaged before calculating group means ± standard error of the mean (SEM). All graphing and statistical testing were performed with the Prism 5.3 graphing and analysis program (Graphpad Software, San Diego, CA). Group comparisons were made with one-way ANOVA using peptide doses as column variables and individual measurements from each clearance period for each rat as row variables. Columns were subdivided into pre-infusion, infusion, and post infusion groups and tested against corresponding values from vehicle-infused rats with Bonferroni's method for multiple comparisons.

Intestinal Circulation Ligation Studies

Rats are prepared as prior for peptide infusion studies with the addition of an infusion of 10% mannitol 0.9% saline at 100µl/min. Following connection of cannula and stabilization of animals, the peritoneal cavity is opened and the bowels are

exteriorized and wrapped in saline soaked gauze. Ligatures are placed around the superior mesenteric artery, the celiac artery and the portal vein. The ligatures are tightened in that order allowing time for pressure in the subsequent vasculature bed to drop before tightening the next ligature. Urine samples are collected every 20 minutes and arterial plasma samples every 40 minutes. Samples are analyzed as described above.

C. Results

The General Effects of the Na^+ Diet

The Na^+ content of the chow fed to the rats had little effect on their overall food consumption. Table 4.2 and Figure 4.2a present the daily consumption for the cohort of rats on the different diets, showing that they ate the same amount of NS or LS chow, but that there was a slight decrease during the HS phase. Significant changes are noted on the graph (asterisks in Figure 4.2a). With food consumption stable, changes in Na^+ content of the food had a significant effect on the animals Na^+ intake and excretion (Figures 4.2b and 4.2c).

Though the change from NS chow to LS Na^+ chow seemed to have little effect on food consumption, there was a significant reduction in water consumed (Figure 4.3a) initially after switching from NS to LS, however water consumption recovered to previous level. The switch from LS to HS chow elicited a three-fold increase in water consumption during the first collection period (3pm to 9pm) and a two-fold increase for the first 24-hour period (Figure 4.3a). This rise in water

consumption continued to increase through the duration of the animals eating HS chow, and correlated with the increase in Na^+ intake (Figure 4.2b).

There were some significant changes in food and water consumption and urine flow rate that would be expected for a circadian sleep cycle and large changes in Na+ consumption. Significance is noted on the graphs.

Animals in the diet study had an average starting weight of 311±11g and during the course of the study had an average weight gain of 3.9±0.5 g/day. There was an unaccounted “metabolic” disappearance of weight in the study as, on average, animals had a 30.6g/day difference between the addition of the water they drank with the food they ate minus the weight of excretion of urine and feces. This loss does seem to be circadian and coincides with when they are active and urinating most.

As a further discrepancy, Na^+ is only recovered at an average rate of 78%. This could be partially accounted for by the fecal contents, which were not monitored. Interestingly, the percent recovered is dependent on the percent Na^+ content of the food. When the animal is on NS, the amount recovered in the urine is ~60%, on LS chow ~50%, and on HS chow ~90%. This implies that a portion of lost Na^+ is in the fecal contents and it is a fixed amount, which comprises a smaller percent of the expected excretion when the intake is higher. Evaporative loss of fluid on cage parts and resulting precipitation of ions on surfaces could also explain some or all of the imbalances.

Circadian Changes in Urinary Ugn and plasma proUgn

Utilizing the sensitive radioligand binding displacement assay, urine samples could be assayed with no purification step. This allowed me to collect samples over shorter times (less than 24 hr) in order to assess of circadian changes in urinary Ugn excretion. The day/ night cycle had a profound effect on this parameter. Excretion was significantly higher during the 9pm to 3am and 3am to 9am periods when the animals were awake, active and consuming food. This is illustrated in Figure 4.4 (black circles).

Plasma sampling was performed on a subset of animals, using an indwelling carotid cannula to take repeated samples from conscious animals every six hours over a 24-hour period. The plasma proUgn levels were also found to be circadian with the same peak level at 3am as Ugn shown in Figure 4.4 (white circles). Interestingly, the urinary Ugn changes in phase with the changes in plasma proUgn levels, consistent with the hypothesis that the plasma propeptide is the source of the Ugn that appears in the urine. ANOVA for both plasma proUgn concentration and urinary Ugn excretion showed that both change significantly with time of day (Tables 4.3 and 4.4 respectively).

Is the amount of proUgn in the plasma sufficient to account for the Ugn that appears in the urine? To make this calculation, it is necessary to know the filtered load of proUgn, which requires a measurement of the animals' GFR. I used published estimates of GFR, taking into account the animals' weights and the time of day. Using the average of 311 g for the rats from the study, I estimate GFR to be 2.65 ml/min while awake and with a 30% reduction for circadian variation,

1.85ml/min while asleep and 2.35 ml/min for the period in the morning when the lights are on but the room sees high traffic of DLAM staff and researchers. My calculations (table 4.5) estimate that 0.30±0.045% of the proUgn filtered load gets converted into Ugn excreted in the urine.

This estimate of the percent of filtered proUgn converted to Ugn is surprisingly low, and shows that the filtered load of propeptide is enormously larger than would be required to produce the Ugn in urine (and would be so even if my estimates of GFR are wrong). It also implies that a small change in proUgn processing within the kidney could significantly affect urinary Ugn: a fractional increase in the percent of proUgn being processed could result in a many-fold change in the level of Ugn excreted.

It must be emphasized that there could also be a renal source for the urinary Ugn, in which case an even smaller percent of the filtered load of proUgn would be converted. As prior studies have not detected proUgn in the urine of normal animals, one might conclude that over 99% of the filtered proUgn is converted into another metabolite or completely degraded.

Plasma ProUgn is Derived Primarily (and Perhaps Exclusively) from Intestinal Secretion

According to the central hypothesis in the Ugn field, proUgn is released from the intestine into the plasma, and delivered to the kidney to regulate salt excretion. To investigate the extent to which plasma proUgn has an enteric source, we ligated the vascular input to and outflow from the intestine and measured plasma levels of proUgn as a function of time after the ligation. As shown in figure 4.5, the plasma

concentration of proUgn fell rapidly after ligation, reaching very low levels (< 15%) within 140 min. Previous studies have shown that renal clearance of radiolabeled recombinant proUgn is rapid (see chapter 2), and the rate of disappearance of exogenous radiolabeled proUgn in these pulse-chase studies is comparable to the rate of loss of endogenous non-radioactive proUgn observed here. Thus, the data suggest that most (and perhaps all) of the circulating pool of plasma proUgn is supplied by the intestine, and are consistent with a high rate of enteric release coupled with a rapid rate of renal clearance.

Urinary Ugn Changes in Response to Dietary Na^+

Analysis of urinary Ugn in samples showed significant changes in response to dietary Na^+ content (Figure 4.6a). The change from NS (0.26%) to LS (0.02%) resulted in a 15% decrease in the daily rate of excretion (NS 130.2±0.2 vs. LS 111.5 ± 9.1). There was little change in the "basal" excretion rate of Ugn when the animals were quiescent (during the 9 am to 9 pm time period), but when active and eating (during the 3am to 9am time period), there was a significant difference between NS chow (day 4) Ugn excretion (31.9±5.8 fmol/min) and the LS chow (day 5) excretion (20.1±3.8 fmol/min, $p< 0.02$, paired t-test) (Figure 4.6a). This trend of significantly less urinary Ugn excretion from 3am to 9am continued through the third day, but a normal-appearing circadian increase had returned by the fourth day. Thus, Ugn excretion was lower than normal while the animals were adapting to the abrupt change in their Na+ intake (i.e. when intake and excretion were not yet in balance – see Days 4-9 Table 4.2), but returned to normal once the animals had regained a state of metabolic equilibrium.

When the animals were switched from LS to HS diet, the 3am collection Urinary Ugn was significantly higher (HS {day 10} 43.6±7.5 fmol/min vs LS {day 9} 23.3±2.6 fmol/min $p<0.05$, paired t-test). The circadian peaks on HS chow were significantly different from the NS chow peaks for every day (Figure 4.6a, day 11, $p<.0.003$; day 12,$p<0.04$; day 13,$p<0.04$; day 14,$p<0.02$). Comparing the quiescent (3pm-9pm) period for the HS animals to the NS animals shows that for the first three days (day1 vs. day 10, 11 and 12) that the "trough" of the circadian peak (i.e. "basal" secretion during the quiescent period) was not significantly different but day 13 and day 14 ($p<0.01$ and $p<0.04$ respectively) the trough was significantly higher. Figure 4.6b shows that the daily excretion of Ugn increased significantly for the duration of the HS diet treatment and appears to have achieved a new steady-state rate by day 3. Figure 4.7a shows that the troughs and the peaks of urinary Ugn correlate closely with the circadian cycle of Na^+ excretion the first two days on HS diet.

Plasma ProUgn Does Not Change in Response to Dietary Na^+

The plasma proUgn data presented in Figure 4.4 were obtained by collecting plasma from an indwelling carotid artery cannula. Unfortunately, the implanted ports did not stay patent for more than 6-7 days, which limited a more extensive analysis during full diet regime, as originally planned. Nevertheless, the ports were used to gather limited data about the effects of dietary Na+ changes on plasma proUgn at specific time points in different sets of animals. Table 4.3 lists these values, showing circadian changes in plasma proUgn that were basically unaffected by diet conditions. The table also shows the results of ANOVA evaluation of different dietary

Na^+ treatments compared with NS. None of the Na^+ changes achieves overall statistical significance. However, two-way ANOAVA reaffirms proUgn variation as a function of time of day regardless of dietary Na^+.

Additional plasma samples were collected from a separate set of animals treated in parallel to those in metabolic cages. These separate animals were sacrificed by guillotine at 4am on specific points during the study. This time was chosen because it is when the circadian changes in plasma proUgn and urinary Ugn levels were both at their highest (Figure 4.4). Plasma from these animals was analyzed by quantitative proUgn western blot assay at four critical time points: adapted to NS, adapted to LS, adapted to HS, and 12 hours after the switch from LS to HS. The results indicate there was no significant change in the plasma proUgn concentration (Figure 4.8a). The value observed for the animals that had become adapted to HS chow was 15-20% higher than other groups, but this tendency did not achieve statistical significance even with the relatively large sample size of ~ 10 animals per treatment group.

In Figure 4.8b, the colored circles illustrate the relationship between urinary Ugn and plasma proUgn levels at these four different dietary Na^+ conditions at 3am. The grey dashed line is the average plasma proUgn value for all diet conditions. During no diet conditions is there a significant difference from this. The red dashed line plots the theoretical values of plasma proUgn that would be required to generate each value of urinary Ugn at a fixed 0.3% conversion rate. It is evident that the actual proUgn values do not fall on the theoretical line, and, indeed, appear to be completely independent of dietary status. There are the three additional time

periods plotted for NS diet (green circles without error bars) that illustrates again the circadian change of Ugn excretion its association with plasma proUgn.

Changes in proUgn mRNA Expression in Response to Dietary Na^+

Because Ugn levels in the urine changed in response to salt diet, q-rtPCR was used to determine whether either the intestine or the kidney increased their levels of the proUgn-encoding mRNA transcript. A salt-dependent change in expression levels would serve as an indirect assessment of whether either tissue might be generating proUgn at a higher rate under any of the dietary conditions.

Figure 4.9a represents the difference in cycle threshold (ΔC_t) values determined by real time RT-PCR amplification between proUgn and ß-Actin (chosen as a control housekeeping gene) in these two tissues. For the intestine, the ß-Actin C_t was consistent across all diets (not shown), and the proUgn C_t decreased slightly for the different diet conditions (0.8 cycle C_t difference between NS and HS adapted). For kidney samples the proUgn gene expression reached threshold more than 2 cycles sooner for HS adapted than for NS, and there was also a slight concurrent increase in C_t for ß-Actin C_t (not shown). Using the Δ-Δ-C_t method (Figure 4.9b) to compute expression changes, there was 70% increase in Ugn expression in the kidney between NS and HS day 1, and a 100% (two–fold) increase by day 5 on HS diet. This Δ-Δ-C_t approximation of expression also showed that intestinal proUgn mRNA levels did not change immediately after the switch to HS, and increased non-significantly by 40% by 5 days after the switch. Thus, the qRT-PCR data suggest that higher mRNA levels may be required to support an

accelerated rate of proUgn synthesis in the kidney under high salt conditions. This would be consistent with a higher rate of renal proUgn secretion, requiring, in turn, a higher rate of de novo synthesis to maintain the tissue pool of propeptide at a normal level. In contrast, intestinal mRNA expression is independent of salt diet. This correlates well with the observation (Figure 4.8) that plasma proUgn (secreted by the intestine – Figure 4.5) also does not change as a function of salt intake. Thus, two lines of evidence (plasma propeptide levels and enteric mRNA levels) argue against the hypothesis that the intestine is the tissue source of a Ugn/proUgn signal that regulates PPN. The mRNA expression data also demonstrate that there is ~50 times more proUgn transcript in the intestine than the kidney (data not shown), in good agreement with past findings.

Excretion of Ugn in Urine After proUgn and Ugn Infusions

Chapter 2 investigated the metabolic fate of radiolabeled proUgn (infused into the plasma). However, these studies were non-quantitative. In order to evaluate the stoichiometric relationship between plasma proUgn and excreted Ugn, we infused known amounts of recombinant proUgn and measured both the resulting plasma levels of propeptide and the excreted amounts of Ugn.

After 60 minutes of intravenous infusion with rat proUgn at 10 nmol/kg BW, plasma proUgn concentration increased from 2.2±0.3 (n=6) to 37±9.6 pmol/ml over the same time period ($p<0.0001$ n=3, unpaired t test). This is significantly higher than would be seen in normal rats, but is within the range that can be achieved in patho-physiological conditions, as such a level is commonly achieved in rats with renal failure produced by a 5/6 reduction in renal mass (N. Moss, unpublished

observation). In Figure 4.10a Ugn excretion is shown as fmol of Ugn excreted in the urine per minute before, during, and after the proUgn infusion. The total recovered amount of Ugn in urine (summed over the infusion and post-infusion periods) was 206±39 pmol/kg, which amounts to 2% of the infused dose of proUgn (Figure 4.10c). This contrasts with plasma proUgn levels, which increased by ~1700% during the infusion rates. The extremely low recoveries of Ugn derived from proUgn suggest either that Ugn production within the tubules is relatively inefficient, or that Ugn may be produced but is largely degraded and/or reabsorbed before it is excreted in the final urine.

To examine this latter possibility, and for comparison with the results of propeptide infusions (Figure 4.10a), urinary Ugn excretion in response to intravenous infusions of rat Ugn itself is shown in Figure 4.10b. The excretion of Ugn in urine increased from 0.125±0.03 pmol/min to a peak of 13.7±1.11 pmol/min during the 10 nmol/kg infusion (Figure 4.10b). This is more than 10 times higher than the excretion achieved with intravenous infusions of the same molar amount of proUgn (Figure 4.10a). The amount of Ugn recovered in urine was ~5000 pmol after the infusion, or about 50% of the total infused amount (Figure 4.10c). The fate of unrecovered Ugn is unknown, but is not due to delayed excretion, as the urine Ugn concentrations returned close to baseline levels in the second hour following the intravenous infusion (Figure 4.10b). It is more likely that several processes reduced the recovery, including degradation within the proximal tubules and removal from the circulation by non-renal clearance mechanisms. However, the relatively robust recovery of infused Ugn (~50%), compared to the relatively poor recovery of Ugn

derived from infused proUgn (~2%, see above), argues that Ugn is not produced stoichiometrically from proUgn within the tubule. In summary, proUgn infusions produce very small increases in urinary Ugn excretion relative to those observed when Ugn itself is infused.

The Ugn concentration in urine provides an index of the intratubular "dose" of the peptide. As shown in Figure 10d, the "dose" of Ugn generated from the 10 nmol/kg proUgn infusion is very low compared to the "dose" generated by the 10 nmol/kg Ugn infusion. Surprisingly, however, in companion studies performed by Nick Moss, the proUgn infusion actually had a greater natriuretic effect than the Ugn infusion (Figure 4.11a vs 4.11b). Since none of the infused proUgn appeared in the urine (i.e. all of it was metabolized and/or reabsorbed before excretion) this observation argues very strongly that proUgn is being processed to something that is distinct from (and more potent than) Ugn. Furthermore, since any such material did not generate a significant signal in my binding assay, it would likely not be derived from the N-terminus of the propeptide.

D. Discussion

Urinary Excretion of Ugn Varies in Proportion to Dietary Na^+ intake, but Plasma Levels of ProUgn Do Not

Analysis of plasma and urine obtained from rats housed in metabolic cages shows that both Ugn and proUgn vary during the normal circadian day/night cycle. The changes in proUgn were limited to the plasma (proUgn was undetectable in urine under all conditions in my study) and had a high correlation to time of day

(Table 3). This circadian rhythm of plasma proUgn is shown in Figure 2; the two highest values occurred when the lights were out and the animals were active and eating (Figure 4.2). The intestinal expression of proUgn mRNA has previously been shown to change in a circadian cycle, with ileum and duodenum levels highest during active hours (25). Data in Figure 4.5 show that the intestine is the primary (and perhaps exclusive) source for circulating proUgn, suggesting that enteric secretion of proUgn also displays a diurnal rhythm.

The urinary Ugn changes are also constrained to a circadian rhythm (Table 4.4). This has previously been observed in humans, and again this cycle is associated with the wakeful phase (24). Figure 4.4 shows that urinary Ugn changes in phase with plasma proUgn supporting the hypothesis that intestinal plasma proUgn is a source for excreted Ugn, and that changes in circulating proUgn would result in changes in Ugn. Note that some circadian protein expression cycles are driven by inherent cyclical changes in gene expression (based on an internal “clock” that is stimulus-independent) while others are due to the cyclic nature of some external stimulus that drives expression (such as photoperiod, or food intake) (66, 71, 146). Based on these concepts, it could be hypothesized that changes in urinary Ugn are derived from an intestinal source that cycles in response to Na^+ intake.

In addition to circadian changes, there is a significant correlation between the amounts of Ugn excreted in the urine and the Na^+ content of the chow being consumed. One-way ANOVA shows that high salt intake significantly affects urinary Ugn excretion. This strongly supports the hypothesis that Ugn is involved in Na^+

homeostasis. Following is a list of changes observed (or not observed) in plasma proUgn and urinary Ugn in relation to dietary Na^+:

- A decrease in food Na^+ content causes a significant transient (18-24 hour) drop in urinary Ugn excretion
- On a low Na^+ diet urinary Ugn excretion is nearly normal after the animal has adapted to a new lower Na+ intake level (48 hours)
- An increase in Na^+ diet causes both transient and significant sustained increases in urinary Ugn
- No significant changes in levels of plasma proUgn in response to dietary Na^+ but proUgn levels do change significantly in a circadian rhythm.
- No significant change in proUgn transcript levels in the intestine but significant changes were seen in the kidney

These data are in good agreement with (but much more far-reaching than) the limited observations of absolute amounts of protein and fold change in response to dietary stimuli that have been previously reported. They support the concept that a change in dietary Na^+ results in a change in the levels of renal metabolites of proUgn, specifically Ugn, that appear in the urine.

In addition to the strong association that I observe between urinary Ugn excretion and Na^+ intake, there is also a strong association between Na^+ excretion and Ugn gene status. Figure 4.7b illustrates results reported by Dr. Mitchell Cohen's group when studying a whole animal Ugn knockout model that they developed (50).

The phenotype of these mice is associated with impaired Na^+ excretion over the first 36 hours after a switch to HS food, as indicated by the pink shaded region. When compared to the graph of my data in figure 6a, which is appropriately lined up, it is evident that the phase of impaired excretion (days 1 and 2) is associated with a transient period of maximal Ugn excretion. The transient peak is then replaced by a prolonged plateau phase of constant excretion at a lower level.

On day 15 of the study, the first day of NS food after being on HS food the animals greatly increased their food intake. Specifically, the first period after the change they ate more chow on average than any other period during the study. Despite this increased food intake, the NS animals only consumed 32.7±2.1 milligrams of Na+ compared to 187.3 ±23.9mg for the same period the prior day on HS chow. During these same periods, the excretion of Ugn was significantly greater on the HS chow that was consumed in less quantity but with a greater Na^+ content (46.7±11.6 vs, 29.4±6.9 fmol/min, t-test $p< 0.03$). From this I conclude that the mass of food in the stomach is unlikely to be responsible for changes in urinary Ugn; rather, it is the Na^+ content of that food.

The Source of Urinary Ugn

The implication of my results, taken as a whole, is that changes in urinary Ugn excretion do accompany shifts in oral Na^+ consumption, but these are not driven by changes in plasma proUgn levels that are generated by the intestine. Rather, my data favor the hypothesis that the “diet-responsive” component of urinary Ugn is coming from the kidney. Evidence that supports this idea includes: (1) the proUgn transcript is expressed in the kidney (Figure 4.9); (2) the proUgn polypeptide

is present as well (Chapter 2, Table 2.2); (3) renal expression of the proUgn transcript is regulated by oral Na+ intake (at least for the shift to high salt), whereas enteric expression is not (Figure 4.9b); (4) plasma proUgn is secreted primarily (and perhaps exclusively) by the intestine (Figure 4.5); (5) but plasma proUgn levels are not affected by dietary Na+ (Figure 4.8a).

proUgn is present in the plasma at very high levels relative to most circulating hormones (134), and Figure 2.5 in Chapter 2 and Figure 4.10 in this Chapter demonstrate that at least some of this circulating propeptide does get converted to Ugn and is excreted in the urine in that form. Quantitative analysis (Table 4.5) reveals that sufficient Ugn can be generated from normal basal levels of plasma proUgn to account for the basal levels of urinary Ugn. At a 0.3% conversion rate this filtered load is adequate to supply the urinary Ugn excreted and exogenous infusions of proUgn convert to Ugn at a rate of 2%, well above that threshold (Figure 4.10). However, the plasma proUgn level does not change in response to dietary Na^+ increases but urinary Ugn does, so there is a disconnect from this 0.3% conversion rate. This implies that the kidney is supplying the increased Ugn and this is reasonable given the renal content of proUgn is 15 times greater than the highest 6-hour excretion period on a molar basis. For renal production to supply the whole Ugn excretion, the conversion rate would have to be greater than 6% to utilize the entire stored kidney pool in one period. An alternative is that both sources contribute to this excreted urinary Ugn. Thus, there may be two components to the Ugn that is excreted in urine: a constant, baseline diurnal rhythm that is generated by cyclical secretion of proUgn into the plasma from the intestine, and a variable “diet-

responsive" transient component that occurs after a switch in intake and is generated by the kidney.

At least one alternative to a renal source of proUgn should be considered. It is possible that proUgn levels in plasma are not in themselves salt-sensitive, but that the processing of plasma proUgn into Ugn is salt sensitive. My data indicate that if plasma proUgn is, in fact, the sole source for urinary Ugn, then <1 percent of the filtered load of proUgn is sufficient to account for all of the urinary Ugn. Thus, if activity of an intrarenal enzyme, such as a brush border endopeptidase, were controlled by Na^+, then a constant filtered load of proUgn would be able to produce these varying amounts of urinary Ugn. This could be complementary to the central idea of the entero-renal axis, as the intestine would be exerting control over natriuresis through subtle changes in plasma proUgn that are magnified by an increased percentage processed into Ugn.

Final Thoughts

The present studies do not support the hypothesis that proUgn plays a central role of an entero-renal signal that responds to an enteric Na^+ load. The absence of any significant changes in intestinal proUgn expression or plasma proUgn levels after changes in dietary Na^+ argue that the mechanism is either extra-intestinal, or is more subtle than a major change in secretion levels. Thus, the role of Ugn or proUgn in salt homeostasis is not as simple as predicted by the PPN model. My observations support the idea that there may be two different tissue sources for urinary Ugn—a renal source that responds to a dietary Na+ stimulus, and a constitutive intestinal source with a circadian rhythm.

Estimations of percent conversion of proUgn to Ugn indicate that if the primary role of enteric proUgn is to produce urinary Ugn, then it does so in a very inefficient manner. With an estimated 0.3% conversion of endogenous proUgn to Ugn at physiological plasma concentrations (2.5 to 4.5 pmol/ml), and a conversion rate of ~2% at 37pmol/ml plasma after 10 nmol/kg exogenous infusion, it might well be that Ugn is not the primary intended product within the kidney, but rather is a byproduct during the production of the true metabolite. In this regard, data presented in figure 11 show that after infusion of equivalent doses of Ugn and proUgn, the response to proUgn is significantly greater than the response to Ugn. This can be contrasted with substantially lower intratubular Ugn concentrations when equal moles of proUgn or Ugn were infused systemically (figure 8d). Thus, a substantially lower filtrate Ugn concentration is inducing a greater natriuretic response when plasma proUgn is the source. The implication is that an alternate metabolite is physiologically active. This is one of the most interesting and crucial areas for future research in the Ugn field.

In addition, my data also raise the intriguing question of whether circulating proUgn might play a role in some homeostatic mechanism that is not predicted by the prevailing PPN model. Such a mechanism could act outside the kidney, though this would require an as-yet unidentified processing mechanism to generate appropriate biologically active metabolites. Plausible target tissues for such extra-renal actions include the adrenal gland, the pancreas, the liver, and the reproductive organs, all of which have been shown to express GC-C either constitutively or in response to developmental or pathophysiological events (22, 74, 129, 145, 182).

Tables

Table 1: primers used for RT-PCR			
primer set	forward primer	reverse primer	probe
A (proUgn)	ca/ccagggtgtctacatcaag	tctcc/ttccaactcattcagc	ftggcttccaagtcc agctg/agaatcq
B (β-actin)	tgcctgacggtcaggtca	caggaaggaaggctggaag	fcactatcggcaatg agcggttccgq

Table 4.1 Primers and Probes for rtPCR Is a diagram of the primers and probes used for q-rtPCR to determine relative amounts of mRNA present for genes of interest in tissues of interest.

	Day															
	1	2	3	4	5	6	7	8	9	10	11	12	13	14	15	16
	0.26% Na^+ Chow				0.02% Na^+ Chow					3.1% Na^+ Chow					0.26% Na	
Food Intake (g)	25.79 ±1.16	25.40 ±0.83	27.68 ±1.24	26.33 ±1.12	26.99 ±1.21	27.53 ±1.55	27.05 ±1.61	25.57 ±1.70	24.61 ±0.92	20.96 ±2.18	22.65 ±1.8	23.89 ±1.70	24.01 ±2.01	23.60 ±1.24	28.42 ±0.66	30.13 ±1.29
Water intake (ml)	31.46 ±1.49	35.02 ±1.50	31.94 ±8.11	29.99 ±3.70	23.64 ±3.03	26.63 ±3.29	28.58 ±3.70	29.42 ±4.14	30.09 ±4.05	67.25 ±9.31	74.82 ±10.3	84.09 ±10.8	88.63 ±12.4	69.21 ±14.9	37.93 ±2.96	35.16 ±3.72
Na+ Intake (mEq)	2.58 ±0.13	2.87 ±0.09	2.98 ±0.14	3.45 ±0.23	0.23 ±0.01	0.24 ±0.01	0.24 ±0.01	0.23 ±0.01	0.22 ±0.01	28.91 ±2.37	31.39 ±1.87	32.95 ±1.86	33.04 ±2.16	31.81 ±1.68	3.21 ±0.07	3.41 ±0.15
UNa+ Excretion (mEq)	1.50 ±0.08	1.76 ±0.04	1.84 ±0.23	1.99 ±0.23	0.54 ±0.07	0.13 ±0.01	0.11 ±0.01	0.11 ±0.01	0.11 ±0.01	16.88 ±0.87	26.94 ±2.31	30.57 ±1.44	31.51 ±2.62	27.89 ±1.44	3.67 ±0.83	1.46 ±0.53
Urine Volume (ml)	11.60 ±0.60	12.48 ±0.44	15.69 ±2.84	14.04 ±1.58	12.25 ±1.33	13.69 ±1.49	14.30 ±0.98	15.09 ±1.69	15.45 ±1.83	42.96 ±4.74	61.59 ±7.05	69.84 ±7.40	71.44 ±9.99	65.02 ±7.24	19.70 ±2.00	16.01 ±0.16
Feces (g)	14.15 ±0.85	16.54 ±1.89	15.03 ±2.17	12.03 ±1.04	11.06 ±0.96	9.41 ±1.51	10.63 ±1.63	10.96 ±2.08	10.58 ±1.63	8.48 ±1.18	8.36 ±0.97	8.23 ±1.32	9.32 ±1.06	9.62 ±1.95	11.70 ±1.16	13.24 ±1.49
Sodium Imbalance (Percent recovered)	58.2	61.5	61.8	57.8	230.6	56.0	45.9	49.7	49.2	58.4	85.8	92.8	95.4	87.7	114.4	42.8
Water Imbalance (Percent recovered)	36.9	35.6	49.1	46.8	51.8	51.4	50.0	51.3	51.4	63.9	82.3	83.1	80.6	93.9	51.9	45.5
Solid Imbalance (Percent recovered)	62.08	65.10	54.30	45.69	40.97	34.18	39.32	42.88	42.97	40.45	36.91	34.46	38.80	40.75	41.15	43.94
Number of Animals	3	3	7	10	10	10	10	10	10	10	10	10	10	10	7	3

Table 4.2 Sodium Diet Study Data The effects of diet changes on the daily amounts of food, water, and Na^+ consumed, Na^+ excreted and urine flow rate for all animals included in the diet study.

proUgn in 24 hour Plasma Collections During Diet Study Intervals (pmol/ml)							
Collection period	Normal salt	Normal to Low	Low Salt Adapted	Low to High	High Salt Adapted	High to Normal	
9PM	3.16	3.25	3.41	2.57	4.14	3.58	Values are in pmol of proUgn per ml Plasma
3AM	4.50	3.74	4.56	4.19	4.65	3.43	
9AM	2.95	2.96	2.98	2.71	3.11	2.84	
3PM	2.93	2.57	2.48	2.21	2.65	2.80	
		1 way ANOVA compared to Normal Salt					
	Mean Difference	-0.2523	-0.02362	-0.463	0.2593	-0.2197	
	p < 0.05	n/s	n/s	n/s	n/s	n/s	
	2 way ANOVA of all Values						
	Source of Variation		% of total variation		P value		
	Diet		11.03		0.1148		
	Time		73.6		< 0.0001		

Table 4.3 Analysis of Diet and Circadian Effects on Plasma proUgn Analysis of plasma samples obtained from animals during Na^+ diet study. Samples were drawn every six hours over a 24-hour time period. 1-way ANOVA was performed for each dietary intervention versus animals fed normal (0.26% Na^+) chow. 2-way ANOVA was performed on the entire data set.

Urinary Ugn Excretion During Diet Study Intervals (fmol/min)							
Collection period	Normal salt	Normal to Low	Low Salt Adapted	Low to High	High Salt Adapted	High to Normal	
9PM	19.26	21.41	19.45	27.43	46.70	29.37	Values are fmol of Ugn Excreted per Minute into Urine
3AM	30.61	20.15	23.31	43.58	47.36	24.11	
9AM	26.39	22.07	18.51	42.45	46.39	22.31	
3PM	16.94	16.47	16.66	21.85	34.28	16.22	
		1 way ANOVA compared to Normal Salt					
	Mean Difference	-3.275	-3.817	10.53	20.38	-0.2975	
	p < 0.05	n/s	n/s	n/s	Yes	n/s	
	2 way ANOVA of all Values						
	Source of Variation		% of total variation		P value		
	Diet		71.78		< 0.0001		
	Time		16.65		0.0032		

Table 4.4 Analysis of Diet and Circadian Effects on Urinary Ugn Analysis of Urinary Ugn in samples obtained from animals during Na^+ diet study. Samples were collected every six hours over a 16-day period. 1-way ANOVA was performed for each dietary intervention versus animals fed normal (0.26% Na^+) chow. 2-way ANOVA was performed on the entire data set. These analyses were carried out using values that represent the mean of 4 animals.

Estimation of percent of Filtered proUgn converted into Ugn						
	Time	GFR (ml/min)	Plasma proUgn (pmol/ml)	Filtered Load proUgn (pmol)	Urinary Ugn (pmol/ period)	Percent of proUgn converted to Ugn
Mean	9pm	1.75	3.73	2346.9	5.90	0.25
SEM	3am	2.65	4.55	4335.9	10.28	0.25
	9am	2.65	3.15	3004.0	9.01	0.30
	3pm	2.3530	2.92	1837.3	7.54	0.41
					Mean	0.30
					SEM	0.045
3am NS (day4)		2.65	4.55	4336.2	10.28	0.25
3am LS (day 9)		2.65	4.59	4380.4	8.39	0.19
3am LS->HS (day 10)		2.65	4.22	4028.4	15.69	0.39
3am HS (day 14)		2.65	5.35	5107.0	17.05	0.33

Table 4.5 Estimation of proUgn to Ugn Conversion with Effects of Diet and Circadian Variation Analysis of the percent of the filtered load of plasma proUgn that is converted to Urinary Ugn.

Figures

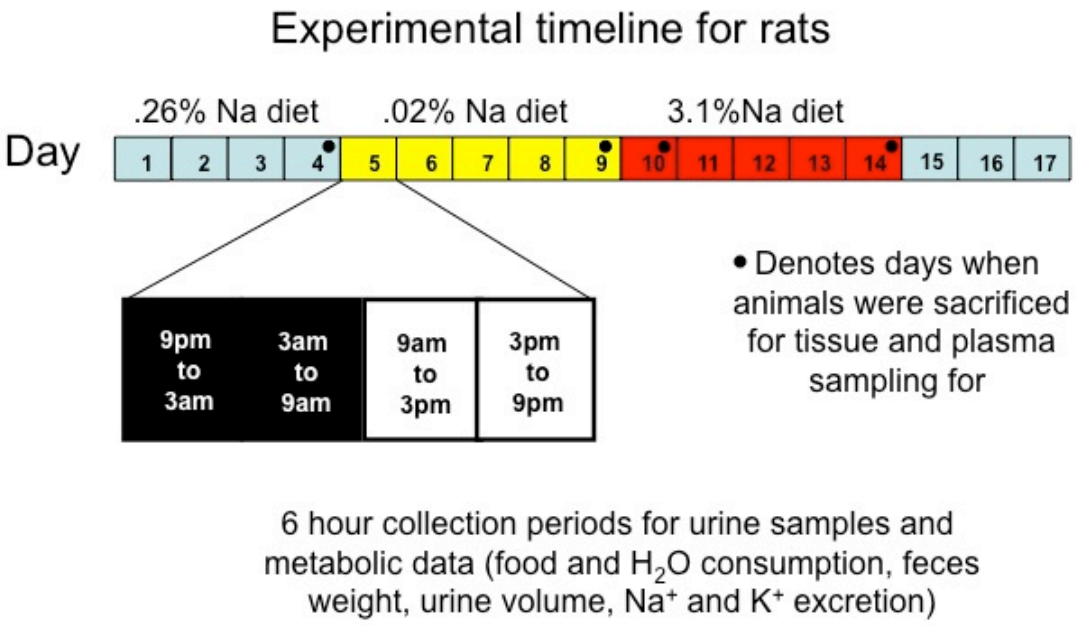

Figure 4.1 Sodium Diet Study Feeding Protocol Schematic illustration of the Na^+ content of the chow and the days and times when biological samples and metabolic data were obtained.

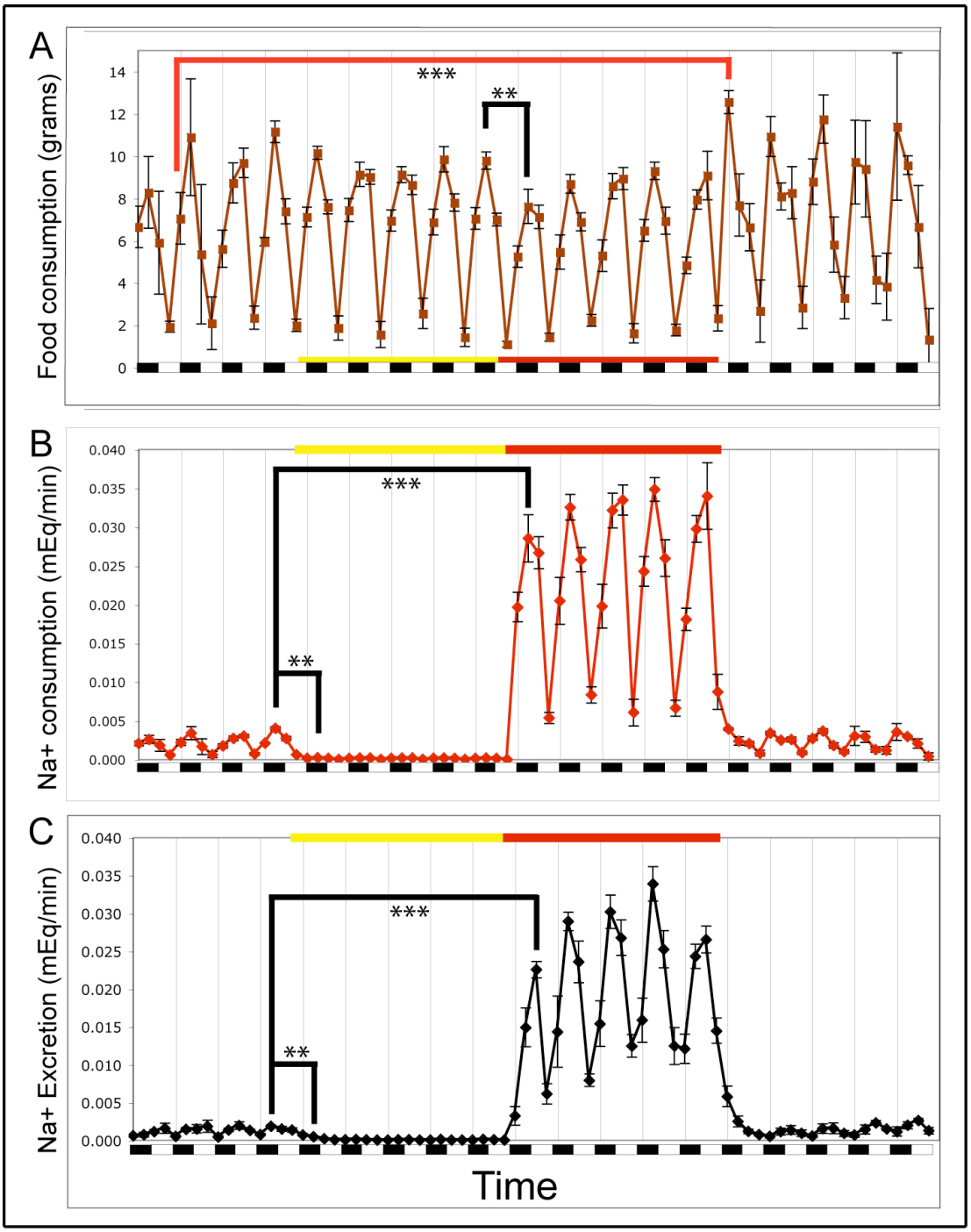

Figure 4.2 Na^+ Handling and Food Consumption During Sodium Diet Study
A) Food consumption in grams (g) for each 6 hour time period over the entire time course of the diet study. **B)** Na^+ consumption in mEq per minute for each 6 hour time period **C)** Na^+ excretion in mEq per minute for each 6-hour time period. An all graphs, vertical lines indicate 9pm and black/white boxes indicate night/day status. The yellow bar indicates 0.02% Na^+ LS chow and the red bar indicates 3.1% Na^+ HS chow. Values are mean ±SEM, n=8-11. Asterisks indicate $p<0.001$ (**) and $p<0.0005$ (***) for paired t-test of values from same animals.

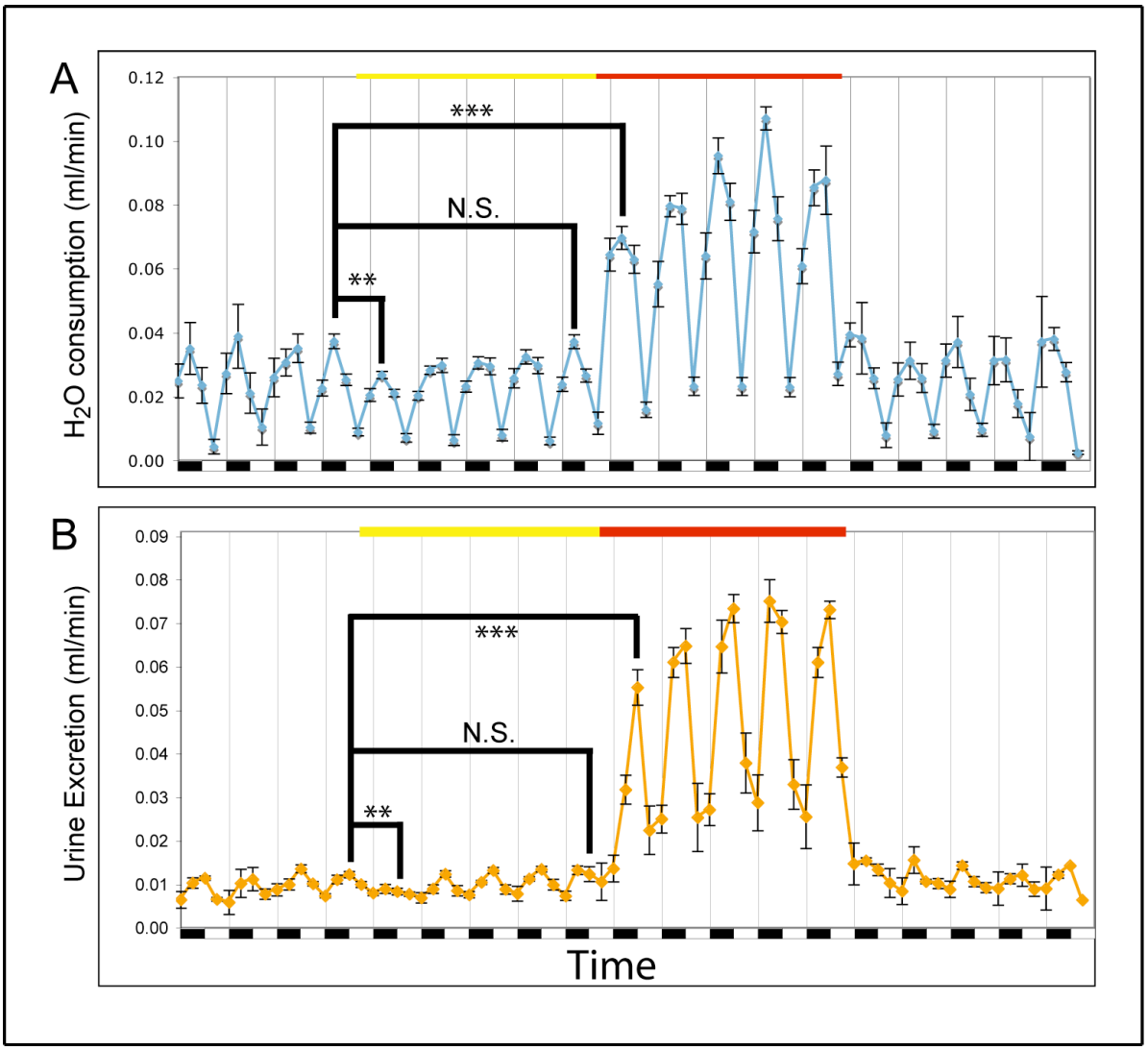

Figure 4.3 Water Handling During Sodium Diet Study A) Water consumption (ml) for each 6 hour time period over the entire time course of the diet study. **B)** Urine excretion (ml per minute). In both graphs, vertical lines indicate 9pm and black/white boxes indicate night/day status. The yellow bar indicates 0.02% Na^+ LS chow and the red bar indicates 3.1% Na^+ HS chow. Values are mean ±SEM, n=8-11. Asterisks indicate $p<0.001$ (**) and $p<0.0005$ (***) for paired t-test of values from same animals.

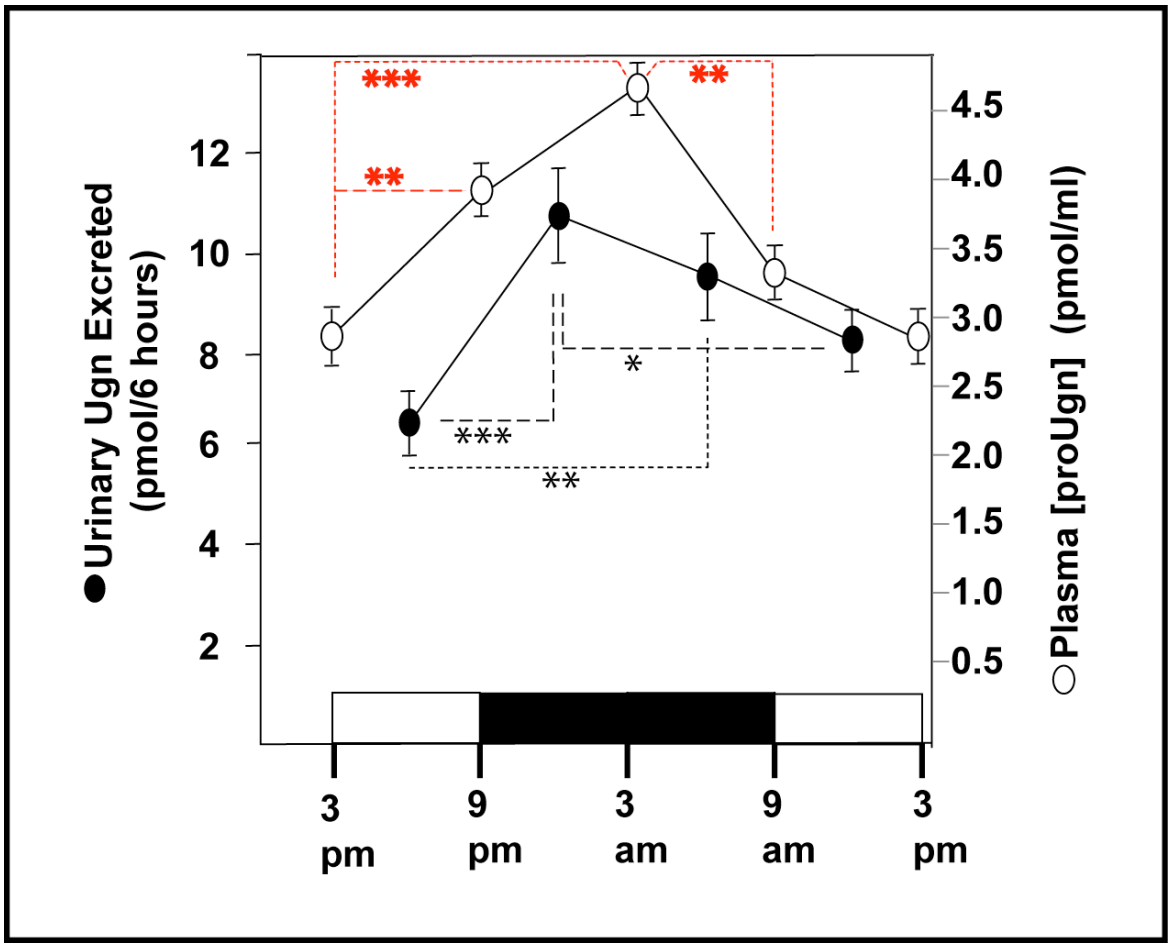

Figure 4.4 Circadian changes in Circulating proUgn and Urinary Ugn Excretion White symbols indicate urinary Ugn excreted in picomoles during the 6-hour time period that the data point is centered on. The black symbols denote plasma proUgn (picomoles/ml) at that time point. Values are mean ±SEM, n=8 for proUgn, n=13 for Ugn. Statistics calculated using a paired t-test comparing each animal's urinary Ugn to its own sample from adjacent time period. * = $p<0.025$ ** = $p<0.005$ *** = $p<0.002$.

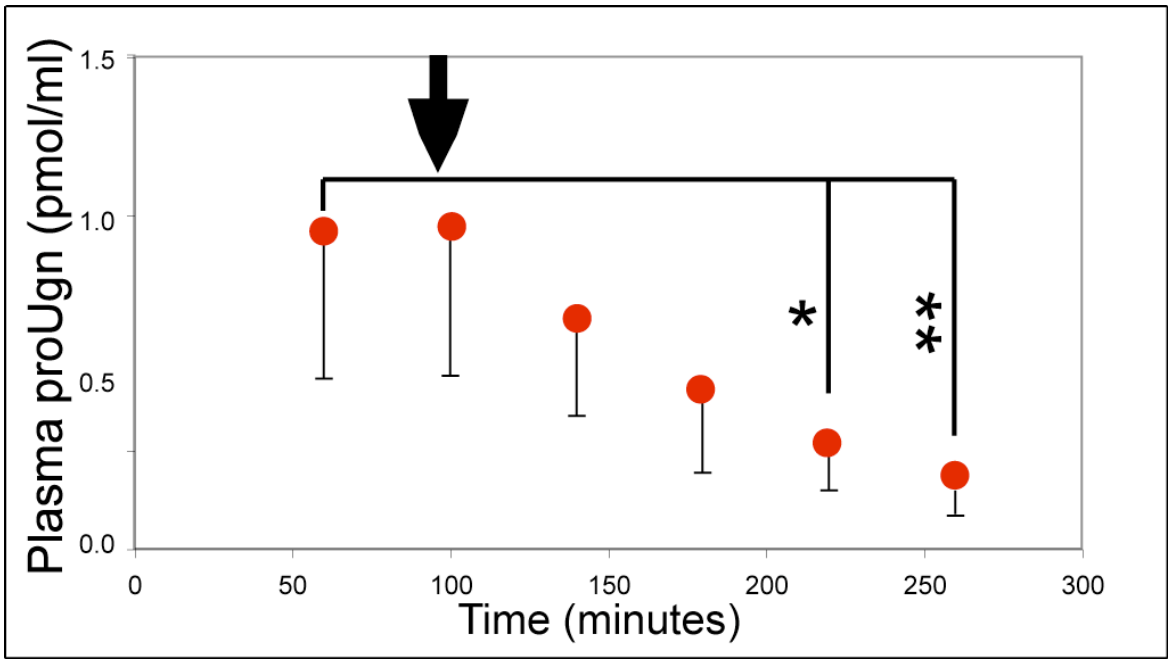

Figure 4.5 Plasma proUgn Levels Change Following Entero-Hepatic Circulation Ligation. The red symbols indicate the amount of proUgn in the plasma at time points following the ligation of intestinal arteries and portal vein (Black arrow). * = $p<0.05$ ** = $p<0.01$, n=3.

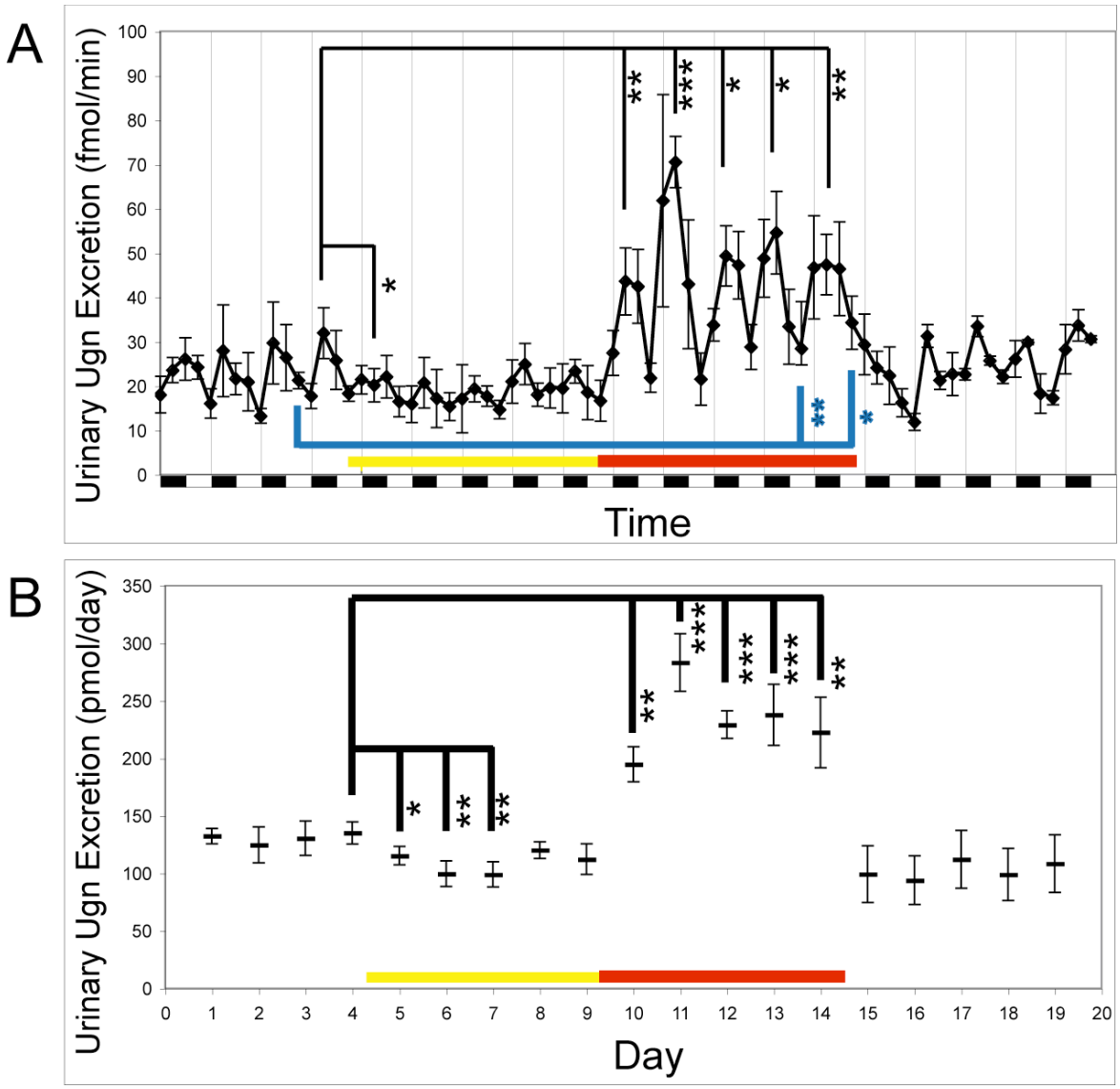

Figure 4.6 Urinary Ugn Excretion During Sodium Diet Study A) Urinary Ugn excretion for each 6 hour time period over the entire time course of the diet study. The vertical lines indicate 9pm and the black/white boxes indicate night/day status. **B)** Black symbols indicate summed 24-hour urinary Ugn excretion (pmol/day). In both graphs the yellow bar indicates 0.02% Na^+ LS chow and the red bar indicates 3.1% Na^+ HS chow. Values are mean ±SEM, n=4. Asterisks indicate $p<0.05$ (*), $p<0.001$ (**) and $p<0.005$ (***) for paired t-test of values from same animals.

A

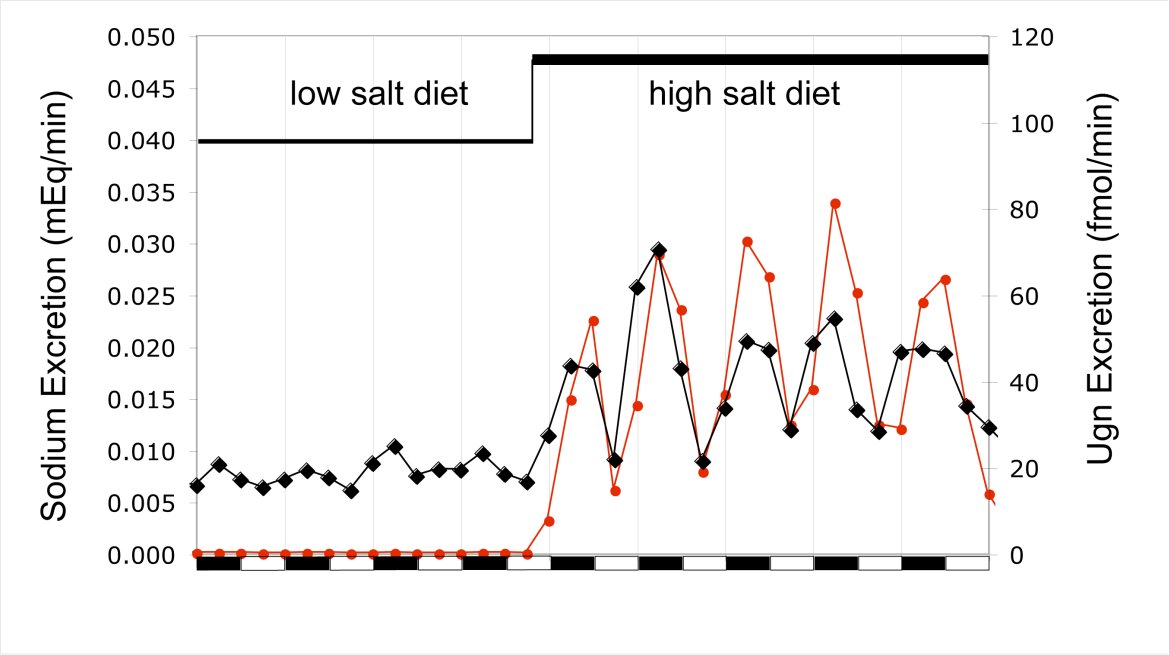

B

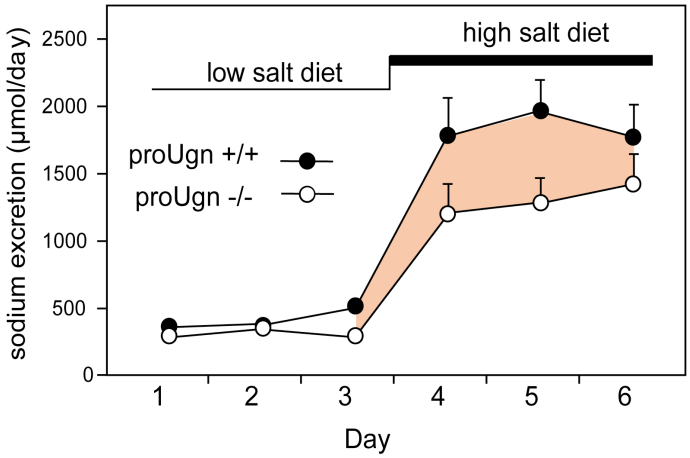

Figure 4.7 Urinary Ugn Excretion Correlated to Na^+ Excretion in Diet Study Animals and Compared to Knockout Mouse Phenotype Data A) The black symbols indicate Ugn excretion in fmol/min. The red symbols indicate Na^+ excretion in mEq/min. Vertical lines correspond to 9pm and black/white boxes indicate night/day status. **B)** Data taken from studies performed by Elitsur et.al. 2006 (50). White symbols indicate Na^+ excretion from proUgn knockout mice. Black symbols indicate Na^+ excretion from wild-type mice. The shaded pink area between the curves highlights the time when Na^+ excretion differs between strains in the study.

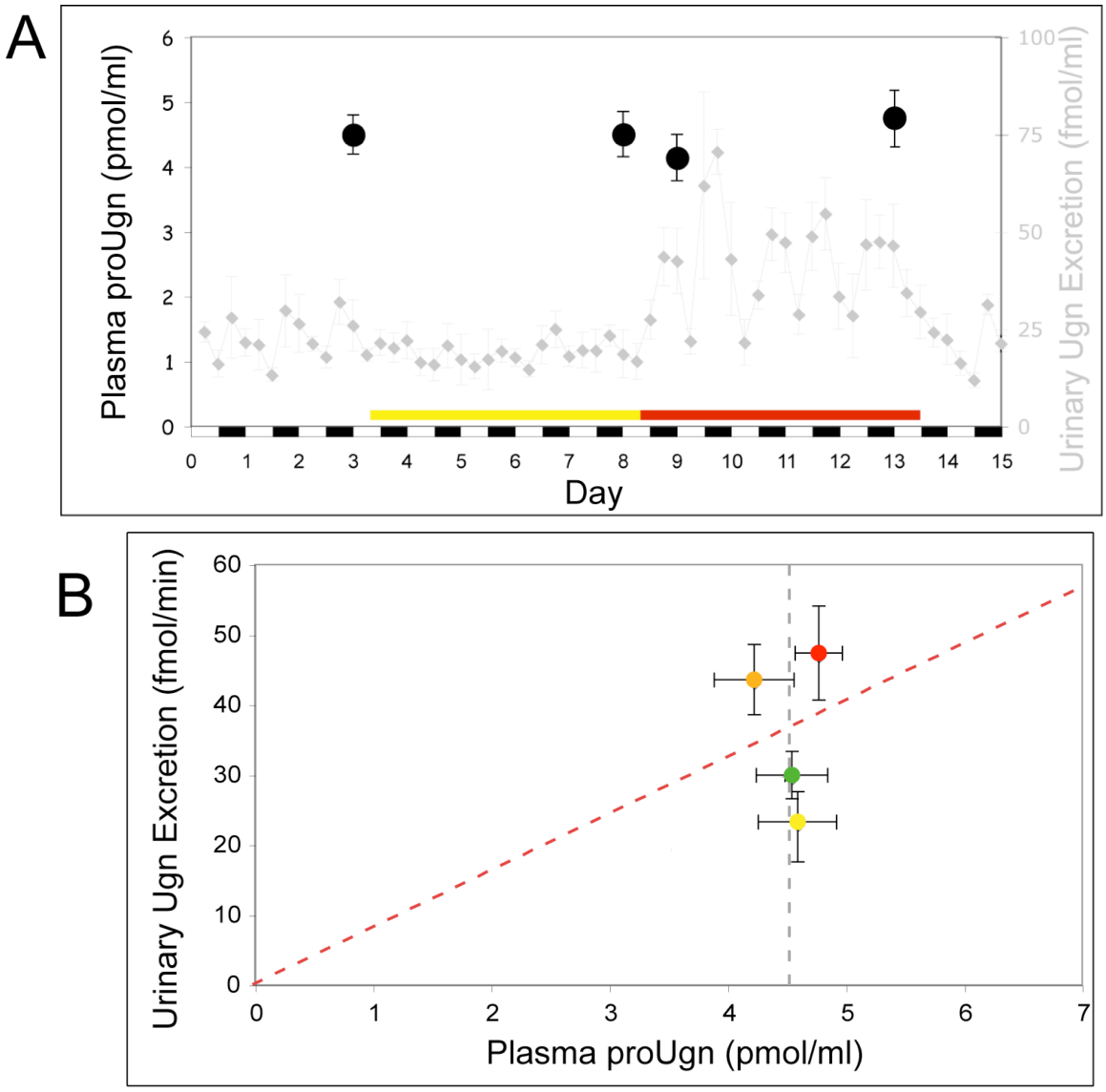

Figure 4.8 Circulating Plasma proUgn During Sodium Diet Study and processing into Urinary Ugn A) Black circles represent the plasma proUgn concentration in pmol/ml at 3am during that diet intervention. Urinary Ugn is gray in the background, for comparison of relative changes. Black/white boxes indicate night/day status. The yellow bar indicates 0.02% Na^+ LS chow and the red bar indicates 3.1% Na^+ HS chow. **B)** Circles represent the plasma proUgn concentration in pmol/ml at 3am during that diet intervention. Green = NS, Yellow = LS, Orange = HS day 1 and Red = HS day 5. The grey dashed line indicates the average plasma value observed at 3am regardless of dietary Na^+. The red dotted line indicates expected urinary Ugn excretion at 0.3% conversion of hypothetical filtered load at each given plasma proUgn value. Values are mean ±SEM, proUgn n=9-11, Ugn n=4.

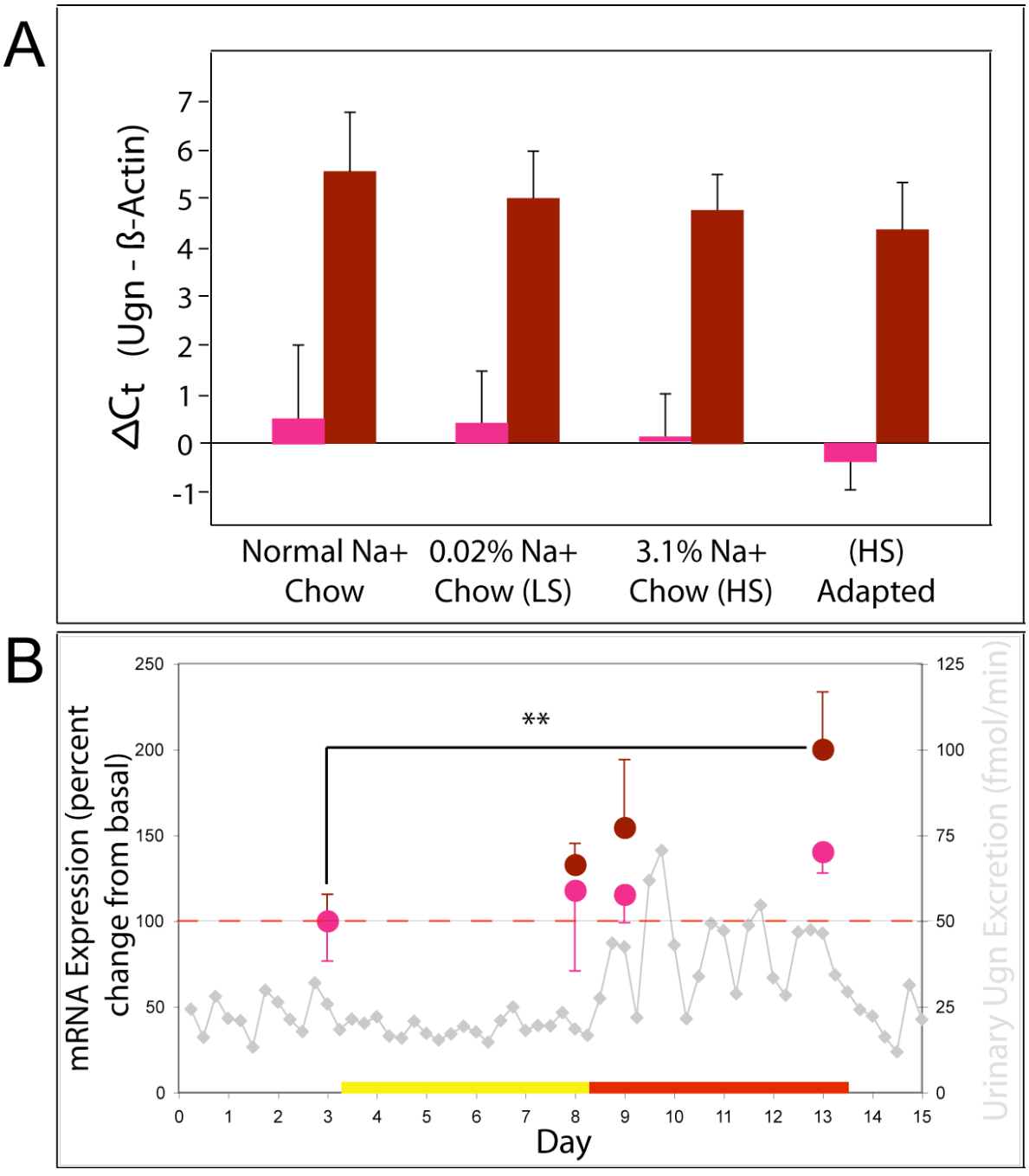

Figure 4.9 Ugn mRNA Expression Changes in Response to Diet A) Difference in cycle times (ΔCt) between ß-Actin and proUgn, determined by quantitative-RT-PCR amplification. Values are plotted against the diet conditions under which tissue samples were collected. The pink bar is intestine, and the burgundy bar is kidney (values are mean ±SEM, n=8-11). **B)** Graph showing the ΔΔCt analysis of the Cycle threshold values from qRT-PCR of kidney and intestinal proUgn mRNA. HS-adjusted is significantly higher that NS for kidney Ugn expression. Urinary Ugn is in the background (grey diamonds and line) for comparison to relative changes. The red dashed line indicates basal expression level of proUgn mRNA, **P<.03.

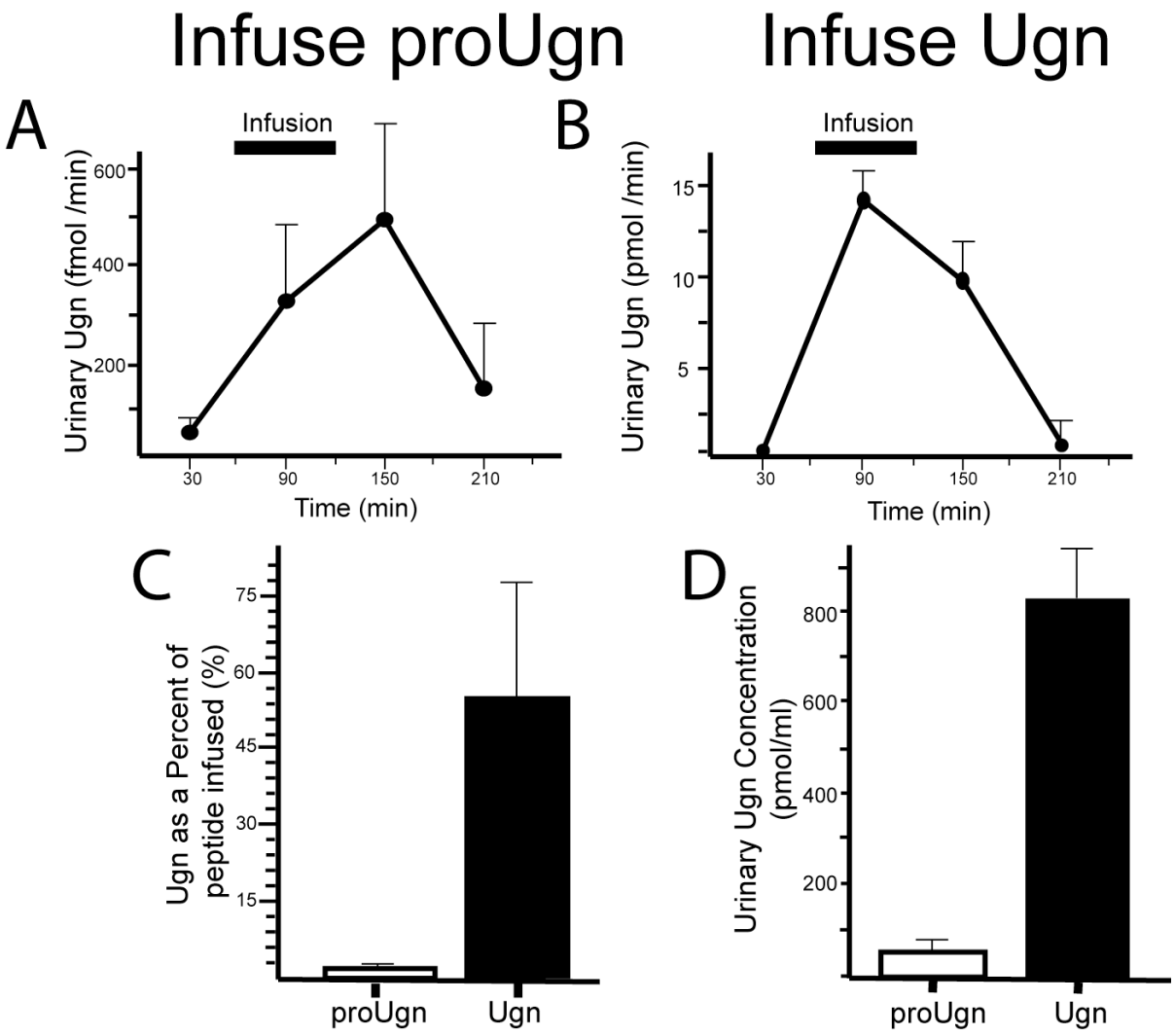

Figure 4.10 Urine Ugn Excretion in Response to Intravenous Infusions of Rat proUgn and Ugn. A) Urine Ugn excretion in fmol/min before, during and after intravenous infusion of 10ng/kg b.w. proUgn. The horizontal bar indicates the 60 min infusion period.. **B)** Urine Ugn excretion in pmol/min before, during and after intravenous infusions of 10ng/kg b.w. Ugn The horizontal bar indicates the 60 min infusion period. **C)** The amounts of Ugn recovered in urine during the infusion and post infusion periods associated with the proUgn and Ugn infusions shown in panels a and b is expressed as a percentage of peptide infused, **D)** Urinary Ugn concentrations (pmol/ml) during the infusion periods illustrated in panels a and b. All values are Mean ± SEM, n=3. As a reference, Urinary Ugn in a conscious animal on a NS diet is excreted at ~25 fmol/min, and the corresponding plasma proUgn concentration is 2 pmol/ml.

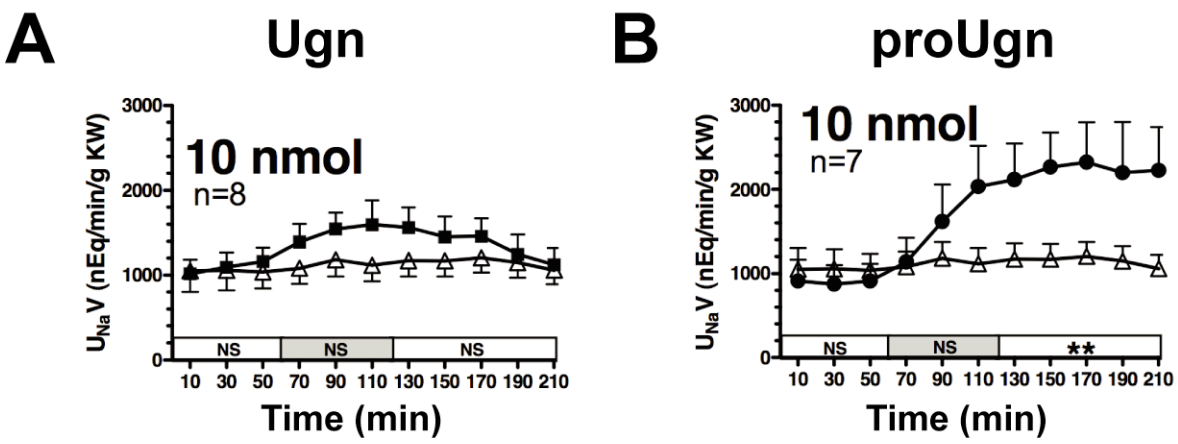

Figure 4.11 Sodium excretion ($U_{Na}V$, nEq/min/gKW) in response to intravenous peptide infusions. A) Response to rat Ugn infusions (filled squares) of 10nmol/kg b.w.. $U_{Na}V$ from a vehicle control group is shown by open triangles. The infusion period is indicated by the shaded section of the bar along the x-axis. **B)** Response to rat proUgn infusions (filled circles) in the amounts indicated. The protocol was the same as for Ugn infusions. **=p<0.01 by 1 way ANOVA with Bonferroni's multiple range testing.

CHAPTER V

SCIENTIFIC DISCUSSION

A. A Role for Prouroguanylin

High blood pressure affects more than 70 million Americans, putting them at a much greater risk for heart disease or a stroke (125). Sodium (Na^+) is a major determinant of blood osmolarity and volume, and therefore its net balance plays a critical role in blood pressure (70). Managing high blood pressure clinically usually involves reducing dietary Na^+. For some individuals these changes in salt intake have no effect, while in others they do. High blood pressure that can be lowered by a reduction in salt intake is referred to as salt-sensitive hypertension. The reason for this difference in individuals is not clearly understood and therefore it is important to understand all the mechanisms involved in Na^+ and volume homeostasis (91).

One mechanism hypothesized to play a role in Na^+ homeostasis is the post-prandial natriuretic response. This is best described as the faster urinary excretion of Na^+ after an oral NaCl load than after an equimolar intravenous NaCl load (24, 100, 152). The current teleological model for post-prandial natriuresis (PPN) is that salt ingestion causes the intestine to secrete a natriuretic endocrine agent, signaling to the kidney to excrete salt in anticipation of the Na^+ that will imminently be absorbed. Thus, PPN is thought to be mediated by an entero-renal endocrine axis. The concept of endocrine signaling between the GI tract and other organs has considerable precedent, as the GI tract is considered the largest endocrine organ in humans (12). There are many different types of endocrine cells throughout the enteric epithelium including the enterochromaffin cells in the small intestine that secrete prouroguanylin (proUgn)(179).

proUgn is a plausible candidate for mediating the entero-renal axis responsible for PPN. It is highly expressed in the proximal intestine where such a signal could originate (11, 113), its well-established digestion product Ugn has the ability to regulate epithelial electrolyte transport (22, 23, 50, 102), and Ugn is present in the urine (83, 99, 141), indicating that it has access to the lumen of the nephron, a relevant target tissue for homeostatic regulation of Na^+ excretion. Evidence from mice where the gene for proUgn has been disabled clearly shows that the polypeptide product(s) encoded by the Ugn gene can affect blood pressure and Na^+ excretion (50, 118)

B. Prouroguanylin, an Unconventional Endocrine Agent

Typical and Atypical Endocrine Axes

Endocrine axes are crucial for homeostasis, and underlying physiological processes as diverse as growth, reproduction, and nutrient management. Typical endocrine axes allow organs to communicate with each other. Some endocrine axes are simple, in that an input to one organ stimulates the release of a bioactive peptide, amine, or other type of signaling molecule into the biological system. This signal travels through the circulation to the target organ and is received as a message that triggers a physiological change. Gastrin is an example of a simple endocrine model. Luminal stimuli in the stomach and intestine induce a specific population of cells, G-cells, to secrete mature, bioactive gastrin into the blood where it travels to the gastric glands and stimulates the production of acid by parietal cells (184).

Some endocrine axes employ intermediate endocrine organs to relay the message, such as the hypothalamic-pituitary-adrenal axis response to stress (30). The hypothalamus secretes vasopressin and corticotropin-releasing hormone, active hormones that regulate the pituitary gland (115, p.1056-1057). This stimulates the secretion of adrenocorticotropic hormone (ACTH) from the pituitary. ACTH is an active hormone that stimulates the adrenal gland to release cortisol, which travels via the circulation to multiple target tissues, eliciting the desired outcomes.

The Renin-Angiotensin-Aldosterone system is an example of endocrine complexity, where multiple steps in the signaling cascade allow for various inputs to generate or modify the signal, which in turn acts on multiple targets (11). Angiotensinogen (the inactive prohormone) is released into the circulation from the liver. Angiotensinogen circulates in unprocessed form until an appropriate stimulus causes the kidney to secrete a protease known as renin. Renin acts within the circulation to process angiotensinogen into angiotensin I, which is subsequently processed by Angiotensin Converting Enzyme (another ectoprotease) into angiotensin II (ang II). AngII then travels to the kidney to relay the message. This is different from most endocrine mechanisms, in that the initial circulating form of the hormone is the biologically inactive precursor, and conversion to active form occurs only after the prohormone has been delivered to the vasculature (88).

Carrier proteins provide another layer of endocrine complexity. Carrier proteins can prolong the half-life of a circulating hormone, and can also control how much free hormone is available to bind a receptor (16, 130). This means that the

effective concentration of the hormone in the plasma is based on both the amount being secreted and the amount of carrier protein in the plasma.

Ugn or proUgn as the Messenger for PPN?

Early work in the field suggested that proUgn might be the endocrine agent of an unconventional endocrine axis. The intestine produces the majority of the proUgn in the body, but the site where this enteric pool of proUgn is converted to Ugn had not been identified. The circulating pool was assumed to be predominantly Ugn, but some larger molecular weight immunoreactive species (proUgn) had also been detected (24, 95). Because of the lack of specificity of the assay used, it was not possible to accurately identify which peptide species were present, or in what amounts (24, 95).

My studies show that very little processing of proUgn takes place within intestinal tissues. The intestinal ratio of proUgn to Ugn is ~20:1. So where is proUgn processed? Does this occur within the circulatory system, or within the renal tubules? My analyses demonstrate that intact proUgn circulates at relatively high levels in plasma, whereas the level of circulating Ugn is below the detection limit of my most sensitive assay. I also analyzed the fate of radiolabeled recombinant proUgn in pulse-chase infusion studies, and found that the propeptide circulates intact, and appears to be only converted to Ugn within the renal tubules after filtration at the glomerulus (chapter 2b). In this study, no mature Ugn was detected in the circulation; all of the radioactivity seen in arterial plasma was full-length proUgn or free amino acids. This is distinct from the typical endocrine axes described above,

where the prohormone is processed to the mature peptide intracellularly at the site of synthesis, and is secreted and delivered to the target in active form.

My data suggest that proUgn acts in an unconventional endocrine axis where the endocrine message is delivered in unprocessed form and the target organ is responsible for some modulation of the signal. This is unusual but not without precedent. T-kininogen is an example as it is secreted as a propeptide and is cleaved into active form at the site where its effect is required (160).

Additional Complexity in the Ugn/proUgn Signaling Axis

There is also the likelihood that the kidney processes proUgn into multiple bioactive metabolites, as revealed by my pulse-chase studies Chapter 2. One of these species eluted from a reverse phase HPLC column with a retention time corresponding to that of an authentic Ugn standard. However the predominant species eluted with a retention time where no known metabolite has previously been identified. In the past, bioactive peptides derived from proUgn have always been identified by T-84 cell bioassay analysis, which means that only GC-C binding ligands have been considered. As it turns out, this is a severe limitation: experiments using GC-C knockout mice (22, 99), peptide infusion studies (135) and cell culture models (76, 101) have all shown that proUgn and Ugn have effects in the kidney that are mediated by some alternate receptor that is distinct from GC-C.

A detailed analysis of the physiologic responses to infused rat Ugn and rat proUgn shows that the two peptides do not act the same (see chapter 4 and 136). When equal molar infusions were compared, proUgn caused greater a natriuresis at one-fifth the concentration of Ugn, while Ugn showed a slightly greater anti-kaliuretic

effect than did proUgn (136). These studies were performed at doses slightly above the physiological range but still within values seen in animals with kidney pathologies. The implication is that proUgn has biological actions that cannot be accounted for by Ugn. It could be that each proUgn molecule is cleaved into multiple bioactive fragments and they have additive or complementary effects.

The kidney itself has also previously been shown to express proUgn, but before my studies it was not known whether any portion of this intrarenal pool of proUgn was processed and stored as Ugn. My early studies (chapter 2) found that the renally stored form was exclusively proUgn and no Ugn could be detected by T-84cell/cGMP analysis. In follow-up studies I also found that Ugn levels in the kidney were below the detection threshold of the improved binding assay detection method for Ugn. This indicates that any secretion of proUgn by the kidney is most likely in the form of the intact propeptide. Processing must occur after (or coincident with) secretion.

Proposed future studies: Two compelling questions are; 1) what are the renal metabolites (excreted in urine) that proUgn is being broken down into (in addition to Ugn), and 2) is urinary Ugn derived from proUgn produced by the kidney or circulating in the plasma and derived from the intestine). To answer both of these questions I propose to use an isolated perfused kidney prep (IPK).

The first phase of this study would be to identify the renal metabolites by infusing large amounts of proUgn peptide into the IPK to see if the isolated organ could be made into a “metabolite factory”. A recirculating perfusate with a very high dose of proUgn might increase the yield of peptide fragments. Our infusion studies

of non-pharmacological doses of proUgn achieved a yield of 2%, much higher than the upper limit of 0.3% seen in whole animals. It is possible this could be improved at much higher doses. This flow through would then be subjected to LC-MS analysis to identify all fragments produced. The parent sequence of any possible fragments is known with precision, which will make the chance of successful identification much greater.

In attempting to answer the question of whether urinary metabolites are derived from the renal pool of proUgn vs. renal processing of the plasma pool of proUgn, the IPK could also be a good solution. If the kidney is the source of altered urinary Ugn levels in response to oral Na^+, I hypothesize the signal that activates the kidney to secrete proUgn and/or its metabolites into the tubular lumen could be either the sympathetic nerves or subtle changes renal pressure or salt delivery. These would all have to be accounted for in any investigation. An in situ preparation might be possible where renal artery and vein would be cannulated with care to minimize perturbations to the renal nerves. Failing this, it might be best to stimulate the renal nerves with an electrode to simulate normal nerve activity and microvascular tone. The perfusate would be a saline solution with no proUgn but some basal amount of BSA for oncotic pressure. Subtle alterations could be made could be made to salinity and pressure of the perfusate to see what might optimize peptide production. The newly developed binding assay would be a key tool for these analyses, as it would allow high throughput analysis of samples form many different conditions, and provide high sensitivity for detection of small amounts of Ugn excretion. The results I expect to see would be measurable levels of Ugn

(and/or other metabolites) in the urine. This may be altered by renal nerve activity or by conditions of slightly increased pressure or salinity

C. Prouroguanylin as a Control Mechanism of Basal Sodium Excretion

Intestinal Prouroguanylin as a Circadian Control Mechanism of Renal Sodium Excretion

Biological circadian rhythms are a phenomenon common among all species on earth (45). There are genes, such as *Clock*, that encode proteins and transcription factors that act as master regulators of many other genes that are expressed in this circadian cycle (71). Many of these are highly conserved from humans down to *Drosophila* (66, 71). Some circadian cycling phenomena are not directly controlled by genes that cycle autonomously, but are instead dictated by environmental cues that are encountered in each 24-hour cycle, such as food intake (146).

Chapter 4 reports my finding that levels of urinary Ugn and plasma proUgn have a circadian rhythm. The data also show that intestinally sourced plasma proUgn could *potentially* be the main precursor for urinary Ugn, as the measured concentration of gut-derived proUgn in the plasma coupled with the observed rate of conversion in the kidney (urinary Ugn ≈ 0.3% of proUgn filtered load) is adequate to provide the basal levels of Ugn in the urine (see Table 4.5). This 0.3% estimated rate of conversion would be constant throughout the 24-hour cycle, as the diurnal changes in these two proteins occur concomitantly.

The basal secretion of proUgn by the intestine into the plasma with circadian periodicity should be sufficient to drive a basal natriuresis in the kidney. Results presented from chapters 2 and 4 show that infusions of proUgn into the plasma induce a significant increase in Na^+ excretion (figure 2.7,136).

My hypothesis is that intratubular Ugn (or some other metabolite) generated from circulating proUgn causes natriuresis at a basal level, and that this is a component of normal urine generation 24 hours a day. Thus, the diurnal cycle of plasma proUgn levels provides a mechanism for enhancement of Na^+ excretion during active hours. This would have the consequence of accelerating Na^+ excretion in the nighttime hours when Na^+ is being ingested. The circadian increase in proUgn secretion from the intestine could actually be triggered by the ingestion of food, or it could be the consequence of spontaneous, free-running cyclic changes in gene expression driven by an internal circadian clock. Either of these ideas would be consistent with the observation by Dr. Mitchell Cohen's group that the hypertension in proUgn -/- mice is salt insensitive (50). Specifically, I suggest that the basal level of intratubular Ugn (generated from basal plasma proUgn) is responsible for a portion of renal Na^+ excretion that is independent of Na+ intake. When this component is missing (due, for example, to knocking out the Ugn gene), then Na^+ is retained, and blood pressure rises until pressure natriuresis is sufficient to eliminate the retained Na+ (shaded portion of Figure 4.7 B).

Proposed future studies: In order to test this, I would propose experiments that use conditional knockout mice in which the gene for Ugn has been disabled exclusively in the intestine. One way to do this would be to place the recombinase

gene under control of the serotonin promoter, which it is highly active in enterochromaffin cells where intestinal proUgn is produced. This should not affect renal expression of proUgn, as the only other tissue where serotonin is known to be expressed is the central nervous system (9). Note that proUgn has not been seen to be expressed in the nervous system (150). This model would be useful to determine whether the changes seen in Ugn excretion in response to high Na+ are from a renal or enteric source. My hypotheses are that 1) the conditional knockout animals would have high blood pressure and little Ugn in the urine on normal Na+ chow (due to confirmation of the prior hypothesis that proUgn is the mediator of a basal level of Na+ excretion through its constitutive release from the intestine), 2) the Ugn present in their urine would represent basal renal excretion and when the Na+ content of the chow is altered, this level will change concomitantly, and 3) these animals would behave like wildtype animals with respect to Na+ excretion when challenged with a large oral NaCl bolus. If a conditional knockout is not attainable to test these hypotheses, an alternative might be to transplant the kidneys of wildtype animals into constitutive, whole body Ugn-/- animals (37, 38).

Another way to investigate the nature of the circadian release of proUgn from the intestine would be through controlled feeding-time diet studies. Animals would be housed in metabolic cages and access to chow would be restricted to short periods where the lights were on and the animals would otherwise be quiescent. The same parameters as used in the previous study would be monitored to determine if circadian plasma proUgn and urinary Ugn levels are altered. If the circadian control mechanism is genetic, I would expect to see a biphasic excretion in Ugn with the

normal active phase increase reduced but a modest increase during the quiescent phase. If the intake of Na+ during the active phase of the circadian cycle is the sole or primary mechanism causing the increased urinary Ugn (environmental cue) then I would expect to see the circadian increase in Ugn excretion associated with the experimentally-adjusted time period when the animals are being fed.

D. Prouroguanylin as a Control Mechanism of Renal Sodium Excretion in Response to High Na+ Intake

Renal Prouroguanylin as a Control Mechanism for Increased Sodium Excretion During High Na+ Diet Consumption

Data presented in chapter 2 show that the kidney is the only tissue in the body that produces a significant amount of proUgn aside from the intestine. The renal pool of proUgn is significantly smaller than the intestinal pool (table 2.2). However, renal proUgn mRNA increased two-fold on the high Na^+ chow conditions. Secretion from the kidney could be a much more efficient way to produce urinary Ugn than the estimated 0.3% conversion of filtered plasma proUgn. Renal Ugn mRNA not only goes up in response to high salt diet but it also goes down in response to low salt intake (see day one of LS period). If plasma proUgn levels (with circadian variation) are not affected by dietary salt intake (as shown by my Chapter 4 studies), and if the rate of conversion of plasma proUgn to Ugn within the kidney is also not affected by salt intake (a reasonable assumption), then changes in urinary Ugn excretion have to be controlled by changes in renal release of Ugn or proUgn. This hypothesis implies that if the kidney makes a basal contribution to urinary Ugn, then the 0.3% conversion rate of endogenous plasma proUgn could be an

overestimate. An intrarenal cellular processing and secretion mechanism that efficiently produced Ugn (100% conversion) would only require mobilizing 6% of the steady-state stored pool of renal proUgn to provide the increased excretion of Ugn noted during high Na+ intake during the diet study. Note that I detected a small amount of free Ugn in the intestine (where proUgn levels are considerably higher than in the kidney), and the intestinal level of free Ugn was ~5% of the proUgn level (pretty close to the 6% processing rate required in the kidney – which would have generated a level of free Ugn that is below the detection limit of my assay). Therefore I hypothesize renal production and excretion of Ugn is the source of the increased excretion of Ugn during high Na^+ intake periods. This is a phase of the diet study that the previous hypothesis failed to address. This is utilization of the same model for different contexts, much the same way my previous diet study showed

Figure 5.1 illustrates how these two proUgn sources might contribute together to the urinary excretion of Ugn during the diet study. The plasma contribution is an estimated excretion based on filtered load of proUgn from observed values (pink shaded region). The renal contribution (burgundy shaded region) is hypothetical, and based on the concept that there is a basal excretion rate that will go down when the dietary Na^+ is restricted and up when dietary Na^+ is boosted. This response of the kidney to dietary Na^+ could be controlled by mechanisms such as the sympathetic nervous system or even renal Na^+ or stretch sensors (8, 147).

Future studies to investigate these hypotheses could include the use of genetic models such as the intestine specific conditional knockout mouse mentioned

in section C. The “inverse” genetic model would be useful to further evaluate this hypothesis. Animals with a kidney specific Ugn knockout or transplant of Ugn-/- kidneys into wildtype animals would be expected to be normotensive. This blood pressure phenotype would be wholly dependent on the basal excretion of Ugn from the renal source. I would expect these animals to have normal levels of plasma proUgn and lower urinary Ugn, but they would still display circadian changes in urinary Ugn that would match parallel circadian changes in plasma proUgn. Additionally I predict that post-prandial Na^+ excretion will be blunted in these animals (i.e. they would have delayed Na^+ excretion after a dietary Na^+ increase, similar to a constitutive Ugn-/- knockout).

The significance of these experiments, if the hypothesis is proven, is that proUgn would be shown to participate in two different mechanistic post-prandial responses; a) a circadian response that increases Na+ excretion constitutively during active hours by increasing enteric secretion of proUgn and, b) an oral salt induced response that increases Na+ excretion in response to renal Ugn supplied by the kidney itself.

E. Final Thoughts

The intestine is a sensing organ that monitors the timing, the volume and the composition of ingested food and modulates the organism in response. I propose that the changes I describe in Chapter 4 (particularly the circadian nature of enteric proUgn signaling) is appropriate for modulating Na^+ excretion to match general circadian changes in Na^+ consumption, but is not appropriate to regulate excretion in

response to the intake of specific loads of Na^+. The circadian changes in plasma proUgn may be triggered by circadian cycles in Na^+ intake, but not in a measured dose relationship as proposed by the original PPN hypothesis. I also speculate that the kidney responds specifically to bolus intakes of Na^+ by secretion of proUgn (or Ugn) into the lumen of the nephron, where it regulates the component of Na^+ excretion that is driven directly by Na^+ ingestion (controlled by an as-yet undescribed mechanism). Thus, the idea that proUgn participates in an entero-renal endocrine axis which mediates post-prandial natriuresis is not supported by my data. The more likely explanation is that proUgn participates in an entero-renal endocrine axis that modulates Na^+ excretion in a circadian cycle to match activity and general Na^+ intake. Additionally, renal proUgn could be a key component of the mechanism that drives post-prandial natriuresis (a response to specific enteric Na^+ loads), but its activation is reliant on a renal sensing mechanism or CNS input.

Figures

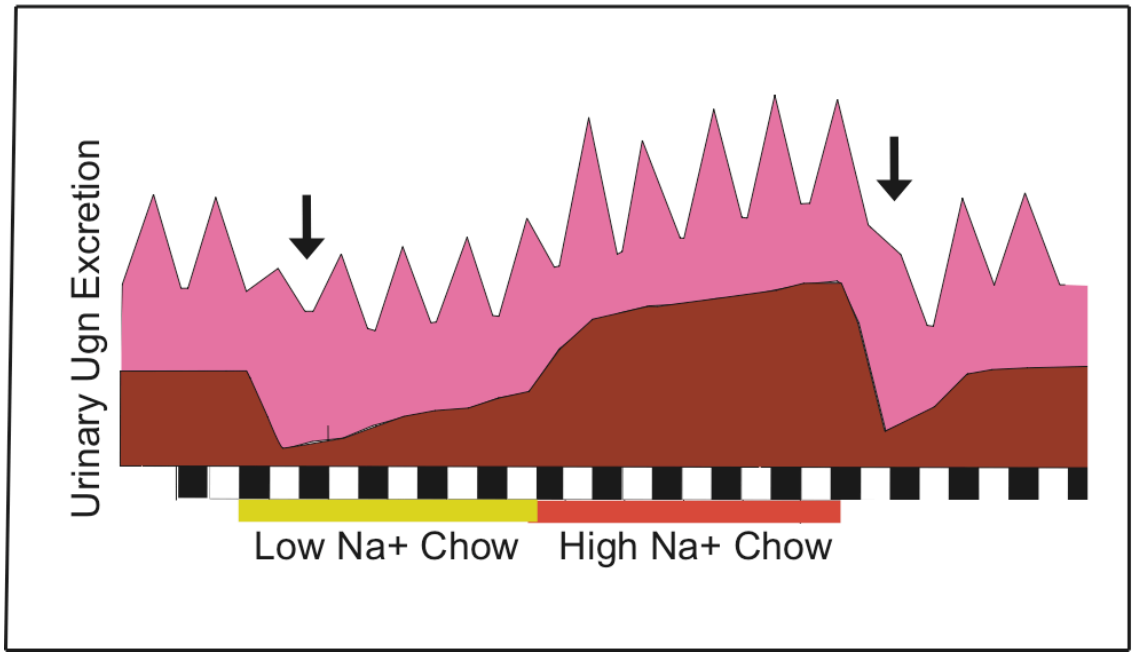

Figure 5.1 Model of hypothetical sources for Urinary Ugn. The black and white boxes indicate night an day. The yellow (0.02%Na+) and red (3.1%Na+) bars indicate Na+ content in the chow. Combined shaded region represents the urinary Ugn excreted and is approximately accurate for my results. The pink shaded region represents a hypothetical amount of Ugn contributed by the filtered plasma proUgn being filtered and processed at less than 0.3%. For these pink areas under the curve each day is approximately integrated to represent a steady state contribution, with no change due to salt status but a circadian variation. The burgundy-shaded region represents the hypothetical contribution from the kidney to affect the changes seen in urinary Ugn that unchanging plasma fails to answer. For the kidney to be playing the role of “salt-responding” organ it would not only have to increase in response to high salt but also have to have a substantial contribution to basal excretion in order to drop in the level observed during these period.

CHAPTER VI

LIST OF PUBLICATIONS

LIST OF PUBLICATIONS

The list below provides citations of the publications to which Robert C. Fellner has contributed. Percent contribution is noted in parentheses.

1. *Qian X, *Moss NG, *Fellner RC and Goy MF. Circulating prouroguanylin is processed to its active natriuretic form exclusively within the renal tubules. *Endocrinology* 149: 4499-4509. (2008)(33%)
* X.Q., N.G.M., and R.C.F. have contributed equally to this work, and the order of authorship is, therefore, arbitrary.

2. *Moss NG, *Fellner RC, Qian X, Yu SJ, Li Z, Nakazato M, Goy MF. Uroguanylin, an intestinal natriuretic peptide, is delivered to the kidney as an unprocessed propeptide. *Endocrinology* 149(9): 4486-98. (2008)(45%)
*N.G.M., and R.C.F. have contributed equally to this work, and the order of authorship is, therefore, arbitrary.

3. Moss NG, Riguera DA, Fellner RC, Cazzolla C, Goy MF. Natriuretic and Antikaliuretic Effects of Uroguanylin and Prouroguanylin in the Rat. *Am J Physiol Renal Physiol*. In Press (2010)(15%)

4. Qian X, Moss NG, Fellner RC, Taylor-Blake B, Goy M. The rat kidney contains high levels of prouroguanylin, (the uroguanylin precursor), but does not express GC-C (the enteric uroguanylin receptor). *Am J Physiol Renal Physiol*. In Press Manuscript #: F-00282-2010R1. (2010)(15%)

REFERENCES

1. Ahlman H, DeMagistris L, Zinner M, Jaffe BM. Release of immunoreactive serotonin into the lumen of the feline gut in response to vagal nerve stimulation. *Science;* 213: 1254-1255. (1981)

2. Akashi YJ, Springer J, Lainscak M, Anker SD. Atrial natriuretic peptide and related peptides. *Clin Chem Lab Med*.; 45(10): 1259-67. (2007)

3. Alfred S. Evans AS, Brachman PS *Bacterial infections of humans: epidemiology and control.* Pg. 270, 3rd ed, New York, NY, Plenum Medical Book Co, (1998)

4. Anand IS, Ferrari R, Kalra GS, Wahi PL, Poole-Wilson PA, Harris PC. Edema of cardiac origin. Studies of body water and sodium, renal function, hemodynamic indexes, and plasma hormones in untreated congestive cardiac failure. *Circulation;* 80(2): 299-305. (1989)

5. Bak M, Thomsen K, Flyvbjerg A. Effects of the somatostatin analogue octreotide on renal function in conscious diabetic rats. *Nephrol Dial Transplant*.; 16(10): 2002-7. (2001)

6. Bell-Reuss E, Trevino DL and Gottschalk CW. Effect of renal sympathetic nerve stimulation on proximal water and sodium reabsorption. *J Clin Invest*; 57: 1104–1107. (1976)

7. Bendtsen JD, Nielsen H, von Heijne G, Brunak S. Improved prediction of signal peptides: *SignalP 3.0. J Mol Bio*l.; 340: 783-795. (2004)

8. Benos DJ. Sensing tension: recognizing ENaC as a stretch sensor. *Hypertension*. 2004 Nov;44(5):616-7. (2004)

9. Berger M, Gray JA, Roth BL. The expanded biology of serotonin. *Annu Rev Med*.; 60: 355-66. (2009)

10. Bie P. Osmoreceptors, vasopressin and control of renal water secretion. *Physiol Rev*.; 60: 961-1048. (1980)

11. Bie P, Damkjaer M. Renin secretion and total body sodium: pathways of integrative control. *Clin Exp Pharmacol Physiol*.;37(2): e34-42. (2010)

12. Boron WF, Boulpaep EL. *Medical Physiology*. W.B. Saunders Company; 1st edition (2002).

13. Bouhnik J, Savoie F, Baussant T, Michaud A, Alhenc-Gelas F, Corvol P. Effect of thyroidectomy on rat T-kininogen. *Am J Physiol*.; 255: E411-5. (1988)

14. Braun T, Voland P, Kunz L, Prinz C, Gratzl M. Enterochromaffin cells of the human gut: sensors for spices and odorants. *Gastroenterology;* 132:1890-01. (2007)

15. Brenner BM, Dallaman BJ, Gunning ME, Zeidel ML. Diverse biological actions of atrial natriuretic peptide. *Physiol Rev*.; 70: 665–99. (1990)

16. Breuner CW and Orchinik M. Beyond Carrier Proteins Plasma binding proteins as mediators of corticosteroid action in vertebrates. Journal of *Endocrinology*; 175, 99–112. (2002)

17. Bulbring E, Lin RC. The effect of intraluminal application of 5-hydroxytryptamine and 5-hydroxytryptophan on peristalsis; the local production of 5-HT and its release in relation to intraluminal pressure and propulsive activity. *J Physiol*.; 140: 381-407. (1958)

18. Burks TF, Long JP. 5-Hydroxytryptamine release into dog intestinal vasculature. *Am J Physiol*.; 211:619-625. (1966)

19. Carey, R. M. Evidence for a splanchnic sodium input monitor regulating renal sodium excretion in man: lack of dependence upon aldosterone. *Circ. Res*.; 43: 19–23. (1978)

20. Carey RM. Aldosterone and cardiovascular disease. *Current Opinion in Endocrinology, Diabetes & Obesity*; 17: 194–198. (2010)

21. Carey RM, Smith JR, Ortt EM. Gastrointestinal control of sodium excretion in sodium-depleted conscious rabbits. *Am J Physiol*.; 230: 1504-1508. (1976)

22. Carrithers SL, Ott CE, Hill MJ, Johnson BR, Cai W, Chang JJ, Shah RG, Sun C, Mann EA, Fonteles MC, Forte LR, Jackson BA, Giannella RA, Greenberg RN. Guanylin and uroguanylin induce natriuresis in mice lacking guanylyl cyclase-C receptor. *Kidney Int;* 65: 40-53. (2004)

23. Carrithers SL, Hill MJ, Johnson BR, O'Hara SM, Jackson BA, Ott CE, Lorenz J, Mann EA, Giannella RA, Forte LR, Greenberg RN. Renal effects of uroguanylin and guanylin in vivo. *Braz J Med Biol Res.;* 32: 1337-44. (1999)

24. Carrithers SL, Eber SL, Forte LR, Greenberg RN. Increased urinary excretion of uroguanylin in patients with congestive heart failure. *Am J Physiol Heart Circ Physiol*.; 278(2): H538-47. (2000)

25. Carrithers SL,Jackson BA, Cai WY, Greenberg RN, Ott CE. Site-specific effects of dietary salt intake on guanylin and Uroguanylin mRNA expression in rat intestine. *Regulatory Peptides*; 107: 87– 95. (2002)

26. Chai W, Danser AH. Is angiotensin II made inside or outside of the cell? *Curr Hypertens Rep.*; 7: 124-127. (2005)

27. Chang MS, Lowe DG, Lewis M, Hellmiss R, Chen E, Goeddel DV. Differential activation by atrial and brain natriuretic peptides of two different receptor guanylate cyclase. *Nature;* 341: 68–72. (1989)

28. Chinkers M, Garbers DL, Chang M-S, Lowe DG, Chin H, Goeddel DV. A membrane form of guanylate cyclase is an atrial natriuretic peptide receptor. *Nature;* 338: 78–83. (1989)

29. Chino N, Kubo S, Miyazato M, Nakazato M, Kangawa K and Sakakibara S. Generation of two isomers with the same disulfide connectivity during disulfide bond formation of human Uroguanylin. *Letters in Peptide Science;* 3: 45-52. (1996)

30. Chrousos GP, Gold PW. The concepts of stress and stress system disorders. Overview of physical and behavioral homeostasis. *JAMA.*; 267(9): 1244-52. (1992)

31. Clauser E, Bouhnik J, Gonzalez MF, Corvol P, Menard J. Influence of converting-enzyme inhibition on rat des-angiotensin I-angiotensinogen. *Am J Physiol.*; 246: E129-33. (1984)

32. Clerico A, Del Ry S, Giannessi D. Measurement of cardiac natriuretic hormones (atrial natriuretic peptide, brain natriuretic peptide, and related peptides) in clinical practice: the need for a new generation of immunoassay methods. *Clin Chem.*; 46: 1529-1534. (2000)

33. Cohen MB, Witte DP, Hawkins JA, Currie MG. Immunohistochemical localization of guanylin in the rat small intestine and colon*. BiochemBiophys ResCommun;* 209: 803-8. (1995)

34. Cohen MB, Hawkins JA, Witte DP. Guanylin mRNA expression in human intestine and colorectal adenocarcinoma. *Lab Invest*; 78: 101–108. (1998)

35. Comrie MM, Cutler CP, Cramb G. Cloning and expression of guanylin from the European eel (Anguilla anguilla). *Biochemical and Biophysical Research Communications;* 281: 1078–1085. (2001)

36. Crane MR, Hugues M, O'Hanley PD, Waldman SA. Identification of two affinity states of low affinity receptors for Escherichia coli heat-stable enterotoxin: correlation of occupation of lower affinity state with guanylate cyclase activation. *Mol Pharmacol.*; 41(6):1073-80. (1992)

37. Crowley SD, Gurley SB, Oliverio MI, Pazmino AK, Griffiths R, Flannery PJ, Spurney RF, Kim HS, Smithies O, Le TH, Coffman TM. Distinct roles for the kidney and systemic tissues in blood pressure regulation by the renin–angiotensin system. *J. Clin. Invest*.; 115: 1092–9. (2005)

38. Crowley SD, Gurley SB, Coffman TM. AT(1) receptors and control of blood pressure. The kidney and more. *Trends Cardiovasc. Med.;* 17:30–4. (2007)

39. Cui L, Blanchard RK, Coy LM, Cousins RJ. Prouroguanylin overproduction and localization in the intestine of zinc-deficient rats. *J Nutr.;* 130: 2726-2732. (2000)

40. Currie MG, Fok KF, Kato J, Moore RJ, Hamra FK, Duffin KL, Smith CE. Guanylin: an endogenous activator of intestinal guanylate cyclase. *Proc Natl Acad Sci* USA; 89:947-951. (1992)

41. de Sauvage FJ, Keshav S, Kuang WJ, Gillett N, Henzel W, Goeddel DV. Precursor structure, expression, and tissue distribution of human guanylin. *Proc Natl Acad Sci* U S A.; 89(19): 9089-93. (1992)

42. Deshmane SP, Parkinson SJ, Crupper SS, Robertson DC, Schulz S, and Scott A. Waldman S. Cytoplasmic Domains Mediate the Ligand-Induced Affinity Shift of Guanylyl Cyclase C. *Biochemistry*; 36, 12921-12929. (1997)

43. Deshmane SP, Canithers SL, Parkinson SJ, Crupper SS Robertson DC and Waldman SJ. Rat guanylyl cyclase C expressed in COS-7 cells exhibits multiple affinities for Escherichia coli heat-stable enterotoxin. *Biochemistry*; 34(28): 9095-102. (1995)

44. Dockray GJ, Varro A, Dimaline R. Gastric endocrine cells: gene expression, processing, and targeting of active products. *Physiol Rev*.; 76: 767-798. (1996)

45. Doherty CJ, Kay SA. Circadian Control of Global Gene Expression Patterns. *Annu. Rev. Genet*.; 44: 419–44. (2010)

46. Dreyfus LA, Frantz JC and Robertson DC. Chemical properties of heat-stable enterotoxins produced by enterotoxigenic Escherichia coli of different host origins, *Infect. Immun.;* 42: 539–548. (1983)

47. Drummer C, Franck W, Heer M, Forssmann W, Gerzer R, and Goetz K. Postprandial natriuresis in humans: further evidence that urodilatin, not ANP, modulates sodium excretion *Am J Physiol*.; 270(Pt 2):F301-10. (1996)

48. Duckert P, Brunak S, Blom N. Prediction of proprotein convertase cleavage sites. *Protein Eng Des Sel.;* 17: 107-112. (2004)

49. Dustan HP, Tarazi RC, Bravo EL. Dependence of arterial pressure on intravascular volume in treated hypertensive patients. *N Engl J Med*.; 286(16): 861-6. (1972)

50. Elitsur N, Lorenz JN, Hawkins JA, Rudolph JA, Witte D, Yang LE, McDonough AA, and Cohen MB. The proximal convoluted tubule is a target for the Uroguanylin-regulated natriuretic response. *Journal of Pediatric Gastroenterology and Nutrition;* 43: S74 Y S81. (2006)

51. Fan X, Hamra FK, London RM, Eber SL, Krause WJ, Freeman RH, Smith CE, Currie MG, Forte LR. Structure and activity of uroguanylin and guanylin from the intestine and urine of rats. *Am J Physiol.;* 273(5 Pt 1): E957-64. (1997)

52. Fan X, Wang Y, London RM, Eber SL, Krause WJ, Freeman RH, Forte LR. Signaling pathways for guanylin and uroguanylin in the digestive, renal, central nervous, reproductive, and lymphoid systems. *Endocrinology;* 138(11):4636-48. (1997)

53. Fan X, Hamra FK, Freeman RH, Eber SL, Krause WJ, Lim RW, Pace VM, Currie MG, Forte LR. Uroguanylin: cloning of preprouroguanylin cDNA, mRNA expression in the intestine and heart and isolation of uroguanylin and prouroguanylin from plasma. *Biochem Biophys Res Commun*.; 219: 457-462. (1996)

54. Field, M., Graf, L. H., Laird, W. J. & Smith, P. L. Heat-stable enterotoxin of Escherichia coli: in vitro effects on guanylate cyclase activity, cyclic GMP concentration, and ion transport in small intestine. *Proc Natl. Acad. Sci*.; 75: 2800–2804. (1978)

55. Fonteles MC, Villar-Palasi C, Fang G, Larner J, Guerrant RL. Partial characterization of an ANF/urodilatin-like substance released from perfused rabbit kidney under hypoxia. *Braz J Med Biol Res*.; 26(1): 75-9. (1993)

56. Fonteles MC, Greenberg RN, Monteiro HS, Currie MG, Forte LR. Natriuretic and kaliuretic activities of guanylin and uroguanylin in the isolated perfused rat kidney. *Am J Physiol*.; 275: F191-F197. (1998)

57. Fonteles MC, Monteiro HS, Soares AM, Santos-Neto MS, Greenberg RN, Lima AA. The lysine-1 analog of guanylin induces intestinal secretion and natriuresis in the isolated perfused kidney. *Braz J Med Biol Res*.; 29(2): 267-71. (1996)

58. Fonteles MC, Havt A, Prata RB, Prata PH, Monteiro HS, Lima AA, Jorge AR, Santos CF, Greenberg RN and Nascimento NR. High-salt intake primes the rat kidney to respond to a subthreshold uroguanylin dose during ex vivo renal perfusion. *Regul Pept.;* 158: 6-13. (2009)

59. Forsberg EJ, Miller RJ. Regulation of serotonin release from rabbit intestinal enterochromaffin cells. *J Pharmacol Exp Ther.;* 227: 755-766. (1983)

60. Forte LR, London RM, Freeman RH, Krause WJ. Guanylin peptides: renal actions mediated by cyclic GMP. *Am J Physiol Renal Physiol*; 278: F180-F191. (2000)

61. Forte LR, Eber SL, Turner JT, Freeman RH, Fok KF, Currie MG. Guanylin stimulation of Cl- secretion in human intestinal T84 cells via cyclic guanosine monophosphate. *J Clin Invest*.; 91(6): 2423-8. (1993)

62. Forte LR, Freeman RH, Krause WJ and London RM. Guanylin peptides: cyclic GMP signaling mechanisms. *Braz J Med Biol Res*, 32(11): 1329-1336. (1999)

63. Forte, LR. A novel role for uroguanylin in the regulation of sodium balance *The Journal of Clinical Investigation;* 112: 1138-1141. (2003)

64. Forte LR, Eber SL, Fan X, London RM, Wang Y, Rowland LM, Chin DT, Freeman RH & Krause WJ. Lymphoguanylin: Cloning and characterization of a unique member of the guanylin peptide family. *Endocrinology,* 140: 1800-1806. (1999)

65. Forte LR. Uroguanylin and guanylin peptides: pharmacology and experimental therapeutics. *Pharmacol Ther.;* 104(2): 137-62. Review. (2004)

66. Franken P, Dijk DJ. Circadian clock genes and sleep homeostasis. *Eur J Neurosci.;* 29(9): 1820-9. (2009)

67. Fukae H, Kinoshita H, Fujimoto S, Kita T, Nakazato M, Eto T. Changes in urinary levels and renal expression of uroguanylin on low or high salt diets in rats. *Nephron;* 92:373-8. (2002)

68. Fukae H, Kinoshita H, Fujimoto S, Nakazato M, Eto T. Plasma concentration of uroguanylin in patients on maintenance dialysis therapy. *Nephron;* 84(3): 206-10. (2000)

69. Garcia KC, de Sauvage FJ, Struble M, Henzel W, Reilly D, Goeddel DV. Processing and characterization of human proguanylin expressed in Escherichia coli. *J Biol Chem*.; 268(30): 22397-401. (1993)

70. Gauer OH, Henry JP and C Behn C. The regulation of extracellular fluid volume. *Annual Review of Physiology;* Vol. 32: 547-595. (1970)

71. Gekakis N, Staknis D, Nguyen HB, Davis FC, Wilsbacher LD, King DP, Takahashi JS, Weitz CJ. Role of the CLOCK protein in the mammalian circadian mechanism. *Science;* 280(5369): 1564-9. (1998)

72. Gerzer R and Drummer C. Is urodilatin involved in the regulation of natriuresis? *J. Cardiovasc. Pharmacol*.; 22, SuppZ. 2: S86-S87. (1993)

73. Giannella RA. Escherichia coli heat-stable enterotoxins, guanylins, and their receptors: what are they and what do they do*? J Lab Clin Med.;* 125(2): 173-81. (1995)

74. Giannella RA, Mann EA. E. coli heat-stable enterotoxin and guanylyl cyclase C: new functions and unsuspected actions. *Trans Am Clin Climatol Assoc.;* 114: 67-85; discussion 85-6. (2003)

75. Gomez-Sanchez EP. The mammalian mineralocorticoid receptor: tying down a promiscuous receptor. *Exp Physiol.;* 95(1): 13-8. (2010)

76. Greenberg RN, Roesch P, Taylor BC, Greenberg VL, Vitali J and Jackson BA. Systemic administration of prouroguanylin in a rat renal clearance model results in natriuresis and increased urinary cyclic GMP. *The FASEB Journal*. 21:578. (2007)

77. Greenberg RN, Hill M, Crytzer J, Krause WJ, Eber SL, Hamra FK, Forte LR. Comparison of effects of uroguanylin, guanylin, and Escherichia coli heat-stable enterotoxin STa in mouse intestine and kidney: evidence that uroguanylin is an intestinal natriuretic hormone. *J Investig Med.;* 45: 276-282. (1997)

78. Guarino A, Cohen M, Thompson M, Dharmsathaphorn K and Giannella R. T84 cell receptor binding and guanyl cyclase activation by Escherichia coli heat-stable toxin. *Am J Physiol Gastrointest Liver Physiol.;* 253: G775-G780. (1987)

79. Guyton AC: Blood pressure control: special role of the kidneys and body fluids. *Science;* 252: 1813-6. (1991)

80. Hall JE, Hall MW. The rennin angiotensin aldosterone systems: renal mechanisms and circulatory homeosatsis. *The Kidney, Physiology and Pathophysiology*. 2nd ed. New York: Raven press, pg. 1455. (1992)

81. Hill O, Cetin Y, Cieslak A, Magert HJ, Forssmann WG. A new human guanylate cyclase-activating peptide (GCAP-II, uroguanylin): precursor cDNA and colonic expression. *Biochim Biophys Acta.;* 1253: 146-149. (1995)

82. Hamra FK, Fan X, Krause WJ, Freeman RH, Chin DT, Smith CE, Currie MG, Forte LR. Prouroguanylin and proguanylin: purification from colon, structure, and modulation of bioactivity by proteases. *Endocrinology;* 137: 257-65. (1996)

83. Hamra FK, Forte LR, Eber SL, Pidhorodeckyj NV, Krause WJ, Freeman RH, Chin DT, Tompkins JA, Fok KF, Smith CE, . Uroguanylin: structure and activity of a second endogenous peptide that stimulates intestinal guanylate cyclase. *Proc Natl Acad Sci USA;* 90: 10464-8. (1993)

84. Hamra FK, Eber SL, Chin DT, Currie MG, Forte LR. Regulation of intestinal uroguanylin/guanylin receptor-mediated responses by mucosal acidity. *Proc Natl Acad Sci U S A.;* 94(6): 2705-10. (1997)

85. Hess R, Kuhn M, Schulz-Knappe P, Raida M, Fuchs M, Klodt J, Adermann K, Kaever V, Cetin Y, Forssmann WG. GCAP-II: isolation and characterization of the circulating form of human uroguanylin. *FEBS Lett.;* 374: 34-38. (1995)

86. Hidaka Y, Ohno M, Hemmasi B, Hill O, Forssmann WG, Shimonishi Y. In vitro disulfide-coupled folding of guanylyl cyclase-activating peptide and its precursor protein. *Biochemistry;* 37: 8498-8507. (1998)

87. Hidaka Y, Shimono C, Ohno M, Okumura N, Adermann K, Forssmann WG, Shimonishi Y. Dual function of the propeptide of prouroguanylin in the folding of the mature peptide: disulfide-coupled folding and dimerization. *J Biol Chem;* 275: 25155-25162. (2000)

88. Ichihara A, Kobori H, Nishiyama A, Navar LG. Renal renin-angiotensin system. *Contrib Nephrol.;* 143: 117-30. (2004)

89. Jaleel M, London RM, Eber SL, Forte LR, Visweswariah SS. Expression of the receptor guanylyl cyclase C and its ligands in reproductive tissues of the rat: a potential role for a novel signaling pathway in the epididymis. *Biol Reprod.;* 67:1975-1980. (2002)

90. Johnson CI, Fabris B, Jandeleit K. Intrarenal renin angiotensin system to the control of intra-renal haemodynamics. *Kidney Int.;* 44: S59-63. (1993)

91. Johnson RJ, M.D., Herrera-Acosta, J M.D., Schreiner, GF M.D., Ph.D., and Rodríguez-Iturbe B, M.D. Subtle Acquired Renal Injury as a Mechanism of Salt-Sensitive Hypertension. *N Engl J Med.;* 346: 913-923. (2002)

92. Karra E, Batterham RL. The role of gut hormones in the regulation of body weight and energy homeostasis. *Mol Cell Endocrinol*.; 316(2):120-8. (2010)

93. Kikuchi M, Fujimoto S, Fukae H, Kinoshita H, Kita T, Nakazato M, Eto T. Role of uroguanylin, a Peptide with natriuretic activity, in rats with experimental nephrotic syndrome. *J Am Soc Nephrol.;*16(2):392-7. (2005)

94. Kim HS, Lee G, John SW, Maeda N and Smithies O. Molecular phenotyping for analyzing subtle genetic effects in mice: application to an angiotensinogen gene titration. *Proc Natl Acad Sci U S A*; 99: 4602-4607. (2002)

95. Kinoshita H, Fujimoto S, Nakazato M, Yokota N, Date Y, Yamaguchi H, Hisanaga S, Eto T. Urine and plasma levels of uroguanylin and its molecular forms in renal diseases. *Kidney Int.;* 52: 1028-34. (1997)

96. Kinoshita H, Nakazato M, Yamaguchi H, Matsukura S, Fujimoto S, Eto T. Increased plasma guanylin levels in patients with impaired renal function. *Clin Nephrol.*; 47: 28-32. (1997)

97. Kinoshita H, Fujimoto S, Fukae H, Yokota N, Hisanaga S, Nakazato M, Eto T. Plasma and urine levels of uroguanylin, a new natriuretic peptide, in nephrotic syndrome. *Nephron;* 81: 160-164. (1999)

98. Kirchheim H, Ehmke H and Persson P, Sympathetic modulation of renal hemodynamics, renin release and sodium excretion. *Klin Wochenschr* (1989); 67: 858–864. (1989)

99. Kita T, Smith CE, Fok KF, Duffin KL, Moore WM, Karabatsos PJ, Kachur JF, Hamra FK, Pid-horodeckyj NV, Forte LR, and Currie, MG. Characterization of human uroguanylin: a member of the guanylin peptide family. *Am J Physiology;* 266: F342-F348. (1994)

100. Kita T, Kitamura K, Sakata J, Eto T. Marked increase of guanylin secretion in response to salt loading in the rat small intestine. *Am J Physiol*.; 277:G960-6. (1999)

101. Klodt J, Kuhn M, Marx UC, Martin S, Rosch P, Forssmann WG, Adermann K. Synthesis, biological activity and isomerism of guanylate cyclase C-activating peptides guanylin and uroguanylin. *J Pept Res.;* 50:222–230. (1997)

102. Kohan DE. Biology of endothelin receptors in the collecting duct. *Kidney Int*.; 76(5): 481-6. (2009)

103. Kokot F, Ficek R. Guanylins - are they of nephrological relevance? *Nephron*.; 84(3): 201-5. (2000)

104. Koller KJ, Lowe DG, Bennett GL, Minamino N, Kangawa K, Matsuo H, Goeddel DV. Selective activation of the B natriuretic peptide receptor by C-type natriuretic peptide (CNP). *Science;* 252: 120-3. (1991)

105. Koopman MG, Koomen GC, Krediet RT, de Moor EA, Hoek FJ, Arisz L. Circadian rhythm of glomerular filtration rate in normal individuals. *Clin Sci (Lond).;* 77(1): 105-11. (1989)

106. Kulaksiz H, Cetin Y. Uroguanylin and guanylate cyclase C in the human pancreas: expression and mutuality of ligand/receptor localization as indicators of intercellular paracrine signaling pathways. *J Endocrinol*.; 170: 267-275.(2001)

107. Kulaksiz H, Rausch U, Vaccaro R, Renda TG, Cetin Y. Guanylin and uroguanylin in the parotid and submandibular glands: potential intrinsic regulators of electrolyte secretion in salivary glands. *Histochem Cell Biol.;* 115: 527-533. (2001)

108. Kulaksiz H, Cetin Y. The electrolyte/fluid secretion stimulatory peptides guanylin and uroguanylin and their common functional coupling proteins in the rat pancreas: a correlative study of expression and cell-specific localization. *Pancreas*; 25: 170-175. (2002)

109. Laney DW,Jr, Bezerra JA, Kosiba JL, Degen SJ, Cohen MB. Upregulation of Escherichia coli heat-stable enterotoxin receptor in regenerating rat liver. *Am J Physiol.;* 266: G899-G906. (1994)

110. Lee SH, Paeng JP, Jung HH, Lee SH, Lee HM, Kwon SY, Lim KJ, Jung KY. Expression of guanylin and uroguanylin mRNA in human nasal mucosa and nasal polyps. *Acta Otolaryngol.;* 124: 179-185. (2004)

111. Lennane RJ, Peart WS, Carey RM, Shaw J: A comparison of natriuresis after oral and intravenous sodium loading in sodium-depleted rabbits: Evidence for a gastrointestinal or portal monitor of sodium intake. *Clin Sci Mol Med.;* 49: 433-436. (1975)

112. Lennane RJ, Carey RM, Goodwin TJ, Peart WS. A comparison of natriuresis after oral and intravenous sodium loading in sodium-depleted man: evidence for a gastrointestinal or portal monitor of sodium intake. *Clin Sci Mol Med;* 49: 437-40. (1975)

113. Li Z, Perkins AG, Peters MF, Campa MJ, Goy MF. Purification, cDNA sequence, and tissue distribution of rat uroguanylin. *Regulatory Peptides*; 68: 45-56. (1997)

114. Li Z, Taylor-Blake B, Light AR, Goy MF. Guanylin, an endogenous ligand for C-type guanylate cyclase, is produced by goblet cells in the rat intestine. *Gastroenterology*; 109: 1863-75. (1995)

115. Limura O, Shimamoto K. Salt and hypertension: water-sodium handling in essential hypertension. *Annals of N Y Acad Sci*.; 676: 105-21. (1993)

116. London RM, Krause WJ, Fan X, Eber SL, Forte LR. Signal transduction pathways via guanylin and uroguanylin in stomach and intestine. *Am J Physiol*.; 273(1 Pt 1): G93-105. (1997)

117. London RM, Eber SL, Visweswariah SS, Krause WJ, Forte LR. Structure and activity of OK-GC: a kidney receptor guanylate cyclase activated by guanylin peptides. *Am J Physiol*.; 276(6 Pt 2): F882-91. (1999)

118. Lorenz JN, Nieman M, Sabo J, Sanford LP, Hawkins JA, Elitsur N, Gawenis LR, Clarke LL, Cohen MB. Uroguanylin knockout mice have increased blood pressure and impaired natriuretic response to enteral NaCl load. *J Clin Invest*.; 112: 1244-54. (2003)

119. Lorenz JN, Gruenstein E. A simple, nonradioactive method for evaluating single-nephron filtration rate using FITC-inulin. *Am J Physiol.;* 276: F172-F177. (1999)

120. Lotan R. Sodium, chloride and water balance in the euryhaline teleost Aphanius dispar (Rüppell) (Cyprinodontidae). *Journal of Comparative Physiology A: Neuroethology, Sensory, Neural, and Behavioral Physiology*; 65 (4): 455-462. (1972)

121. Loutzenhiser R, Griffin K, Williamson G, and Bidani A. Renal autoregulation: new perspectives regarding the protective and regulatory roles of the underlying mechanisms. *Am J Physiol Regul Integr Comp Physiol;* 290: R1153-R1167. (2006)

122. Lowe DG, Chang MS, Hellmis R, Chen E, Singh S, Garbers DL, et al. Human atrial natriuretic peptide receptor defines a new paradigm for second messenger signal transduction. *EMBO* J; 8: 1377–84. (1989)

123. Lucas A, Pitari GM, Kazerounian S, Ruiz-Stewart I, Park J and Schulz S. Guanylyl cyclases and signaling by cyclic GMP. *Pharmacol Rev*.; 52: 375–414. (2000)

124. Luippold G, Beilharz M, Wehrmann M, Unger L, Gross G, Mühlbauer B. Effect of dopamine D3 receptor blockade on renal function and glomerular size in diabetic rats. *Naunyn Schmiedebergs Arch Pharmacol*.; 371(5): 420-7. (2005)

125. MacMahon S, Peto R, Cutler J, Collins R, Sorlie P, Neaton J, Abbott R, Godwin J, Dyer A, Stamler J. Blood pressure, stroke, and coronary heart disease. Part 1, Prolonged differences in blood pressure: prospective observational studies corrected for the regression dilution bias. *Lancet;* 335: 765-74. (1990)

126. Magert HJ, Reinecke M, David I, Raab HR, Adermann K, Zucht HD, Hill O, Hess R, Forssmann WG. Uroguanylin: gene structure, expression, processing as a peptide hormone, and co-storage with somatostatin in gastrointestinal D-cells. *Regul Pept.*; 73: 165-176. (1998)

127. Mann EA, Jump ML, Wu J. Mice lacking the guanylyl cyclase C receptor are resistant to STa-induced intestinal secretion. *Biochem Biophys Res Commun*.; 239: 463–466. (1997)

128. Markert T, Vaandrager AB, Gambaryan S, Pöhler D, Häusler C, Walter U, De Jonge HR, Jarchau T, Lohmann SM. Endogenous expression of type II cGMP-dependent protein kinase mRNA and protein in rat intestine. Implications for cystic fibrosis transmembrane conductance regulator. *J Clin Invest.;* 96(2): 822-30. (1995)

129. Marx UC, Klodt J, Meyer M, Gerlach H, Rösch P, Forssmann WG, Adermann K. One peptide, two topologies: structure and interconversion dynamics of human uroguanylin isomers. *J Pept Res.;* 52(3): 229-40. (1998)

130. Mendel CM. The Free Hormone Hypothesis: Distinction from the Free Hormone Transport Hypothesis*. Journal of Anthology*; 13(2):Apr/May (1992)

131. Miyazato M, Nakazato M, Yamaguchi H, Date Y, Kojima M, Kangawa K, Matsuo H, Matsukura S. Cloning and characterization of a cDNA encoding a precursor for human uroguanylin. *Biochem Biophys Res Commun.*; 219: 644-648. (1996)

132. Miyazato M, Nakazato M, Matsukura S, Kangawa K, Matsuo H. Uroguanylin gene expression in the alimentary tract and extra-gastrointestinal tissues. *FEBS Lett.;* 398:170-174. (1996)

133. Moss NG. Renal function and renal afferent and efferent nerve activity. *Am J Physiol.;* 243(5): F425-33. (1982)

134. Moss NG, Fellner RC, Qian X, Yu SJ, Li Z, Nakazato M, Goy MF. Uroguanylin, an intestinal natriuretic peptide, is delivered to the kidney as an unprocessed propeptide. *Endocrinology.;* 149(9): 4486-98. (2008)

135. Moss NG, Riguera DA, Solinga RM, Kessler MM, Zimmer DP, Arendshorst WJ, Currie MG, Goy MF. The natriuretic peptide uroguanylin elicits physiologic actions through 2 distinct topoisomers. *Hypertension; 53*(5): 867-76. (2009)

136. Moss NG, Riguera DA, Fellner RC, Cazzolla C, Goy MF. Natriuretic and Antikaliuretic Effects of Uroguanylin and Prouroguanylin in the Rat. *Am J Physiol Renal Physiol.* In Press (2010)

137. Motulsky, H.J. *Analyzing Data with GraphPad Prism.* GraphPad Software Inc., San Diego CA. (1999) www.graphpad.com.

138. Nakazato M. Guanylin family: new intestinal peptides regulating electrolyte and water homeostasis. *J Gastroenterol*. 2001 Apr;36(4):219-25. (2001)

139. Nakazato M, Yamaguchi H, Date Y, Miyazato M, Kangawa K, Goy MF, Chino N, Matsukura S. Tissue distribution, cellular source, and structural analysis of rat immunoreactive uroguanylin. *Endocrinology;* 139(12): 5247-54. (1998)

140. Nakazato M, Yamaguchi H, Kinoshita H, Kangawa K, Matsuo H, Chino N, Matsukura S. Identification of biologically active and inactive human uroguanylins in plasma and urine and their increases in renal insufficiency. *Biochem Biophys Res Commun.;* 220: 586-593. (1996)

141. Narayan H, Mohammed N, Quinn PA, Squire IB, Davies JE, Ng LL. Activation of a novel natriuretic endocrine system in humans with heart failure. *Clin Sci* (Lond).; 121(5): 367-74. (2010)

142. Nath SK, Desjeux JF. Human intestinal cell lines as in vitro tools for electrolyte transport studies with relevance to secretory diarrhea. *J Diarrhoeal Dis Res*.; 8(4): 133-42. (1990)

143. Newton P, Harrison P, Clulow S. A novel method for determination of the affinity of protein: protein interactions in homogeneous assays. *Biomol Screen*.; 13(7): 674-82. (2008)

144. Nilsson O, Ahlman H, Geffard M, Dahlstrom A, Ericson LE Bipolarity of duodenal enterochromaffin cells in the rat*. Cell Tissue Res*.; 248: 49-54. (1987)

145. Ohyama Y, Miyamoto K, Morishita Y, Matsuda Y, Kojima M, Minamino N, Kangawa K, Matsuo H. HS-142-1, a novel antagonist for natriuretic peptides, has no effect on the third member of membrane bound guanylate cyclases (GC-C) in T84 cells. *Life Sci*.; 52(17): PL153-7. (1993)

146. Oike H, Nagai K, Fukushima T, Ishida N, Kobori M. High-salt diet advances molecular circadian rhythms in mouse peripheral tissues. *Biochem Biophys Res Commun*.; Oct 1. (2010)

147. Orlov SN, Mongin AA. Salt-sensing mechanisms in blood pressure regulation and hypertension. *Am J Physiol Heart Circ Physiol*.; 293(4): H2039-53. (2007)

148. Packer, M. New concepts in the pathophysiology of heart failure: beneficial and deleterious interaction of endogenous haemodynamic and neurohormonal mechanisms.; *J Intern Med.* Apr;239(4):327-33. (1996)

149. Pass G, Freeth G. The rat. *ANZCCART News;* 6: 1-4. (1993)

150. Perkins A, Goy MF, Li Z. Uroguanylin is expressed by enterochromaffin cells in the rat gastrointestinal tract. *Gastroenterology*; 113:1007-14. (1997)

151. Pons M, Tranchot J, L'Azou B, Cambar J. Circadian rhythms of renal hemodynamics in unanesthetized, unrestrained rats. *Chronobiol Int.;* 11(5): 301-8. (1994)

152. Potthast R, Ehler E, Scheving LA, Sindic A, Schlatter E and Kuhn M. High Salt Intake Increases Uroguanylin Expression in Mouse Kidney. *Endocrinology;* 142: 3087-3097. (2001)

153. Qian X, Prabhakar S, Nandi A, Visweswariah SS, Goy MF. Expression of GC-C, a receptor-guanylate cyclase, and its endogenous ligands uroguanylin and guanylin along the rostrocaudal axis of the intestine. *Endocrinology*; 141: 3210-24. (2000)

154. Qian X, Moss NG, Fellner RC and Goy MF. Circulating prouroguanylin is processed to its active natriuretic form exclusively within the renal tubules. *Endocrinology;* 149: 4499-4509. (2008)

155. Rathaus M, Bernheim J. Oxygen species in the microvascular environment: regulation of vascular tone and the development of hypertension. *Nephrol Dial Transplant*.; 17(2): 216-21. (2002)

156. Rawlings JM, Lucas ML, Russel RI. Measurement of jejunal surface pH in situ by plastic pH electrodes in patients with coeliac disease. *Scan J Gastroenterol*; 22: 377–84. (1987)

157. Rehfeld JF. The new biology of gastrointestinal hormones. *Physiol Rev*.; 78: 1087-1108. (1998)

158. Reid I.A., Morris B.J., Ganong W.F. The renin–angiotensin system. *Annual Rev Physiol.;* 40: 377–410. (1978)

159. Sack RB. Human diarrheal disease caused by enterotoxigenic Escherichia coli. *Annual Rev. Microbiology;* 29: 333-53. (1975)

160. Sakamoto W, Yoshikawa K, Yokoyama A, Kohri M. T-kinin is released from T-kininogen by consecutive cleavage by cathepsin E-like proteinase and 72 kDa proteinase. *Biochim Biophys Acta.*; 884(3): 607-9. (1986)

161. Santos-Neto MS, Carvalho AF, Monteiro HS, Forte LR, Fonteles MC. Interaction of atrial natriuretic peptide, urodilatin, guanylin and uroguanylin in the isolated perfused rat kidney. *Regul Pept.;* 136: 14–22. (2006)

162. Scheving LA and Jin W. Circadian regulation of uroguanylin and Guanylin in the rat intestine. *Am J Physiol Cell Physiol*.; 277: 1177-1183. (1999).

163. Schlatter E, Cermak R, Forssmann WG, Hirsch JR, Kleta R, Kuhn M, Sun D, Schafer JA. cGMP-activating peptides do not regulate electrogenic electrolyte transport in principal cells of rat CCD. *Am J Physiol*.; 271: F1158-F1165. (1996)

164. Schulz S, Green CK, Yuen PS, Garbers DL. Guanylyl cyclase is a heat-stable enterotoxin receptor. *Cell;* 63: 941-8. (1990)

165. Schulz S, Chrisman TD, and Garbers DL. Cloning and Expression of Guanylin: Its Existence in Various Mammalian Tissues. *Journal of Bio Chem*; 267(23): 16019-16021. (1992)

166. Schulz S, Lopez MJ, Kuhn M, Garbers DL. Disruption of the guanylyl cyclase-C gene leads to a paradoxical phenotype of viable but heat-stable enterotoxin-resistant mice. *J Clin Invest*. 1997 Sep 15;100(6):1590-5.

167. Scott RO, Thelin WR, and Milgram SL. A Novel PDZ Protein Regulates the Activity of Guanylyl Cyclase C, the Heat-stable Enterotoxin Receptor. *J Biol Chem*.; 277(25): 22934-41. (2002)

168. Sellers ZM, Mann E, Smith A, Ko KH, Giannella R, Cohen MB, Barrett KE, Dong H. Heat-stable enterotoxin of Escherichia coli (STa) can stimulate duodenal HCO3(-) secretion via a novel GC-C- and CFTR-independent pathway. *FASEB* J.; 22(5): 1306-16. (2008)

169. Shailubhai K, Yu HH, Karunanandaa K. Uroguanylin treatment suppresses polyp formation in the Apc(Min/?) mouse and induces apoptosis in human colon adenocarcinoma cells via cyclic GMP. *Cancer Res;* 60: 5151–5157. (2000)

170. Sindić A, Schlatter E. Mechanisms of actions of guanylin peptides in the kidney. *Pflugers Arch.;* 450(5): 283-91. (2005)

171. Sindić A, Velic A, Başoglu C, Hirsch JR, Edemir B, Kuhn M, Schlatter E. Uroguanylin and guanylin regulate transport of mouse cortical collecting duct independent of guanylate cyclase C. *Kidney Int.;* 68(3): 1008-17. (2005)

172. Sindić A, Hirsch JR, Velic A, Piechota H, Schlatter E 2005 Guanylin and uroguanylin regulate electrolyte transport in isolated human cortical collecting ducts. *Kidney Int* 67:1420-1427 (2005)

173. Sindić A, Başoglu C, Cerçi A, Hirsch JR, Potthast R, Kuhn M, Ghanekar Y, Visweswariah SS, Schlatter E. Guanylin, uroguanylin, and heat-stable enterotoxin activate guanylate cyclase C and/or a pertussis toxin-sensitive G protein in human proximal tubule cells*. J Biol Chem.;* 277(20): 17758-64. (2002)

174. Singer DR, Markandu ND, Buckley MG, Miller MA, Sagnella GA, MacGregor GA. Contrasting endocrine responses to acute oral compared with intravenous sodium loading in normal humans. *Am J Physiol.;* 274: F111-F119. (1998)

175. Skorecki KL, Brenner BM. Body fluid homeostasis in man. A contemporary overview. *Am J Med.;* 70: 77-88. (1981)

176. Skorecki KL, Brenner BM. Body fluid homeostasis in congestive heart failure and cirrhosis with ascites. *Am J Med.;* 72(2): 323-38. (1982)

177. Steinbrecher KA, Rudolph JA, Luo G, Cohen MB. Coordinate upregulation of guanylin and uroguanylin expression by hypertonicity in HT29-18-N2 cells. *Am J Physiol Cell Physiol*.; 283: C1729-C1737. (2002)

178. Sudoh T, Kangawa K, Minamino N, Matsuo H. A new natriuretic peptide in porcine brain. *Nature;* 332: 78–81. (1988)

179. Sudoh T, Minamino N, Kangawa K, Matsuo H. C-type natriuretic peptide (CNP): a new member of natriuretic peptide family identified in porcine brain. *Biochem Biophys Res Commun.;* 168: 863–70. (1990)

180. Takei Y, Yuge S. The intestinal guanylin system and seawater adaptation in eels. *Gen Comp Endocrinol.;* 152(2-3): 339-51. (2007)

181. Tanaka S. Comparative aspects of intracellular proteolytic processing of peptide hormone precursors: studies of proopiomelanocortin processing. *Zoolog Sci.*; 20: 1183-1198. (2003)

182. Vaandrager AB. Structure and function of the heat-stable enterotoxin receptor/guanylyl cyclase C. *Mol. Cell Biochem.;* 230: 73-83. (2002)

183. Valentin JP, Sechi SA, Qui C, Schambelan M and Humphreys MH. Urodilatin binds to and activates renal receptors for atrial natriuretic peptide. *Hypertension;* 21: 432-438. (1993)

184. Varro A, Yegen B, Dockray GJ. Control of tissue progastrin concentrations in the rat. *Exp Physiol.;* 78: 327-336. (1993)

185. Villarreal D, Freeman RH, Brands MW. ANF and postprandial control of sodium excretion in dogs with compensated heart failure. *Am J Physiol.;* 258: R232-R239. (1990)

186. Voogel AJ, Koopman MG, Hart AA, van Montfrans GA, Arisz L. Circadian rhythms in systemic hemodynamics and renal function in healthy subjects and patients with nephrotic syndrome. *Kidney International;* 59(5): 1873-80. (2001)

187. Wang T, Kawabata M, Haneda M, Takabatake T. Effects of uroguanylin, an intestinal natriuretic peptide, on tubuloglomerular feedback*. Hypertens Res.;* 26(7): 577-82. (2003)

188. Whitaker TL, Witte DP, Scott MC, Cohen MB. Uroguanylin and guanylin: distinct but overlapping patterns of messenger RNA expression in mouse intestine. *Gastroenterology;* 113: 1000-1006. (1997)

189. Yan W, Wu F, Morser J, Wu Q. Corin, a transmembrane cardiac serine protease, acts as a pro-atrial natriuretic peptide-converting enzyme. *Proc Natl Acad Sci USA*.; 97: 8525-8529. (2000)

190. Yuge S, Inoue K, Hyodo S, and Takei Y. A Novel Guanylin Family (Guanylin, Uroguanylin, and Renoguanylin) in Eels*. J of Bio Chem*; 278(25):22726–33. (2003)

191. Yuge S, Yamagami S, Inoue K, Suzuki N and Takei N. Identification of two functional guanylin receptors in eel: Multiple hormone-receptor system for osmoregulation in fish intestine and kidney. *General and Comparative Endocrinology;* 149: 10–20. (2006)